

1 *Title: A strong test of the Maximum Entropy Theory of Ecology*

2 *Article type: Note*

3 *Author affiliation: Xiao Xiao<sup>1,2,\*</sup>, Daniel J. McGlinn<sup>1,2</sup>, and Ethan P. White<sup>1,2</sup>*

4 <sup>1</sup>Department of Biology, Utah State University, 5305 Old Main Hill, Logan, UT 84322-5305;

5 <sup>2</sup>Ecology Center, Utah State University, 5205 Old Main Hill, Logan, UT 84322-5205

6 \*Corresponding author

7 *Email addresses: [xiao@weecology.org](mailto:xiao@weecology.org); [ethan@weecology.org](mailto:ethan@weecology.org); [daniel.mcglinn@usu.edu](mailto:daniel.mcglinn@usu.edu)*

8 *Keywords: biodiversity, body size distributions, macroecology, maximum entropy, species*

9 *abundance distribution, unified theory*

10 *Online supplementary material: Appendices A to E, Figure B1, Figure D1*

11 *Figures to print in color: Figure 1, Figure 2*

12 **Abstract**

13 The Maximum Entropy Theory of Ecology (METE) is a unified theory of biodiversity that  
14 predicts a large number of macroecological patterns using only information on the species  
15 richness, total abundance, and total metabolic rate of the community. We evaluated four major  
16 predictions of METE simultaneously at an unprecedented scale using data from 60 globally  
17 distributed forest communities including over 300,000 individuals and nearly 2000 species.  
18 METE successfully captured 96% and 89% of the variation in the species abundance distribution  
19 and the individual size distribution, but performed poorly when characterizing the size-density  
20 relationship and intraspecific distribution of individual size. Specifically, METE predicted a  
21 negative correlation between size and species abundance, which is weak in natural communities.  
22 By evaluating multiple predictions with large quantities of data, our study not only identifies a  
23 mismatch between abundance and body size in METE, but also demonstrates the importance of  
24 conducting strong tests of ecological theories.

## 25 **Introduction**

26           The structure of ecological communities can be quantified using a variety of  
27 relationships, including many of the most well-studied patterns in ecology such as the  
28 distribution of individuals among species (the species abundance distribution or SAD), the  
29 increase of species richness with area (the species area relationship or SAR), and the  
30 distributions of energy consumption and body size (Brown 1995; Rosenzweig 1995; McGill et  
31 al. 2007; White et al. 2007). With the increasing consensus that these patterns are not fully  
32 independent, a growing number of unified theories have been proposed to identify links between  
33 the patterns and unite them under a single framework (e.g., Hanski and Gyllenberg 1997;  
34 Hubbell 2001; Harte 2011; see McGill 2010 for a review). Among these unified theories there  
35 are generally two different approaches, one based on processes and the other based on  
36 constraints. With the process-based approach, characteristics of the community are captured by  
37 explicitly modeling a few key ecological processes (e.g., Hanski and Gyllenberg 1997; Hubbell  
38 2001). While this approach has the potential to directly establish connection between patterns  
39 and processes, it has been found that the same empirical patterns can result from different  
40 processes (Cohen 1968; Pielou 1975), and process-specific parameters are often hard to obtain  
41 (Hubbell 2001; Jones and Muller-Landau 2008). Alternatively, the constraint-based approach  
42 suggests that many macroecological patterns are emergent statistical properties arising from  
43 general constraints on the system, while processes are only indirectly incorporated through their  
44 effect on the constraints (e.g., Harte 2011; Locey and White 2013). This approach attempts to  
45 provide a general explanation of the observed patterns that does not rely on specific processes,  
46 which allows predictions to be made with little detailed information about the system.

47           One of the newest and most parsimonious constraint-based approaches is the Maximum  
48 Entropy Theory of Ecology (METE; Harte et al. 2008; Harte et al. 2009; Harte 2011). METE  
49 adopts the Maximum Entropy Principle from information theory, which identifies the most likely  
50 (least biased) state of a system given a set of constraints (Jaynes 2003). Assuming that the  
51 allocation of individuals and energy consumption within a community is constrained by three  
52 state variables (total species richness, total number of individuals, and total energy  
53 consumption), METE makes predictions for the SAD as well as multiple patterns related to  
54 energy use. Spatial patterns such as the SAR and the endemics area relationship can also be  
55 predicted with an additional constraint on the area sampled (Harte et al. 2008; Harte et al. 2009;  
56 Harte 2011). METE is one of the growing number of theoretical approaches that attempt to  
57 synthesize traditionally distinct areas of macroecology dealing with the distributions of  
58 individuals and the distributions of energy and biomass (Dewar and Porté 2008; Morlon et al.  
59 2009; O'Dwyer et al. 2009), and thus provides a very general characterization of the structure of  
60 ecological systems. With no tunable parameters and no specific assumptions about biological  
61 processes, it can potentially be applied to any community where the values of the state variables  
62 can be obtained.

63           Previous studies have evaluated the performance of METE with separate datasets for  
64 different patterns and have shown that METE generally provides good characterizations of these  
65 patterns across geographical locations and taxonomic groups (Harte et al. 2008; Harte et al.  
66 2009; Harte 2011; White et al. 2012a; McGlinn et al. 2013). However, these tests are relatively  
67 weak as they focus on one pattern at a time (McGill 2003). As a unified theory with multiple  
68 predictions, METE allows stronger tests to be made by testing the ability of the theory to  
69 characterize multiple patterns simultaneously for the same data (McGill 2003; McGill et al.

70 2006). In this study, we conduct a strong test of the non-spatial predictions of METE using data  
71 from 60 globally distributed forest communities to simultaneously evaluate four predictions of  
72 the theory (Fig. 1) including the SAD (the distribution of individuals among species) and  
73 energetic analogs of the individual size distribution (ISD; the distribution of body size among  
74 individuals regardless of their species identity) (Enquist and Niklas 2001; Muller-Landau et al.  
75 2006), the size-density relationship (SDR; the correlation between species abundance and  
76 average individual size within species) (Cotgreave 1993), and the intraspecific individual size  
77 distribution (iISD; the distribution of body size among individuals within a species) (Gouws et  
78 al. 2011). Our analysis shows mixed support for METE across its four predictions, with METE  
79 successfully capturing the variation in two patterns while failing for the other two. We discuss  
80 the ecological implications of our findings, as well as the importance of conducting strong multi-  
81 pattern tests in the evaluation of ecological theories.

## 82 **Methods**

### 83 1. Predicted patterns of METE

84 METE assumes that allocation of individuals and energy consumption within a  
85 community is constrained by three state variables: species richness ( $S_0$ ), total number of  
86 individuals ( $N_0$ ), and total metabolic rate summed over all individuals in the community ( $E_0$ )  
87 (Harte et al. 2008; Harte et al. 2009; Harte 2011). Define  $R(n, \varepsilon)$  as the joint probability that a  
88 species randomly picked from the community has abundance  $n$  and an individual randomly  
89 picked from such a species has metabolic rate between  $(\varepsilon, \varepsilon + \Delta\varepsilon)$ , two constraints are then  
90 established on the ratio between the state variables:

$$91 \quad \sum_{n=1}^{N_0} \int_{\varepsilon=1}^{E_0} d\varepsilon \cdot nR(n, \varepsilon) = \frac{N_0}{S_0} \quad (1)$$

92 which represents the average abundance per species, and

93 
$$\sum_{n=1}^{N_0} \int_{\varepsilon=1}^{E_0} d\varepsilon \cdot n\varepsilon R(n, \varepsilon) = \frac{E_0}{S_0} \quad (2)$$

94 which represents the average total metabolic rate per species. Note that the lower limit of  
 95 individual metabolic rate is set to be 1, and all measures of metabolic rate are rescaled  
 96 accordingly.

97 The forms of the four macroecological patterns that METE predicts can then be derived  
 98 from  $R(n, \varepsilon)$  (see Harte 2011 and **Appendix A** for detailed derivation) and are given by the  
 99 following four equations. SAD takes the form

100 
$$\Phi(n) \approx \frac{1}{cn} e^{-(\lambda_1 + \lambda_2)n} \quad (3)$$

101 which is an upper-truncated Fisher's log-series distribution. Here  $\lambda_1$  and  $\lambda_2$  are Lagrange  
 102 multipliers obtained by applying the Maximum Entropy Principle with respect to the constraints,  
 103 and  $C$  is the proper normalization constant. The Individual-level Energy Distribution (which is  
 104 the energetic equivalent of the ISD) takes the form

105 
$$\Psi(\varepsilon) = \frac{S_0}{N_0 Z} \cdot \frac{e^{-\gamma}}{(1-e^{-\gamma})^2} \cdot (1 - (N_0 + 1)e^{-\gamma N_0} + N_0 e^{-\gamma(N_0+1)}) \quad (4)$$

106 where  $\gamma = \lambda_1 + \lambda_2 \cdot \varepsilon$ . Conditioned on abundance  $n$ , the Species-level Energy Distribution (which is  
 107 the energetic equivalent of the iISD) is given by

108 
$$\Theta(\varepsilon|n) = \frac{n\lambda_2 e^{-\lambda_2 n \varepsilon}}{e^{-\lambda_2 n} - e^{-\lambda_2 n E_0}} \quad (5)$$

109 which is an exponential distribution with parameter  $\lambda_2 n$ . The expected value of the iISD  $\Theta(\varepsilon|n)$   
 110 then gives the Average Species Energy Distribution (which is the energetic equivalent of the  
 111 SDR), i.e., the expected average metabolic rate (size) for individuals within a species with  
 112 abundance  $n$ :

113 
$$\bar{\varepsilon}(n) = \frac{1}{n\lambda_2(e^{-\lambda_2 n} - e^{-\lambda_2 n E_0})} \cdot [e^{-\lambda_2 n}(\lambda_2 n + 1) - e^{-\lambda_2 n E_0}(\lambda_2 n E_0 + 1)] \quad (6)$$

114 2. Data

115 METE predicts the iISD to be an exponential distribution (Eqn 5; also see Fig. 1D) where  
116 the smallest size class is the most abundant, regardless of species identity or abundance.  
117 However, most animal species exhibit interior modes of adult body size (e.g., Koons et al. 2009;  
118 Gouws et al. 2011; but see Harte 2011) and large variation in minimum (and maximum) body  
119 size among species associated with these modal values (Gouws et al. 2011). In other words, the  
120 body sizes of conspecifics are clustered around some intermediate value, while individuals that  
121 are much larger or smaller are rare. Consequently, assembling all individuals across species in  
122 such communities often yields multimodal ISD (Thibault et al. 2011), as opposed to  
123 monotonically decreasing predicted by METE (Eqn 4; also see Fig. 1B). As such animal  
124 communities are expected a priori to violate two of the predictions of METE. Therefore, to  
125 ensure that the performance of METE was not trivially rejected because of the life history trait of  
126 determinate growth, in our analysis we focused exclusively on trees, which are known to have  
127 iISDs (Condit et al. 1998) and ISDs (Enquist and Niklas 2001; Muller-Landau et al. 2006) that  
128 are well characterized by monotonically declining distributions and which arguably have the  
129 greatest prevalence of high quality individual level size data among indeterminately growing  
130 taxonomic groups.

131 We compiled forest plot data from previous publications, publicly available databases,  
132 and data obtained through personal communication (Table 1). All plots have been fully surveyed  
133 with size measurement for all individuals above plot-specific minimum thresholds. For those  
134 plots where surveys have been conducted multiple times, we adopted data from the most recent  
135 one unless otherwise specified (see Table 1). Individuals that were dead, not identified to  
136 species/morphospecies, and/or missing size measurements were excluded. Individuals with size  
137 measurements below or equal to the designated minimum thresholds were excluded as well,

138 because it is unclear whether these size classes were thoroughly surveyed. Overall our analysis  
139 encompassed 60 plots that were at least 1 ha in size and had a richness of at least 14 (Table 1),  
140 with 1943 species/morphospecies and 379022 individuals in total.

### 141 3. Analyses

142 The scaling relationship between diameter and metabolic rate can be described with good  
143 approximation by metabolic theory as  $B \propto D^2 \cdot e^{-E/kT}$ , where  $B$  is metabolic rate,  $D$  is diameter,  
144  $T$  is temperature,  $E$  is the activation energy, and  $k$  is the Boltzmann's constant (West et al. 1999;  
145 Gillooly et al. 2001). Assuming that  $E$  is constant across species and  $T$  is constant within a  
146 community, the temperature-dependent term  $e^{-E/kT}$  is constant within a community, and can be  
147 dropped when the metabolic rate of individuals are rescaled. We thus used  $(D/D_{min})^2$  as the  
148 surrogate for individual metabolic rate, where  $D_{min}$  is the diameter of the smallest individual in  
149 the community, which sets the minimal individual metabolic rate to be 1 following METE's  
150 assumption (see Eqn 2). Applying alternative models that more accurately capture nonlinearities  
151 between diameter, mass and metabolic rate did not have any qualitative effect on our results  
152 (**Appendix B**). For individuals with multiple stems, we adopted the pipe model to combine the  
153 records, i.e.,  $D = \sqrt{\sum d_i^2}$ , where  $d_i$ 's were diameter of individual stems (Ernest et al. 2009). Since  
154 metabolic rate scales as  $D^2$ , the pipe model preserves the total area as well as the total metabolic  
155 rate for all stems combined.

156 We obtained the Lagrange multipliers  $\lambda_1$  and  $\lambda_2$  in each community with inputs  $S_0$ ,  $N_0$ ,  
157 and  $E_0$  (i.e., the sum over the rescaled individual metabolic rates) (see **Appendix A**). Predictions  
158 for the four ecological patterns were obtained from Eqns 3-6 and further transformed to facilitate  
159 comparison with observations. For the SAD and the ISD, we converted the predicted probability  
160 distributions (Eqns 3 & 4) to rank distributions of abundance (i.e., abundance at each rank from



161 the most abundant species to the least abundant species) and size (i.e., scaled metabolic rate at  
162 each rank from the largest individual to the smallest individual across all species) (Harte et al.  
163 2008; Harte 2011; White et al. 2012a), which were compared with the empirical rank  
164 distributions of abundance and size. For the SDR, predicted average metabolic rate was obtained  
165 from Eqn 6 for species with abundance  $n$ , which was compared to the observed average  
166 metabolic rate for that species. For the iISD, we converted the predicted exponential distribution  
167 (Eqn 5) into a rank distribution of individual size for each species, and compared the scaled  
168 metabolic rate predicted at each rank to the observed value. Alternative analyses for the two  
169 continuous distributions, the ISD and the iISD, did not change our results (**Appendix C**).

170 The explanatory power of METE for each pattern was quantified using the coefficient of  
171 determination  $R^2$ , which was calculated as

$$172 \quad R^2 = 1 - \frac{\sum_i [\log_{10}(obs_i) - \log_{10}(pred_i)]^2}{\sum_i [\log_{10}(obs_i) - \overline{\log_{10}(obs_i)}]^2} \quad (7)$$

173 where  $obs_i$  and  $pred_i$  were the  $i$ th observed value and METE's prediction, respectively. Both  
174 observed and predicted values were log-transformed for homoscedasticity. Note that  $R^2$  measures  
175 the proportion of variation in the observation explained by the prediction; it is based on the 1:1  
176 line when the observed values are plotted against the predicted values, not the regression line.  
177 Thus it is possible for  $R^2$  to be negative, which is an indication that the prediction is worse than  
178 taking the average of the observation.

## 179 **Results**

180 The results for all forest plots combined are summarized in Fig.2, with observations  
181 plotted against predictions for each macroecological pattern. METE provides excellent  
182 predictions for the SAD ( $R^2 = 0.96$ ) and the ISD ( $R^2 = 0.89$ ), though the largest size classes

183 deviate slightly but consistently in the ISD. However, the SDR ( $R^2 = -2.24$ ) and the iISD ( $R^2 =$   
184 0.15) are not well characterized by the theory.

185 Further examination of the four macroecological patterns within each community  
186 (**Appendix D**, Fig. A4; also see insets in Fig. 2) confirms METE's ability to consistently  
187 characterize the SAD (all  $R^2$  values  $> 0.60$ , 59/60  $R^2$  values  $> 0.8$ ) and the ISD (all  $R^2$  values  $>$   
188 0.48, 49/60  $R^2$  values  $> 0.8$ ), as well as its inadequacy in characterizing the SDR (all  $R^2$  values  
189 below zero) and the iISD (maximal  $R^2 = 0.30$ , 49/60  $R^2$  values  $< 0$ ).

## 190 **Discussion**

191 Macroecological theories increasingly attempt to make predictions across numerous  
192 ecological patterns (McGill 2010), by either directly modeling ecological processes or imposing  
193 constraints on the system. Among the constraint-based theories, METE is unique in that it makes  
194 simultaneous predictions for two distinct sets of ecological patterns, synthesizing traditionally  
195 separate areas of macroecology dealing with distributions of individuals and distributions related  
196 to body size and energy use (see also Dewar and Porté 2008; Morlon et al. 2009; O'Dwyer et al.  
197 2009). Using only information on the species richness, total abundance, and total energy use as  
198 inputs, METE attempts to characterize various aspects of community structure without tunable  
199 parameters or additional assumptions, making it one of the most parsimonious of the current  
200 unified theories.

201 Our analysis shows that METE accurately captures the general form of the SAD  
202 (allocation of individuals among species) and ISD (allocation of energy/biomass among  
203 individuals) within and among 60 forest communities (Fig. 2A, B; Fig. A4). The SAD and the  
204 ISD are among the most well-studied patterns in ecology, and numerous models exist for both  
205 patterns. For instance, with metabolic theory and demographic equilibrium models, Muller-

206 Landau *et al.* (2006) identified four possible predictions for the ISD under different assumptions  
207 of growth and mortality rates. For the SAD more than twenty models have been proposed  
208 (Marquet *et al.* 2003; McGill *et al.* 2007), ranging from purely statistical to mechanistic.

209 Our study demonstrates METE's high predictive power for these two patterns, but it does  
210 not imply that it is the best model when each pattern is considered independently. Indeed, our  
211 results reveal a slight but consistent departure of individuals in the largest size class from the ISD  
212 predicted by METE, which may result from mortality unrelated to energy use (Muller-Landau *et al.*  
213 *al.* 2006). Moreover, while METE does generally outperform the most common model of the  
214 species abundance distribution (White *et al.* 2012a), model comparisons for the ISD using AIC  
215 suggest that the maximum likelihood Weibull distribution (one of the distributions for tree  
216 diameter in Muller-Landau *et al.* 2006) almost always outperforms METE (though METE's  
217 performance is comparable to that of the other two distributions, the exponential and the Pareto;  
218 see **Appendix E**). Quantitatively comparing theories that make multiple predictions is  
219 challenging and there is no general approach for properly comparing models that make different  
220 numbers of predictions. When comparing general theories to single prediction models with  
221 tunable parameters it is not surprising that theories such as METE fail to provide the best  
222 quantitative fit (White *et al.* 2012b). However, as a constraint-based unified theory, METE's  
223 strength lies in its ability to link together ecological phenomena that were previously considered  
224 distinct, and to make predictions based on first principles with minimal inputs. The agreement  
225 between METE's predictions and the observed SAD and ISD supports the notion that the  
226 majority of variation in these macroecological patterns can be characterized by variation in the  
227 state variables  $S_0$ ,  $N_0$ , and  $E_0$  alone (Harte 2011; Supp *et al.* 2012; White *et al.* 2012a).

228           While METE performs well in characterizing the SAD and ISD, it performs poorly when  
229 predicting the distribution of energy at the species level (Fig. 2C, D; Fig. A4). These deviations  
230 from the predictions reveal a mismatch between the predicted metabolic rate of individuals and  
231 their species' abundances. METE predicts a monotonically decreasing relationship between  
232 species abundance and average intraspecific metabolic rate, i.e., species with higher abundance  
233 are also smaller in size on average and are more likely to contain smaller individuals (Eqns 5, 6,  
234 Fig. 1C). Evaluating the total (instead of average) intraspecific metabolic rate, this relationship  
235 translates roughly into Damuth's energetic equivalence rule (Damuth 1981), where the total  
236 energy consumption within a species does not depend on species identity or abundance (Harte et  
237 al. 2008; Harte 2011). While Damuth's rule has been argued to apply at global scales (Damuth  
238 1981; White et al. 2007), our results indicate that it does not hold locally, in concordance with a  
239 number of previous studies (Brown and Maurer 1987; Blackburn and Gaston 1997; White et al.  
240 2007).

241           The consistency of our results across 60 forest communities (as well as confirmative  
242 evidence from a concurrent study of a single herbaceous plant community; Newman *et al.* in  
243 review) provides strong evidence for METE's mixed performance among the four  
244 macroecological patterns. However, several limitations of the study are worth noting. First, we  
245 only analyzed a single taxonomic group (trees). This was in part because individual level size  
246 data collected in standardized ways is available for a large number of tree communities, and in  
247 part based on a prior knowledge that the form of the ISD and the iISD (Condit et al. 1998;  
248 Enquist and Niklas 2001; Muller-Landau et al. 2006) had a reasonable chance of being well  
249 characterized by the theory (see **Methods**). While we know that the SAD predictions of the  
250 theory perform well in general (White et al. 2012a), further tests are necessary to determine if the

251 simultaneous good fit of the ISD predictions is supported in other taxonomic groups. There is  
252 some evidence that this result holds in invertebrate communities (Harte 2011). Second, we  
253 estimated the metabolic rate of individuals based on predictions of metabolic theory rather than  
254 direct measurement. While our results were not sensitive to the use of other equations used for  
255 estimating metabolic rate (**Appendix B**), it is possible that directly measured metabolic rates  
256 could result in different fits to the theory (but see Newman *et al.* in review, which adopts a  
257 different method to obtain metabolic rate yet reaches similar conclusions).

258         Models and theories can be evaluated at multiple levels which yield different strengths of  
259 inference (McGill 2003; McGill et al. 2006), progressing from matching theory to empirical  
260 observations on a single pattern, to testing against a null hypothesis, to evaluating multiple a  
261 priori predictions, to eventually comparing between multiple competing models. With  
262 quantitative predictions on various ecological patterns, METE and other unified theories allow  
263 for simultaneous examination of multiple predictions, which provides a much stronger test  
264 compared to curve-fitting for a single pattern and can often reveal important insight into theories  
265 that are otherwise overlooked by single pattern tests (e.g., Adler 2004). As a comprehensive  
266 analysis on the performance of METE in predicting abundance and energy distributions in the  
267 same datasets, our study demonstrates the importance of moving towards stronger tests in  
268 ecology, especially when multiple intercorrelated predictions are available; while previous  
269 studies have shown that METE does an impressive job characterizing a single pattern (White et  
270 al. 2012a; McGlenn et al. 2013), concurrently evaluating all predictions of the theory identifies a  
271 mismatch between species' abundance and individual size that consistently deviates from  
272 empirical patterns.

273           The fact that METE fails to provide good characterization of all four patterns of  
274 community structure and performs more poorly than alternative models in some cases can be  
275 interpreted in two ways. First, the aspects of community structure that are poorly characterized  
276 by the theory may be more adequately characterized by explicitly modeling ecological processes.  
277 For example, O’Dwyer *et al.* (2009) has developed a model that incorporates individual  
278 demographic rates of birth, death, and growth, which likewise yields predictions of abundance  
279 and body size distributions. It is worth noting, however, that the process-based approach and the  
280 constraint-based approach do not have to be mutually exclusive. While O’Dwyer *et al.* (2009)  
281 suggested that size-related patterns may reflect ecological processes, the agreement between their  
282 model and METE in the predicted SAD (both log-series), as well as METE’s excellent  
283 performance for the ISD, support the idea that information in the underlying processes can be  
284 summarized in constraints alone for some macroecological patterns. Alternatively, the constraint-  
285 based approach may be sufficient in characterizing patterns of abundance and of body size, but  
286 the current form of METE may be incorrect. Specifically, its limitations revealed in our analyses  
287 may be remedied by either relaxing the current constraints to remove the association between  
288 species level body size and abundance from the theory, or by adding additional constraints to the  
289 system so that energetic equivalence among species no longer holds (J. Harte, pers. comm.).  
290 While the success of METE in characterizing the SAD and the ISD adds to the growing support  
291 for the constraint-based approach for studying macroecological patterns, further work is clearly  
292 needed to develop unified theories for community structure whether they are based on specific  
293 biological processes or emergent statistical properties.

294

295 **Acknowledgements**

296 We thank John Harte, Erica Newman, the rest of the Harte Lab, and members of the Weecology  
297 Lab for extensive feedback on this research, general insights into MaxEnt, and for being  
298 incredibly supportive of our efforts to evaluate METE. Nathan G. Swenson provided data for  
299 wood density in Luquillo forest plot and gave insightful comments. Robert K. Peet provided data  
300 for the North Carolina forest plots. The Serimbu (provided by T. Kohyama), Lahei (provided by  
301 T. B. Nishimura), and Shirakami (provided by T. Nakashizuka) datasets were obtained from the  
302 PlotNet Forest Database. The ACA Amazon (provided by N. Pitman) and DeWalt Bolivia  
303 (provided by S. DeWalt) datasets were obtained from SALVIAS. The BCI forest dynamics  
304 research project was made possible by National Science Foundation grants to Stephen P.  
305 Hubbell: DEB-0640386, DEB-0425651, DEB-0346488, DEB-0129874, DEB-00753102, DEB-  
306 9909347, DEB-9615226, DEB-9615226, DEB-9405933, DEB-9221033, DEB-9100058, DEB-  
307 8906869, DEB-8605042, DEB-8206992, DEB-7922197, support from the Center for Tropical  
308 Forest Science, the Smithsonian Tropical Research Institute, the John D. and Catherine T.  
309 MacArthur Foundation, the Mellon Foundation, the Small World Institute Fund, and numerous  
310 private individuals, and through the hard work of over 100 people from 10 countries over the  
311 past two decades. The UCSC Forest Ecology Research Plot was made possible by National  
312 Science Foundation grants to Gregory S. Gilbert (DEB-0515520 and DEB-084259), by the  
313 Pepper-Giberson Chair Fund, the University of California, and the hard work of dozens of UCSC  
314 students. These two projects are part the Center for Tropical Forest Science, a global network of  
315 large-scale demographic tree plots. The Luquillo Experimental Forest Long-Term Ecological  
316 Research Program was supported by grants BSR-8811902, DEB 9411973, DEB 0080538, DEB  
317 0218039, DEB 0620910 and DEB 0963447 from NSF to the Institute for Tropical Ecosystem  
318 Studies, University of Puerto Rico, and to the International Institute of Tropical Forestry USDA

319 Forest Service, as part of the Luquillo Long-Term Ecological Research Program. The U.S.  
320 Forest Service (Dept. of Agriculture) and the University of Puerto Rico gave additional support.  
321 This research was supported by a CAREER award from the U.S. National Science Foundation to  
322 E. P. White (DEB-0953694).

## 323 **References**

- 324 Adler, P. B. 2004. Neutral models fail to reproduce observed species-area and species-time  
325 relationships in Kansas grasslands. *Ecology* 85:1265–1272.
- 326 Baribault, T. W., R. K. Kobe, and A. O. Finley. 2011. Data from: Tropical tree growth is  
327 correlated with soil phosphorus, potassium, and calcium, though not for legumes. *Ecological*  
328 *Monographs*. Dryad Digital Repository.
- 329 Baribault, T. W., R. K. Kobe, and A. O. Finley. 2012. Tropical tree growth is correlated with soil  
330 phosphorus, potassium, and calcium, though not for legumes. *Ecological Monographs* 82:189–  
331 203.
- 332 Blackburn, T. M., and K. J. Gaston. 1997. A critical assessment of the form of the interspecific  
333 relationship between abundance and body size in animals. *The Journal of Animal Ecology*  
334 66:233–249.
- 335 Brown, J. H. 1995. *Macroecology*. University Of Chicago Press.
- 336 Brown, J. H., and B. A. Maurer. 1987. Evolution of species assemblages: Effects of energetic  
337 constraints and species dynamics on the diversification of the North American avifauna. *The*  
338 *American Naturalist* 130:1–17.
- 339 Cohen, J. E. 1968. Alternate derivations of a species-abundance relation. *The American*  
340 *Naturalist* 102:165–172.
- 341 Condit, R. 1998a. *Tropical forest census plots*. Springer-Verlag and R. G. Landes Company,  
342 Berlin, Germany, and Georgetown, Texas.
- 343 Condit, R. 1998b. Ecological implications of changes in drought patterns: shifts in forest  
344 composition in Panama. *Climatic Change* 39:413–427.
- 345 Condit, R., S. Aguilar, A. Hernández, R. Pérez, S. Lao, G. Angehr, S. P. Hubbell, et al. 2004.  
346 Tropical forest dynamics across a rainfall gradient and the impact of an El Niño dry season.  
347 *Journal of Tropical Ecology* 20:51–72.



- 348 Condit, R., R. Sukumar, S. P. Hubbell, and R. B. Foster. 1998. Predicting population trends from  
349 size distributions: a direct test in a tropical tree community. *The American Naturalist* 152:495–  
350 509.
- 351 Cotgreave, P. 1993. The relationship between body size and population abundance in animals.  
352 *Trends in Ecology & Evolution* 8:244–248.
- 353 Damuth, J. 1981. Population density and body size in mammals. *Nature* 290:699–700.
- 354 DeWalt, S. J., G. Bourdy, L. R. ChÁvez de Michel, and C. Quenevo. 1999. Ethnobotany of the  
355 Tacana: Quantitative inventories of two permanent plots of Northwestern Bolivia. *Economic*  
356 *Botany* 53:237–260.
- 357 Dewar, R. C., and A. Porté. 2008. Statistical mechanics unifies different ecological patterns.  
358 *Journal of Theoretical Biology* 251:389–403.
- 359 Enquist, B. J., and K. J. Niklas. 2001. Invariant scaling relations across tree-dominated  
360 communities. *Nature* 410:655–660.
- 361 Ernest, S. K. M., E. P. White, and J. H. Brown. 2009. Changes in a tropical forest support  
362 metabolic zero-sum dynamics. *Ecology Letters* 12:507–515.
- 363 Gilbert, G. S., E. Howard, B. Ayala-Orozco, M. Bonilla-Moheno, J. Cummings, S. Langridge, I.  
364 M. Parker, et al. 2010. Beyond the tropics: forest structure in a temperate forest mapped plot.  
365 *Journal of Vegetation Science* 21:388–405.
- 366 Gillooly, J. F., J. H. Brown, G. B. West, V. M. Savage, and E. L. Charnov. 2001. Effects of size  
367 and temperature on metabolic rate. *Science* 293:2248–2251.
- 368 Gouws, E. J., K. J. Gaston, and S. L. Chown. 2011. Intraspecific body size frequency  
369 distributions of insects. *PLoS ONE* 6:e16606.
- 370 Hanski, I., and M. Gyllenberg. 1997. Uniting two general patterns in the distribution of species.  
371 *Science* 275:397–400.
- 372 Harte, J. 2011. *Maximum entropy and ecology: a theory of abundance, distribution, and*  
373 *energetics*. Oxford University Press.
- 374 Harte, J., A. B. Smith, and D. Storch. 2009. Biodiversity scales from plots to biomes with a  
375 universal species-area curve. *Ecology Letters* 12:789–97.
- 376 Harte, J., T. Zillio, E. Conlisk, and A. B. Smith. 2008. Maximum entropy and the state-variable  
377 approach to macroecology. *Ecology* 89:2700–2711.
- 378 Hubbell, S. P. 2001. *The unified neutral theory of biodiversity and biogeography*. Princeton  
379 University Press.

- 380 Hubbell, S. P., R. Condit, and R. B. Foster. 2005. Barro Colorado forest census plot data.
- 381 Hubbell, S. P., R. B. Foster, S. T. O'Brien, K. E. Harms, R. Condit, B. Wechsler, S. J. Wright, et  
382 al. 1999. Light-gap disturbances, recruitment limitation, and tree diversity in a neotropical forest.  
383 *Science* 283:554–557.
- 384 Jaynes, E. T. 2003. *Probability theory: the logic of science*. (G. L. Bretthorst, ed.). Cambridge  
385 University Press.
- 386 Jones, F. A., and H. C. Muller-Landau. 2008. Measuring long-distance seed dispersal in complex  
387 natural environments: an evaluation and integration of classical and genetic methods. *Journal of*  
388 *Ecology* 96:642–652.
- 389 Kohyama, T., E. Suzuki, T. Partomihardjo, and T. Yamada. 2001. Dynamic steady state of patch-  
390 mosaic tree size structure of a mixed dipterocarp forest regulated by local crowding. *Ecological*  
391 *Research* 16:85–98.
- 392 Kohyama, T., E. Suzuki, T. Partomihardjo, T. Yamada, and T. Kubo. 2003. Tree species  
393 differentiation in growth, recruitment and allometry in relation to maximum height in a Bornean  
394 mixed dipterocarp forest. *Journal of Ecology* 91:797–806.
- 395 Koons, D. N., R. D. Birkhead, S. M. Boback, M. I. Williams, and M. P. Greene. 2009. The effect  
396 of body size on cottonmouth (*Agkistrodon piscivorus*) survival, recapture probability, and  
397 behavior in an Alabama swamp. *Herpetological Conservation and Biology* 4:221–235.
- 398 Locey, K. J., and E. P. White. 2013. How species richness and total abundance constrain the  
399 distribution of abundance. (D. Storch, ed.) *Ecology Letters*.
- 400 Marquet, P. A., J. A. Keymer, and H. Cofre. 2003. Breaking the stick in space: of niche models,  
401 metacommunities and patterns in the relative abundance of species. In T. M. Blackburn & K. J.  
402 Gaston, eds., *Macroecology: Concepts and Consequences* (pp. 64–86). Blackwell Science  
403 Oxford.
- 404 McDonald, R. I., R. K. Peet, and D. L. Urban. 2002. Environmental correlates of oak decline and  
405 red maple increase in the North Carolina piedmont. *Castanea* 67:84–95.
- 406 McGill, B. 2003. Strong and weak tests of macroecological theory. *Oikos* 102:679–685.
- 407 McGill, B. J. 2010. Towards a unification of unified theories of biodiversity. *Ecology Letters*  
408 13:627–642.
- 409 McGill, B. J., R. S. Etienne, J. S. Gray, D. Alonso, M. J. Anderson, H. K. Benecha, M. Dornelas,  
410 et al. 2007. Species abundance distributions: moving beyond single prediction theories to  
411 integration within an ecological framework. *Ecology Letters* 10:995–1015.

- 412 McGill, B. J., B. A. Maurer, and M. D. Weiser. 2006. Empirical evaluation of neutral theory.  
413 Ecology 87:1411–1423.
- 414 McGlinn, D. J., X. Xiao, and E. P. White. 2013. An empirical evaluation of four variants of a  
415 universal species–area relationship. PeerJ 1:e212.
- 416 Morlon, H., E. P. White, R. S. Etienne, J. L. Green, A. Ostling, D. Alonso, B. J. Enquist, et al.  
417 2009. Taking species abundance distributions beyond individuals. Ecology letters 12:488–501.
- 418 Muller-Landau, H. C., R. S. Condit, K. E. Harms, C. O. Marks, S. C. Thomas, S.  
419 Bunyavejchewin, G. Chuyong, et al. 2006. Comparing tropical forest tree size distributions with  
420 the predictions of metabolic ecology and equilibrium models. Ecology Letters 9:589–602.
- 421 Nakashizuka, T., M. Saito, K. Matsui, A. Makita, T. Kambayashi, T. Masaki, T. Nagaike, et al.  
422 2003. Monitoring beech (*Fagus crenata*) forests of different structure in Shirakami Mountains.  
423 Tohoku Journal of Forest Science 8:67–74.
- 424 Nishimura, T. B., and E. Suzuki. 2001. Allometric differentiation among tropical tree seedlings  
425 in heath and peat-swamp forests. Journal of Tropical Ecology 17:667–681.
- 426 Nishimura, T. B., E. Suzuki, T. Kohyama, and S. Tsuyuzaki. 2006. Mortality and growth of trees  
427 in peat-swamp and heath forests in central Kalimantan after severe drought. Plant Ecology  
428 188:165–177.
- 429 O’Dwyer, J. P., J. K. Lake, A. Ostling, V. M. Savage, and J. L. Green. 2009. An integrative  
430 framework for stochastic, size-structured community assembly. Proceedings of the National  
431 Academy of Sciences of the United States of America 106:6170–6175.
- 432 Palmer, M. W., R. K. Peet, R. A. Reed, W. Xi, and P. S. White. 2007. A multiscale study of  
433 vascular plants in a North Carolina Piedmont forest. Ecology 88:2674–2674.
- 434 Peet, R. K., and N. L. Christensen. 1987. Competition and tree death. BioScience 37:586–595.
- 435 Pielou, E. C. 1975. Ecological diversity. Wiley, New York, New York, USA.
- 436 Pitman, N. C. A., C. E. Cerón, C. I. Reyes, M. Thurber, and J. Arellano. 2005. Catastrophic  
437 natural origin of a species-poor tree community in the world’s richest forest. Journal of Tropical  
438 Ecology 21:559–568.
- 439 PlotNet. 2007. PlotNet Forest Database.
- 440 Pyke, C. R., R. Condit, S. Aguilar, and S. Lao. 2001. Floristic composition across a climatic  
441 gradient in a neotropical lowland forest. Journal of Vegetation Science 12:553–566.

442 Ramesh, B. R., M. H. Swaminath, S. V. Patil, R. Pélissier, P. D. Venugopal, S. Aravajy, C.  
443 Elouard, et al. 2010. Forest stand structure and composition in 96 sites along environmental  
444 gradients in the central Western Ghats of India. *Ecology* 91:3118–3118.

445 Reed, R. A., R. K. Peet, M. W. Palmer, and P. S. White. 1993. Scale dependence of vegetation-  
446 environment correlations: A case study of a North Carolina piedmont woodland. *Journal of*  
447 *Vegetation Science* 4:329–340.

448 Rosenzweig, M. L. 1995. *Species diversity in space and time*. Cambridge University Press.

449 Supp, S. R., X. Xiao, S. K. M. Ernest, and E. P. White. 2012. An experimental test of the  
450 response of macroecological patterns to altered species interactions. *Ecology* 93:2505–2511.

451 Thibault, K. M., E. P. White, A. H. Hurlbert, and S. K. M. Ernest. 2011. Multimodality in the  
452 individual size distributions of bird communities. *Global Ecology and Biogeography* 20:145–  
453 153.

454 Thompson, J., N. Brokaw, J. K. Zimmerman, R. B. Waide, E. M. Everham, D. J. Lodge, C. M.  
455 Taylor, et al. 2002. Land use history, environment, and tree composition in a tropical forest.  
456 *Ecological Applications* 12:1344–1363.

457 West, G. B., J. H. Brown, and B. J. Enquist. 1999. A general model for the structure and  
458 allometry of plant vascular systems. *Nature* 400:664–667.

459 White, E. P., S. K. M. Ernest, A. J. Kerkhoff, and B. J. Enquist. 2007. Relationships between  
460 body size and abundance in ecology. *Trends in Ecology & Evolution* 22:323–330.

461 White, E. P., K. M. Thibault, and X. Xiao. 2012a. Characterizing species abundance distributions  
462 across taxa and ecosystems using a simple maximum entropy model. *Ecology* 93:1772–1778.

463 White, E. P., X. Xiao, N. J. B. Issac, and R. M. Sibly. 2012b. Methodological tools. In R. M.  
464 Sibly, J. H. Brown, & A. Kodric-Brown, eds., *Metabolic Ecology: A Scaling Approach*. Wiley,  
465 Chichester, UK.

466 Xi, W., R. K. Peet, J. K. Decoster, and D. L. Urban. 2008. Tree damage risk factors associated  
467 with large, infrequent wind disturbances of Carolina forests. *Forestry* 81:317–334.

468 Zimmerman, J. K., E. M. E. III, R. B. Waide, D. J. Lodge, C. M. Taylor, and N. V. L. Brokaw.  
469 1994. Responses of tree species to hurricane winds in subtropical wet forest in Puerto Rico:  
470 Implications for tropical tree life histories. *The Journal of Ecology* 82:911–922.

471

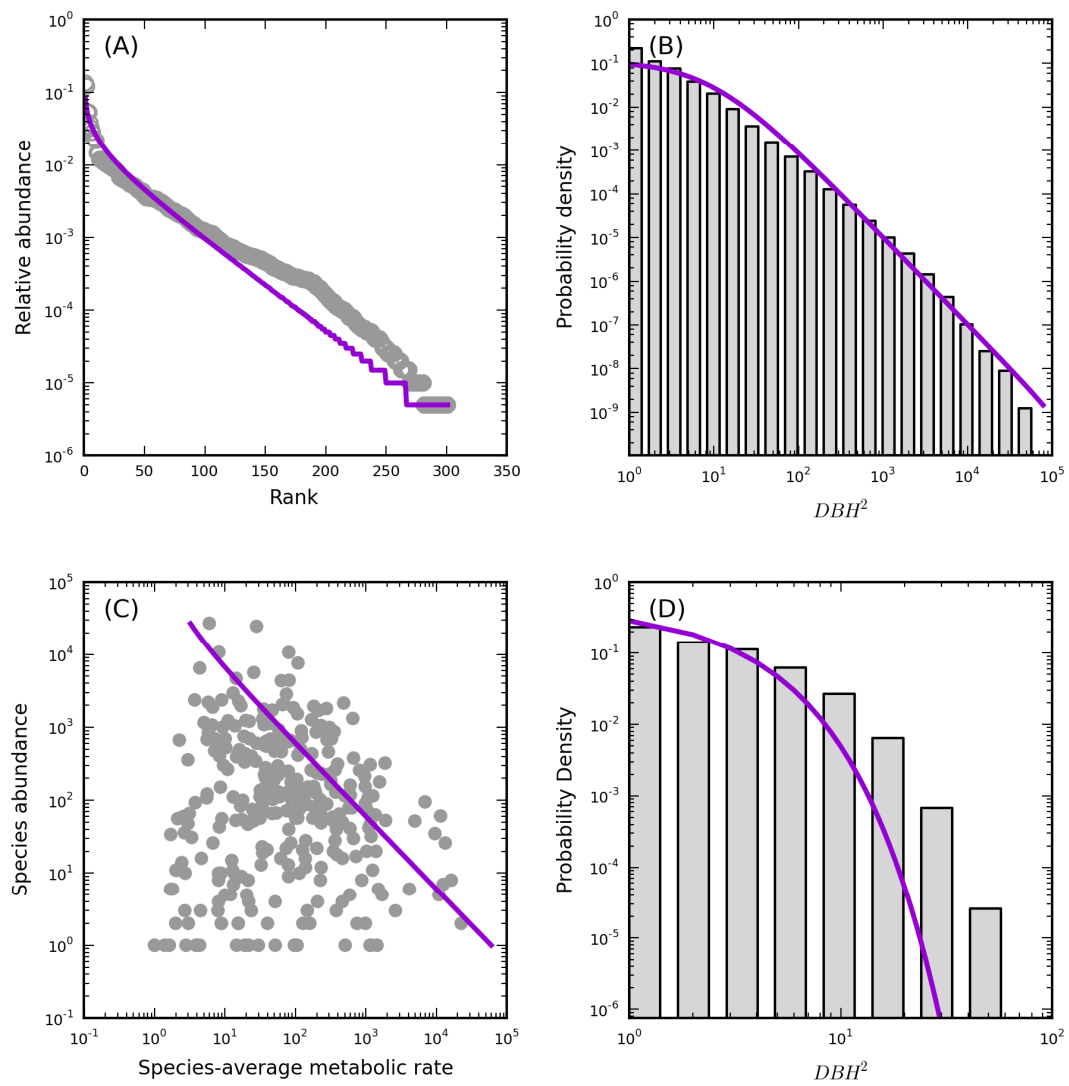
472 **Figure Legends**

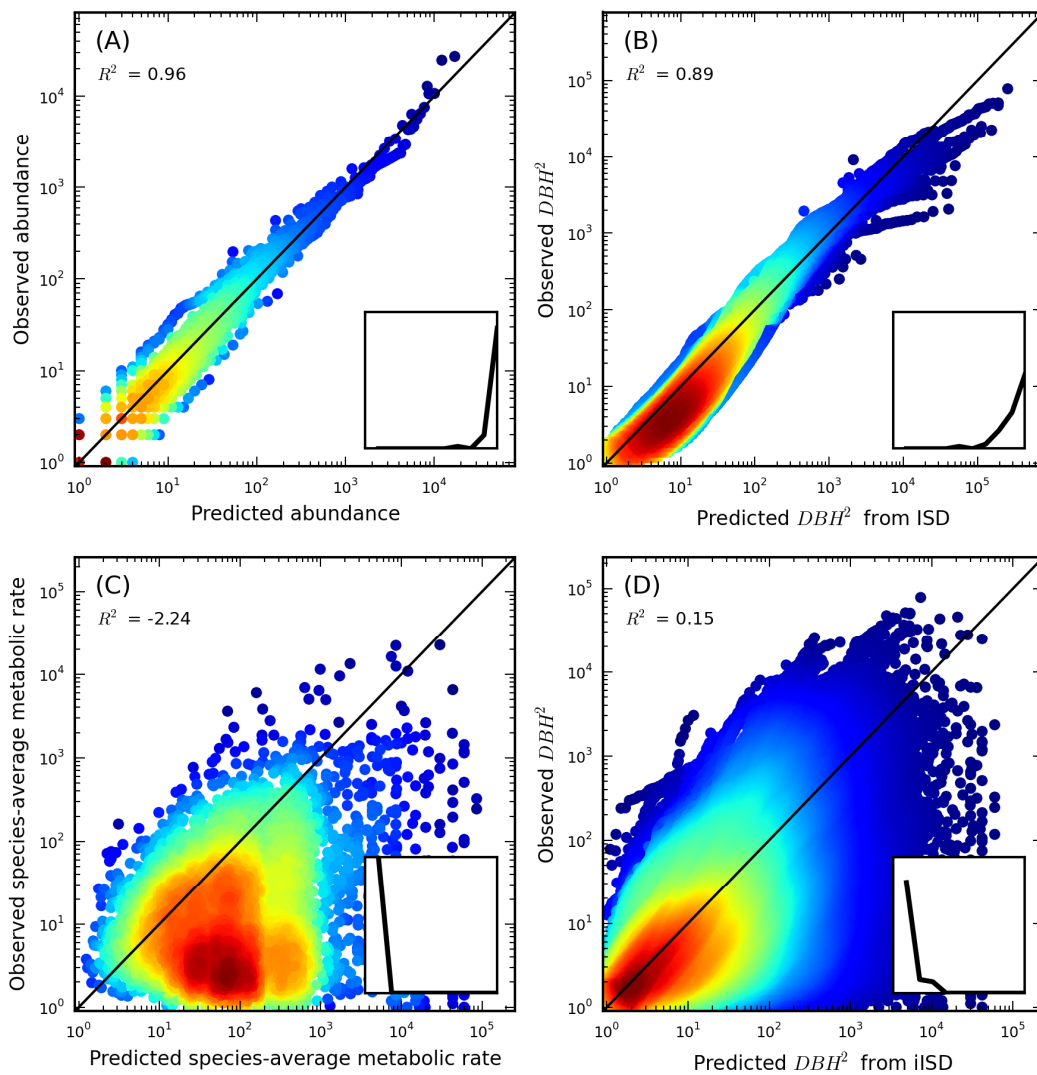
473 **Figure 1.** An illustration of the four patterns with data from Barro Colorado Island: A) Rank-  
474 abundance distribution; B) Individual size distribution (ISD); C) Size-density relationship  
475 (SDR); D) Intraspecific individual size distribution (iISD) of the most abundant species,  
476 *Hybanthus prunifolius*. Grey dots or bars in each panel represent empirical observations and  
477 magenta curve represents METE's prediction.

478

479 **Figure 2.** METE's predictions are plotted against empirical observations across 60 communities  
480 for A) SAD (each data point is the abundance of a species at a single rank in one community), B)  
481 ISD (each data point is the metabolic rate of an individual at a single rank in one community), C)  
482 SDR (each data point is the average metabolic rate within one species in one community), and  
483 D) iISD (each data point is the metabolic rate of an individual at a single rank belonging to a  
484 specific species in one community). The diagonal black line in each panel is the 1:1 line. The  
485 points are color-coded to reflect the density of neighbouring points, with warm (red) colors  
486 representing higher densities and cold (blue) colors representing lower densities. The inset  
487 reflects the distribution of  $R^2$  among 60 communities from negative (left) to 1 (right).

488 **Figure 1.**





Dataset	Description	Area of Individual Plots (ha)	Number of Plots	Survey Year	References
Serimbu	Tropical rainforest	1	2	1995*	1, 2, 3
La Selva	Tropical wet forest	2.24	5	2009	4, 5
ACA Amazon Forest Inventories	Tropical moist forest	1	1	2000-2001	6
BCI	Tropical moist forest	50	1	2010	7, 8, 9
DeWalt Bolivia forest plots	Tropical moist forest	1	2	N/A	10
Lahei	Tropical moist forest	1	3	1998	3, 11, 12
Luquillo	Tropical moist forest	16	1	1994-1996 <sup>†</sup>	13, 14
Sherman	Tropical moist forest	5.96	1	1999	15, 16, 17
Cocoli	Tropical moist forest	4	1	1998	15, 16, 17
Western Ghats	Wet evergreen / moist / dry deciduous forests	1	34	1996-1997	18
UCSC FERP	Mediterranean mixed evergreen forest	6	1	2007	19
Shirakami	Beech forest	1	2	2006	3, 20
Oosting	Hardwood forest	6.55	1	1989	21, 22
North Carolina forest plots	Mixed hardwoods / pine forest	1.3 – 5.65	5	1990-1993 <sup>‡</sup>	23, 24, 25

493 <sup>1</sup>Kohyama et al. (2001) <sup>2</sup>Kohyama et al. (2003) <sup>3</sup>PlotNet (2007) <sup>4</sup>Baribault et al. (2011)  
494 <sup>5</sup>Baribault et al. (2012) <sup>6</sup>Pitman et al. (2005) <sup>7</sup>Condit (1998a) <sup>8</sup>Hubbell et al. (2005)  
495 <sup>9</sup>Hubbell et al. (1999) <sup>10</sup>DeWalt et al. (1999) <sup>11</sup>Nishimura et al. (2006)  
496 <sup>12</sup>Nishimura and Suzuki (2001) <sup>13</sup>Zimmerman et al. (1994) <sup>14</sup>Thompson et al. (2002)  
497 <sup>15</sup>Condit (1998b) <sup>16</sup>Condit et al. (2004) <sup>17</sup>Pyke et al. (2001) <sup>18</sup>Ramesh et al. (2010)  
498 <sup>19</sup>Gilbert et al. (2010) <sup>20</sup>Nakashizuka et al. (2003) <sup>21</sup>Reed et al. (1993) <sup>22</sup>Palmer et al. (2007)  
499 <sup>23</sup>McDonald et al. (2002) <sup>24</sup>Peet and Christensen (1987) <sup>25</sup>Xi et al. (2008)

\* One plot has a more recent survey in 1998, however it lacks species ID.

<sup>†</sup> We chose Census 2 because information for multiple stems is not available in Census 3, and the unit of diameter is unclear in Census 4.

<sup>‡</sup> We chose survey individually for each plot based on expert opinion to minimize the effect of hurricane disturbance.



## Appendix A. Derivation for the Equations

The equations we adopted in our analysis (see **Methods: 1. Predicted patterns of METE**) are largely identical to those in Harte (2011), except for a few minor modifications. Below we briefly summarize the derivations, and derive those that are slightly different. See Harte (2011) for the step-by-step procedure.

**Table A1.** List of equations in our analysis and the location of their counterparts in Harte (2011).

Equation in this study	Equation in Harte 2011
Eqn 1	Eqn 7.2
Eqn 2	Eqn 7.3
Eqn 3	N/A
Eqn 4	N/A
Eqn 5	Eqn 7.25
Eqn 6	N/A

The distribution of central significance on which all other predictions are based is  $R(n, \varepsilon)$ , the joint probability that a species randomly picked from the community has abundance  $n$  and an individual randomly picked from such a species has metabolic rate between  $(\varepsilon, \varepsilon + \Delta\varepsilon)$ . By maximizing information entropy  $I = -\sum_{n=1}^{N_0} \int_{\varepsilon=1}^{E_0} d\varepsilon \cdot R(n, \varepsilon) \log(R(n, \varepsilon))$  with respect to the constraint on average abundance per species

$$\sum_{n=1}^{N_0} \int_{\varepsilon=1}^{E_0} d\varepsilon \cdot nR(n, \varepsilon) = \frac{N_0}{S_0} \quad (\text{Eqn 1 in the main text; Eqn 7.2 in Harte 2011})$$

and the constraint on total metabolic rate per species

$$\sum_{n=1}^{N_0} \int_{\varepsilon=1}^{E_0} d\varepsilon \cdot n\varepsilon R(n, \varepsilon) = \frac{E_0}{S_0} \quad (\text{Eqn 2 in the main text; Eqn 7.3 in Harte 2011})$$

16 as well as the normalization condition  $\sum_{n=1}^{N_0} \int_{\varepsilon=1}^{E_0} d\varepsilon \cdot R(n, \varepsilon) = 1$  (Eqn 7.1 in Harte 2011),  $R(n, \varepsilon)$   
 17 can be obtained as

$$18 \quad R(n, \varepsilon) = \frac{1}{Z} e^{-\lambda_1 n} e^{-\lambda_2 n \varepsilon} \quad (\text{Eqn 7.13 in Harte 2011})$$

19 where the normalization constant  $Z$  is given by

$$20 \quad Z = \sum_{n=1}^{N_0} \int_{\varepsilon=1}^{E_0} d\varepsilon \cdot e^{-\lambda_1 n} e^{-\lambda_2 n \varepsilon} \quad (\text{Eqn 7.14 in Harte 2011})$$

21 With reasonable approximations, the Lagrange multipliers  $\lambda_1$  and  $\lambda_2$  are given by

$$22 \quad \sum_{n=1}^{N_0} e^{-(\lambda_1 + \lambda_2) \cdot n} / \sum_{n=1}^{N_0} \frac{e^{-(\lambda_1 + \lambda_2)n}}{n} \approx \frac{N_0}{S_0} \quad (\text{Eqn 7.26 in Harte 2011})$$

$$23 \quad \lambda_2 \approx \frac{S_0}{E_0 - N_0} \quad (\text{Eqn 7.27 in Harte 2011})$$

## 24 **Derivation for equations not found in Harte (2011):**

### 25 1. Species-abundance distribution (SAD; Eqn 3 in main text)

26 From Eqn 7.23 in Harte (2011):

$$27 \quad \Phi(n) = \int_{\varepsilon=1}^{E_0} d\varepsilon \cdot R(n, \varepsilon) = \frac{e^{-(\lambda_1 + \lambda_2)n} - e^{-(\lambda_1 + E_0 \lambda_2)n}}{\lambda_2 Z n} \quad (\text{Eqn A1})$$

28 Note that this distribution is properly normalized, i.e.,  $\sum_{n=1}^{N_0} \Phi(n) = 1$ .

29 Given that  $E_0$  is large, the second term in the numerator,  $e^{-(\lambda_1 + E_0 \lambda_2)n}$ , is much smaller than the  
 30 first term  $e^{-(\lambda_1 + \lambda_2)n}$ . Dropping the second term,

$$31 \quad \Phi(n) \approx \frac{e^{-(\lambda_1 + \lambda_2)n}}{\lambda_2 Z n} \quad (\text{Eqn A2})$$

32 This approximation leads to the familiar Fisher's log-series distribution, upper-truncated at  $N_0$ .

33 However, the form in Eqn A2 is not properly normalized, which can cause problems when the

34 SAD is converted to the RAD (rank-abundance distribution). To ensure the proper normalization  
 35 of  $\Phi(n)$ , we replace the constant term in the Eqn A2,  $\lambda_2 Z$ , with constant  $C$ , where

$$36 \quad C = \sum_{n=1}^{N_0} \frac{e^{-(\lambda_1 + \lambda_2)n}}{n} \quad (\text{Eqn A3})$$

37 2. The energetic analog of the individual size distribution (ISD; Eqn 4 in main text)

38 From Eqn 7.6 in Harte (2011):

$$\begin{aligned}
 \Psi(\varepsilon) &= \frac{S_0}{N_0} \sum_{n=1}^{N_0} n \cdot R(n, \varepsilon) \\
 &= \frac{S_0}{N_0 Z} \sum_{n=1}^{N_0} n \cdot e^{-\lambda_1 n} e^{-\lambda_2 n \varepsilon} \\
 &= \frac{S_0}{N_0 Z} \sum_{n=1}^{N_0} n \cdot e^{-(\lambda_1 + \lambda_2 \varepsilon)n} \\
 &= \frac{S_0}{N_0 Z} \cdot e^{-(\lambda_1 + \lambda_2 \varepsilon)} \cdot \frac{1 - (N_0 + 1)e^{-N_0(\lambda_1 + \lambda_2 \varepsilon)} + N_0 e^{-(N_0 + 1)(\lambda_1 + \lambda_2 \varepsilon)}}{(1 - e^{-(\lambda_1 + \lambda_2 \varepsilon)})^2} \\
 &= \frac{S_0}{N_0 Z} \cdot \frac{e^{-\gamma}}{(1 - e^{-\gamma})^2} \cdot (1 - (N_0 + 1)e^{-\gamma N_0} + N_0 e^{-\gamma(N_0 + 1)}) \quad (\text{Eqn A4})
 \end{aligned}$$

39 where  $\gamma = \lambda_1 + \lambda_2 \cdot \varepsilon$ . Note that Eqn A4 is not identical to Eqn 7.24 in Harte (2011), which contains  
 40 a minor error (J. Harte, pers. comm.). However, the trivial difference is unlikely to invalidate or  
 41 significantly change any published results.  
 42

43 3. The energetic analog of the size-density relationship (Eqn 6 in main text)

44 From Eqn 7.25 in Harte (2011):

$$\Theta(\varepsilon|n) = \frac{n\lambda_2 e^{-\lambda_2 n \varepsilon}}{e^{-\lambda_2 n} - e^{-\lambda_2 n E_0}} \quad (\text{Eqn A5})$$

46 Then

$$\begin{aligned}
 \bar{\varepsilon}(n) &= \int_{\varepsilon=1}^{E_0} d\varepsilon \cdot \varepsilon \cdot \Theta(\varepsilon|n) \\
 &= \int_{\varepsilon=1}^{E_0} d\varepsilon \cdot \varepsilon \cdot \frac{n\lambda_2 e^{-\lambda_2 n \varepsilon}}{e^{-\lambda_2 n} - e^{-\lambda_2 n E_0}} \\
 &= \frac{n\lambda_2}{e^{-\lambda_2 n} - e^{-\lambda_2 n E_0}} \int_{\varepsilon=1}^{E_0} d\varepsilon \cdot \varepsilon \cdot e^{-\lambda_2 n \varepsilon} \\
 &= \frac{1}{n\lambda_2(e^{-\lambda_2 n} - e^{-\lambda_2 n E_0})} \cdot [e^{-\lambda_2 n}(\lambda_2 n + 1) - e^{-\lambda_2 n E_0}(\lambda_2 n E_0 + 1)] \quad (\text{Eqn A6})
 \end{aligned}$$

## 48 **Appendix B. Alternative Scaling Relationship between Diameter and Metabolic Rate**

49 While we converted diameter ( $D$ ) to metabolic rate ( $B$ ) with  $B \propto D^2$  in our analyses,  
50 alternative relationships between diameter and metabolic rate have been proposed. Specifically,  
51 it has been suggested that the aboveground biomass of tropical trees is a function of diameter,  
52 wood density, and forest type (Chave et al. 2005), while the relationship between aboveground  
53 biomass and metabolic rate is a biphasic, mixed-power function (Mori et al. 2010). Here we  
54 demonstrate that adopting this alternative scaling relationship does not quantitatively change our  
55 results.

56 We compiled species-specific wood density (wood specific gravity; WSG) from previous  
57 publications (Reyes et al. 1992; Chave et al. 2009; Zanne et al. 2009; Wright et al. 2010;  
58 Swenson et al. 2012). Since WSG information is not available for every species, we included  
59 only communities of tropical forest where no less than 70% of individuals belonged to species  
60 with known WSG to ensure the accuracy of our analysis. This criterion was met by five  
61 communities (BCI, Cocoli, Plots 4 and 5 in LaSelva, and Luquillo) out of all 60 that we  
62 examined. Individuals in these communities for which WSG information were not available were  
63 assigned average WSG value across all species in the WSG compilation.

64 We obtained metabolic rate of each individual using the alternative scaling relationships  
65 specified in Chave et al. (2005) and Mori et al. (2010). METE was then applied to each  
66 community following the steps described in **Methods** in the main text, and its predictions were  
67 compared to the observed values for the ISD, the SDR, and the iISD (Fig. B1). Though the  
68 patterns differ slightly in shape with metabolic rates obtained from the alternative method, the  
69 explanatory power of METE for each pattern does not change qualitatively, i.e., METE  
70 characterizes the ISD with high accuracy but is unable to explain much variation in the SDR or

71 the iISD, regardless of the method used to calculate metabolic rate (compare Fig. B1 with  
72 corresponding communities in Fig. D1).

73 **Figure B1.** METE's predictions are plotted against observed values for A) SAD (which remains  
74 unchanged), B) ISD, C) SDR, and D) iISD for each of the five communities individually. Here  
75 the metabolic rate was obtained with alternative scaling method, which slightly changes the  
76 shape of the ISD, the size-density relationship, and the iISD, without significant impact on the  
77 explanatory power of METE. (See Pages 42 – 46)

## Appendix C. Alternative Analyses for the ISD and the iISD

78

79

80

81

82

83

84

85

86

87

In our analyses in the main text, we converted all three probability distributions (SAD, ISD, and iISD) into distributions of rank, and compared the predicted values at each rank against the observed values. While this approach has been widely adopted (Harte et al. 2008; Harte 2011; White et al. 2012), it may not be entirely adequate for continuous distributions such as the ISD and the iISD, where empirical measurements are usually rounded off to decimals and thus may not be directly comparable to the truly continuous values obtained from the predicted distributions of rank. Here we conduct additional analyses for the ISD and the iISD with alternative approaches directly applied on the probability distributions without converting them to distributions of rank to demonstrate the robustness of our results.

88

89

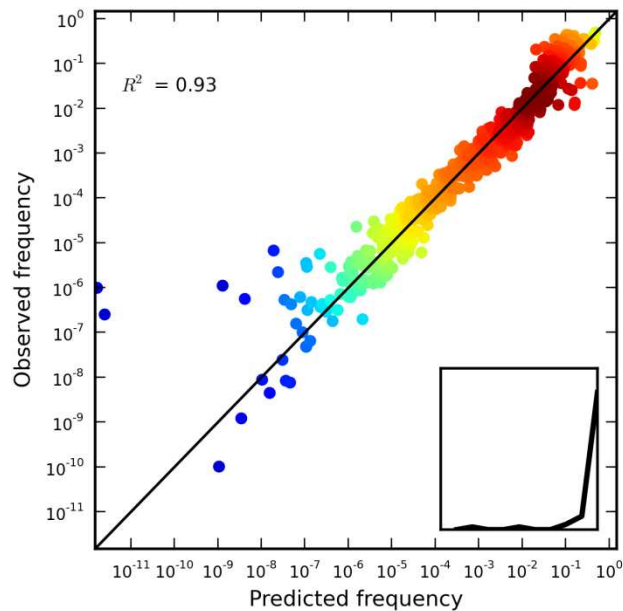
90

91

92

93

For the ISD, we grouped the scaled individual metabolic rates into  $\log(1.7)$  bins (i.e., 1-1.7, 1.7-2.89, 2.89-4.913, etc.), which resulted in 10 to 21 bins for each forest community. The predicted frequency for each bin was then calculated from the cumulative distribution of  $\Psi(\varepsilon)$  (Eqn 4 in the main text) and compared with the observed frequency. The predictive power of METE for the ISD does not change qualitatively when the ISD is analyzed as frequencies ( $R^2 = 0.93$ ; Fig. C1) instead of as ranked metabolic rates ( $R^2 = 0.89$ ; Fig. 2B in the main text).



94

95 **Figure C1.** Plot METE’s predictions against empirical observations across 60 communities for  
 96 the ISD, which is analyzed as binned frequencies. The diagonal black line is the 1:1 line. The  
 97 points are color-coded to reflect the density of neighbouring points, with warm (red) colors  
 98 representing higher densities and cold (blue) colors representing lower densities. The inset in the  
 99 lower right corner shows the distribution of  $R^2$  among individual communities from below zero  
 100 (left) to 1 (right).

101

102 The iISDs for most species contain too few individuals for the above analysis with binned  
 103 frequencies. Instead, we directly looked at the shape of the distribution. METE predicts that the  
 104 iISD for each species within a community follows an exponential distribution left-truncated at 1,  
 105 with the parameter of the distribution proportional to the abundance of the species (see Eqn 5 in  
 106 main text). Deviation from METE’s prediction can occur in one or both of two ways: 1. The  
 107 observed iISDs are not well characterized by exponential distributions; 2. Assuming that the  
 108 iISDs can be characterized by exponential distributions (which may or may not be true), the

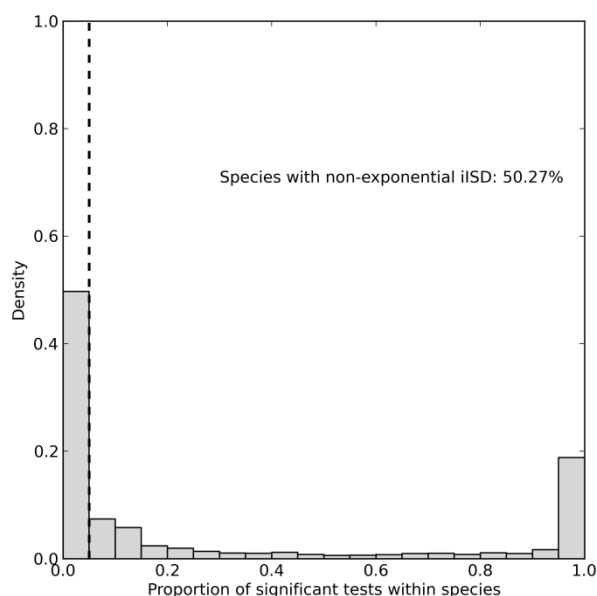
109 parameter of the distributions that best capture the observed iISDs differ from those predicted by  
110 METE (Eqn 5 in main text). Here we show that METE's prediction for iISD fails in both aspects,  
111 which is consistent with our results in the main text (Fig. 2D).

### 112 1. Characterizing iISDs with exponential distributions

113 In each community, we fitted an exponential distribution left-truncated at 1 (the minimal  
114 rescaled metabolic rate within each community) to rescaled individual metabolic rates for each  
115 species with at least 5 individuals, and obtained the maximum likelihood (MLE) parameter of the  
116 distribution. For each species, 5,000 independent samples were drawn from a left-truncated  
117 exponential distribution with the MLE parameter, where the sample size was equal to the  
118 abundance of the species. The two-sample Kolmogorov-Smirnov test was then applied to  
119 evaluate if the empirical iISD differ significantly from each sample drawn from the left-truncated  
120 exponential distribution. If the proportion of tests (among all 5,000) where the empirical iISD  
121 and the randomly generated sample differ in distribution is higher than the significance level ( $\alpha$ )  
122 of the tests, the empirical iISD for the focal species does not conform to a left-truncated  
123 exponential distribution.

124 Fig. C2 shows a histogram of proportions of Kolmogorov-Smirnov tests that are  
125 significant at  $\alpha = 0.05$  among species (with abundance  $\geq 5$ ) across all 60 communities. Overall  
126 the iISDs for more than half of the species are deemed to be significantly different from the left-  
127 truncated exponential distribution, which implies that the form of iISD predicted by METE does  
128 not hold.



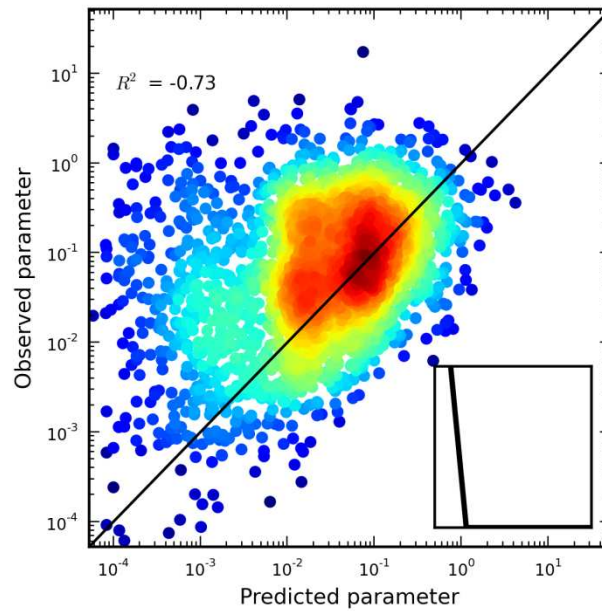


129

130 **Figure C2.** Histogram of the proportion of Kolmogorov-Smirnov tests that are significant for  
 131 each species. The dashed vertical line represents the significance level of the tests  $\alpha = 0.05$ .  
 132 Species for which the proportion of tests (among 5,000) with significant results is higher than  
 133 0.05 have iISDs that differ significantly from the left-truncated exponential distribution.

134 2. Comparing MLE parameter with METE's predicted parameter

135 We further compared the MLE parameter of left-truncated exponential distribution for  
 136 each species to the parameter predicted by METE ( $\lambda_2 n$ ; see Eqn 5 in main text) (Fig. C3). Note  
 137 that this analysis is biased in favor of METE, as we have already shown that left-truncated  
 138 exponential distribution does not provide a good characterization of empirical iISD for most  
 139 species (Fig. C2). The fact that the  $R^2$  for the iISD is below zero even when METE is evaluated  
 140 with this biased analysis further strengthens our conclusion that METE is unable to meaningfully  
 141 capture any variation in the iISD.



142

143 **Figure C3.** The iISD parameter predicted by METE is plotted against the MLE parameter for the  
144 empirical distribution for each species (with no fewer than 5 individuals) in each of the 60  
145 communities. The diagonal black line is the 1:1 line. The points are color-coded to reflect the  
146 density of neighbouring points, with warm (red) colors representing higher densities and cold  
147 (blue) colors representing lower densities. The inset reflects the distribution of  $R^2$  among 60  
148 communities from negative (left) to 1 (right).

149

## Appendix D. Evaluation of METE within Communities

150 **Figure D1.** METE's predictions for A) SAD, B) ISD, C) SDR, and D) iISD are plotted against  
151 observed patterns in each of the 60 forest communities. In A), the grey circles represent observed  
152 abundance of species in each community at each rank from the most abundant to the least  
153 abundant. In B), the grey bars represent the proportion of individuals within each size bin in each  
154 community. In C), each grey dot represents one species with a specific abundance and species-  
155 average metabolic rate in the community. The magenta curves in subplots A), B), and C)  
156 represent the relationships predicted by METE. In D), the size for each individual within a  
157 species predicted by METE is plotted against its observed size, while the diagonal line is the 1:1  
158 line. (See Pages 47 – 106)

## Appendix E. Model Comparison for ISD

Muller-Landau et al. (2006) proposed four possible distributions (exponential, Pareto, Weibull, and quasi-Weibull) for diameter in old-growth forests, under different assumptions of growth and mortality. Here we compare the fit of three of the four distributions (exponential, Pareto, and Weibull) to the fit of the ISD predicted by METE (Eqn 8) using data from the 60 forest communities. The quasi-Weibull distribution, which has been shown to provide the best fit for the majority of communities (Muller-Landau et al. 2006), is not evaluated due to the difficulty in obtaining its maximum likelihood parameters when it is left-truncated.

All distributions are left-truncated to account for the fact that individuals below the minimal threshold in each community were excluded from the datasets. With the minimal size rescaled as 1 across communities (see **Methods**), the left-truncated exponential distribution takes the form

$$f(D) = \lambda e^{-\lambda(D-1)} \quad (\text{Eqn E1})$$

the left-truncated Pareto distribution takes the form

$$f(D) = \frac{\alpha}{D^{\alpha+1}} \quad (\text{Eqn E2})$$

the left-truncated Weibull distribution takes the form

$$f(D) = \frac{k}{\lambda} \left(\frac{D}{\lambda}\right)^{k-1} e^{-(D/\lambda)^k} / e^{-(1/\lambda)^k} \quad (\text{Eqn E3})$$

where the diameter  $D \geq 1$  for all three distributions.

Parameters in Eqns E1, E2 and E3 were obtained with maximum likelihood method (MLE) for each community. While analytical solutions exist for parameters in Eqn E1 and Eqn E2, MLE solutions for parameters in Eqn E3 can only be obtained numerically. The three distributions of  $D$  were then transformed into distributions of  $D^2$  (surrogate for metabolic rate; see Methods) to be consistent with METE's prediction (Eqn 8) as:

182 
$$g(D^2) = \frac{1}{2D} f(D) \quad (\text{Eqn E4})$$

183 where  $f(D)$  is the left-truncated exponential, Pareto, or Weibull distribution in Eqns E1, E2 or  
 184 E3.

185 The fit of the ISD predicted by METE and the other three distributions was evaluated  
 186 with Akaike’s Information Criterion (AIC; Burnham and Anderson 2002).  $AIC_c$ , a second-order  
 187 variant of AIC which corrects for finite sample size, was computed for each distribution as

188 
$$AIC_c = 2k - 2 \ln(L) + \frac{2k(k+1)}{n-k-1} \quad (\text{Eqn E5})$$

189 where  $k$  is the number of parameters in the corresponding distribution,  $n$  is the number of  
 190 individuals in the community, and  $L$  is the likelihood of the distribution across all individuals  
 191 (Burnham and Anderson 2002). Within a community, the distribution with a lower  $AIC_c$  value  
 192 provides a better fit.

193 Our results show that overall the Weibull distribution provides the best fit for the ISD,  
 194 which outperforms the other three distributions (i.e., has the smallest  $AIC_c$  value) in 50 out of 60  
 195 communities. While METE is exceeded by the Weibull distribution in all except 3 communities,  
 196 its performance is comparable to that of the other two distributions, with METE outperforming  
 197 the exponential distribution in 24 communities and the Pareto distribution in 33 (Table E1).

198 **Table E1.** The  $AIC_c$  value of the four distributions of ISD across communities. The distribution  
 199 with the best fit (lowest  $AIC_c$  value) for each community is in red.

Dataset	Site	$AIC_c$ -exponential	$AIC_c$ -Pareto	$AIC_c$ -Weibull	$AIC_c$ -METE
FERP	FERP	85971.15	82823.11	<b>81893.76</b>	88390.74
ACA	eno-2	3047.892	3123.951	<b>3037.737</b>	3048.544
WesternGhats	BSP104	8447.378	8232.82	<b>8147.375</b>	8597.933
WesternGhats	BSP11	9670.786	9737.739	<b>9565.319</b>	9756.008

WesternGhats	BSP12	8072.348	7580.985	<b>7580.105</b>	8005.097
WesternGhats	BSP16	6505.854	6465.984	<b>6371.536</b>	6473.227
WesternGhats	BSP27	4158.854	4352.934	<b>4154.657</b>	4168.587
WesternGhats	BSP29	5200.085	5601.832	<b>5186.167</b>	5246.872
WesternGhats	BSP30	<b>5228.032</b>	5550.478	5229.22	5272.148
WesternGhats	BSP36	5363.257	4997.568	<b>4994.507</b>	5613.485
WesternGhats	BSP37	6648.723	<b>5882.951</b>	5940.894	6702.201
WesternGhats	BSP42	4862.353	4579.541	<b>4572.774</b>	4912.597
WesternGhats	BSP5	6316.684	<b>5868.932</b>	5879.056	6344.512
WesternGhats	BSP6	8362.132	8224.467	<b>8144.515</b>	8368.706
WesternGhats	BSP65	10730.14	10597.32	10418.12	<b>10323.55</b>
WesternGhats	BSP66	6127.039	6078.716	<b>5969.159</b>	6118.758
WesternGhats	BSP67	5733.979	6116.641	<b>5713.447</b>	5970.901
WesternGhats	BSP69	9639.039	9839.743	<b>9566.506</b>	9677.272
WesternGhats	BSP70	7568.366	7643.62	7475.877	<b>7471.337</b>
WesternGhats	BSP73	<b>13866.8</b>	14638.34	13867.97	14056.6
WesternGhats	BSP74	10384.88	10164.99	<b>10043.66</b>	10178.07
WesternGhats	BSP75	<b>3828.718</b>	4032.776	3830.225	3844.366
WesternGhats	BSP79	10012.15	10192.38	<b>9943.069</b>	10014.63
WesternGhats	BSP80	10351.04	10721.97	<b>10333.53</b>	10392.1
WesternGhats	BSP82	7775.241	8109.038	<b>7766.727</b>	7779.842
WesternGhats	BSP83	<b>10080.84</b>	10603.67	10082.84	10184.62
WesternGhats	BSP84	9941.77	10676.22	<b>9906.56</b>	10087.81
WesternGhats	BSP85	4090.759	4051.023	<b>3986.417</b>	4092.965

WesternGhats	BSP88	9539.878	10007.25	9532.9	<b>9468.538</b>
WesternGhats	BSP89	7758.469	8040.773	<b>7746.257</b>	7749.632
WesternGhats	BSP90	7802.77	8287.765	<b>7800.707</b>	7891.673
WesternGhats	BSP91	8443.673	9081.623	<b>8392.871</b>	8709.277
WesternGhats	BSP92	5010.321	5156.128	<b>4980.47</b>	5037.136
WesternGhats	BSP94	4995.435	5113.566	<b>4949.09</b>	4997.738
WesternGhats	BSP98	6338.305	6535.699	<b>6312.535</b>	6336.033
WesternGhats	BSP99	8329.191	8461.831	<b>8238.427</b>	8268.363
BCI	bci	1663761	1595835	<b>1580094</b>	1616953
BVSF	BVPlot	2801.075	2851.043	<b>2790.895</b>	2792.688
BVSF	SFPlot	2452.828	2427.723	<b>2409.388</b>	2413.466
Cocoli	cocoli	73752.32	68152.93	<b>67835.59</b>	75938.32
Lahei	heath1	9947.228	9966.227	<b>9841.178</b>	9888.052
Lahei	heath2	9795.598	9650.197	<b>9595.179</b>	9618.001
Lahei	peat	9183.332	9040.189	<b>8961.699</b>	9030.188
LaSelva	1	5518.14	5434.672	<b>5376.494</b>	5555.8
LaSelva	2	5504.011	5548.332	<b>5444.005</b>	5489.366
LaSelva	3	6337.174	6328.63	<b>6237.519</b>	6294.73
LaSelva	4	5445.745	5527.303	<b>5402.815</b>	5409.85
LaSelva	5	4410.166	4318.777	<b>4281.463</b>	4440.427
Luquillo	lfdp	534427.2	515126.9	<b>509926.5</b>	525725.7
NC	12	45716.48	44860.83	<b>44212.08</b>	45592.31
NC	13	36251.18	34948.55	<b>34539.55</b>	36220.19
NC	14	56695.06	52506.98	<b>52273.61</b>	55964.15

NC	4	36203.17	36553.64	<b>35587.05</b>	36447.78
NC	93	34667.37	33277.48	<b>32934.38</b>	34730.18
Oosting	Oosting	74293.18	69837.5	<b>69718.9</b>	74739.21
Serimbu	S-1	7887.232	7471.463	<b>7463.06</b>	7981.97
Serimbu	S-2	8507.118	8123.406	<b>8102.843</b>	8614.922
Shirakami	Akaishizawa	3105.173	3104.759	<b>3057.59</b>	3188.967
Shirakami	Kumagera	<b>3473.692</b>	3680.852	3473.805	3597.692
Sherman	sherman	191735.8	188206	<b>185424</b>	190339.9

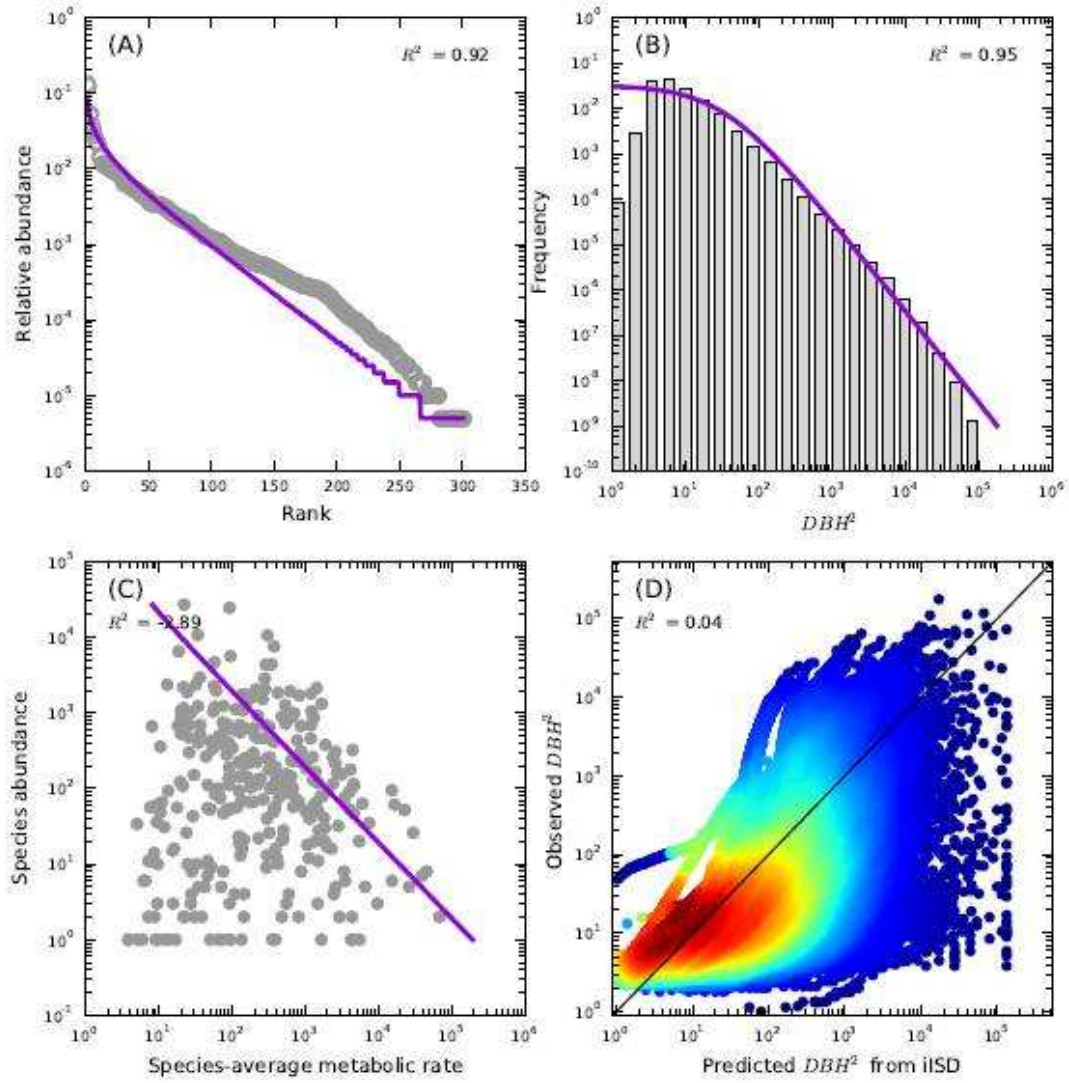


200 **References**

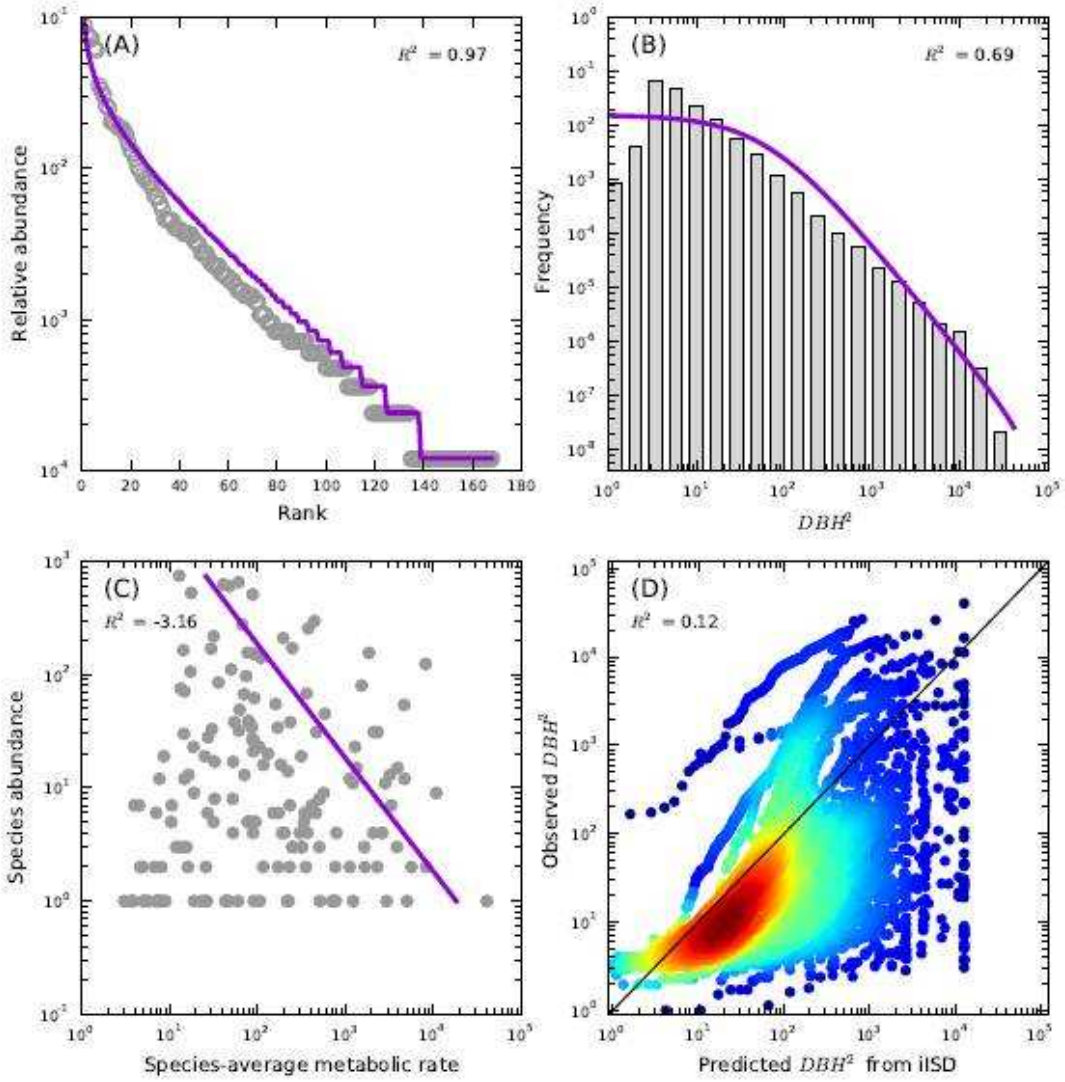
- 201 Burnham, K. P., and D. R. Anderson. 2002. Model selection and multimodel inference: a  
202 practical information-theoretic approach. Springer-Verlag, New York, New York, USA.
- 203 Chave, J., C. Andalo, S. Brown, M. a Cairns, J. Q. Chambers, D. Eamus, H. Fölster, et al. 2005.  
204 Tree allometry and improved estimation of carbon stocks and balance in tropical forests.  
205 *Oecologia* 145:87–99.
- 206 Chave, J., D. Coomes, S. Jansen, S. L. Lewis, N. G. Swenson, and A. E. Zanne. 2009. Towards a  
207 worldwide wood economics spectrum. *Ecology Letters* 12:351–366.
- 208 Harte, J. 2011. Maximum entropy and ecology: a theory of abundance, distribution, and  
209 energetics. Oxford University Press.
- 210 Harte, J., T. Zillio, E. Conlisk, and A. B. Smith. 2008. Maximum entropy and the state-variable  
211 approach to macroecology. *Ecology* 89:2700–2711.
- 212 Mori, S., K. Yamaji, A. Ishida, S. G. Prokushkin, O. V Masyagina, A. Hagihara, a T. M. R.  
213 Hoque, et al. 2010. Mixed-power scaling of whole-plant respiration from seedlings to giant trees.  
214 *Proceedings of the National Academy of Sciences of the United States of America* 107:1447–  
215 1451.
- 216 Muller-Landau, H. C., R. S. Condit, K. E. Harms, C. O. Marks, S. C. Thomas, S.  
217 Bunyavejchewin, G. Chuyong, et al. 2006. Comparing tropical forest tree size distributions with  
218 the predictions of metabolic ecology and equilibrium models. *Ecology Letters* 9:589–602.
- 219 Reyes, G., S. Brown, J. Chapman, and A. E. Lugo. 1992. Wood densities of tropical tree species.  
220 Gen. Tech. Rep. SO-88. New Orleans, LA: U.S. Dept of Agriculture, Forest Service, Southern  
221 Forest Experiment Station.
- 222 Swenson, N. G., J. C. Stegen, S. J. Davies, D. L. Erickson, J. Forero-Montaña, A. H. Hurlbert,  
223 W. J. Kress, et al. 2012. Temporal turnover in the composition of tropical tree communities:  
224 functional determinism and phylogenetic stochasticity. *Ecology* 93:490–499.
- 225 White, E. P., K. M. Thibault, and X. Xiao. 2012. Characterizing species abundance distributions  
226 across taxa and ecosystems using a simple maximum entropy model. *Ecology* 93:1772–1778.
- 227 Wright, S. J., K. Kitajima, N. J. B. Kraft, P. B. Reich, I. J. Wright, D. E. Bunker, R. Condit, et al.  
228 2010. Functional traits and the growth–mortality trade-off in tropical trees. *Ecology* 91:3664–  
229 3674.
- 230 Zanne, A. E., G. Lopez-Gonzalez, D. A. Coomes, J. Ilic, S. Jansen, S. L. Lewis, R. B. Miller, et  
231 al. 2009. Data from: Towards a worldwide wood economics spectrum. *Ecology Letters*. Dryad  
232 Digital Repository.

Figure B1.

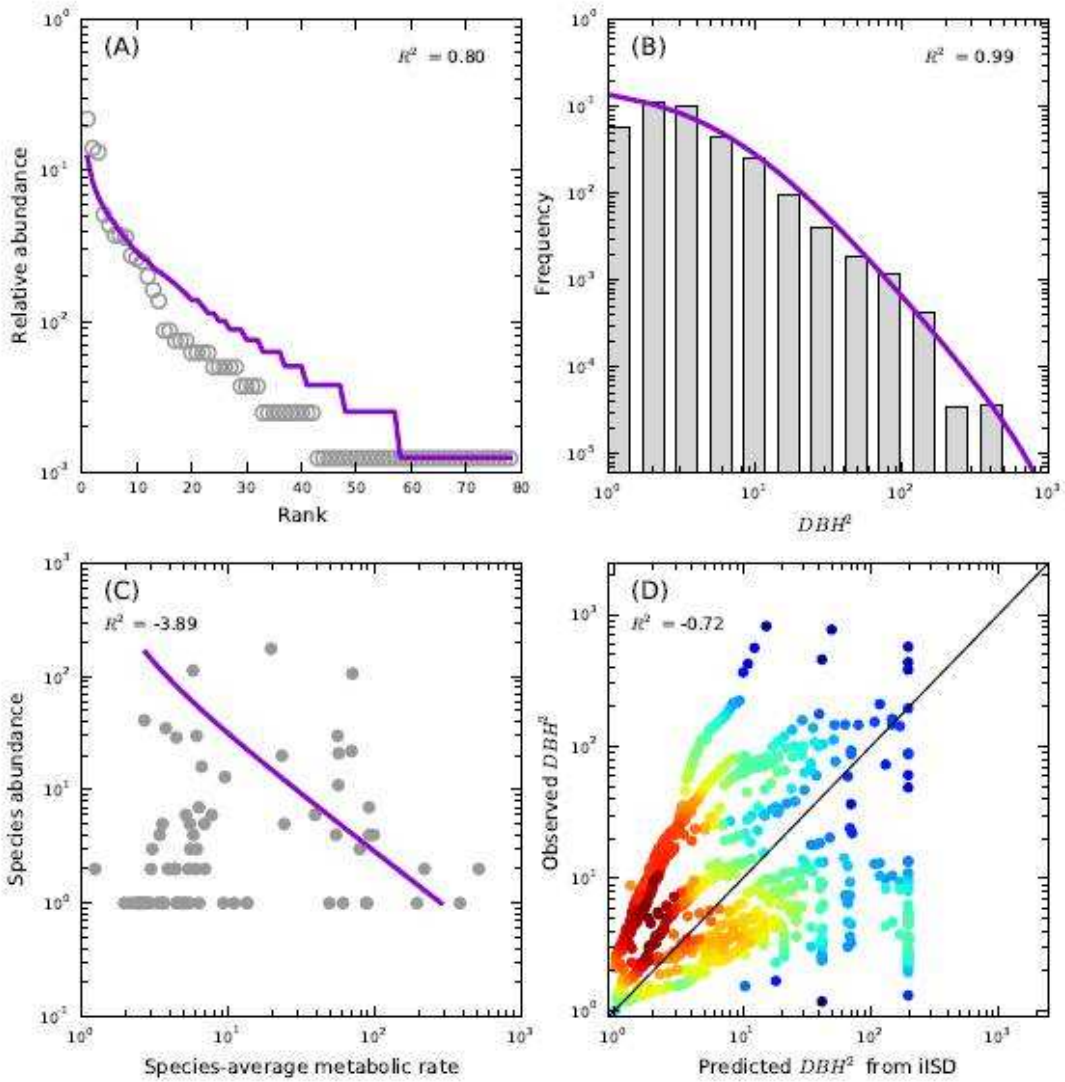
BCI\_alt,bci



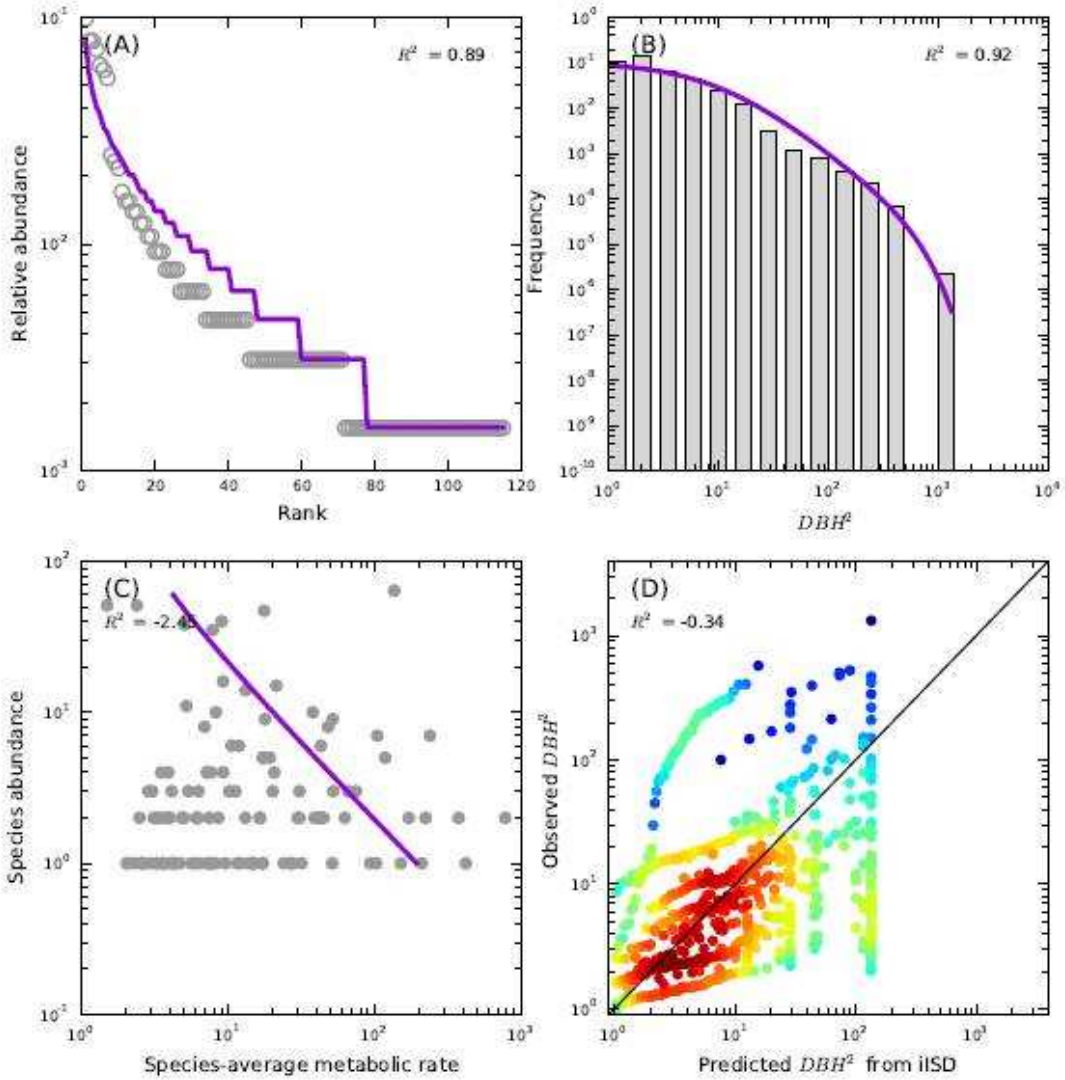
Cocoli\_alt,cocoli



LaSelva\_alt,4



LaSelva\_alt,5



Luquillo\_alt,lfdp

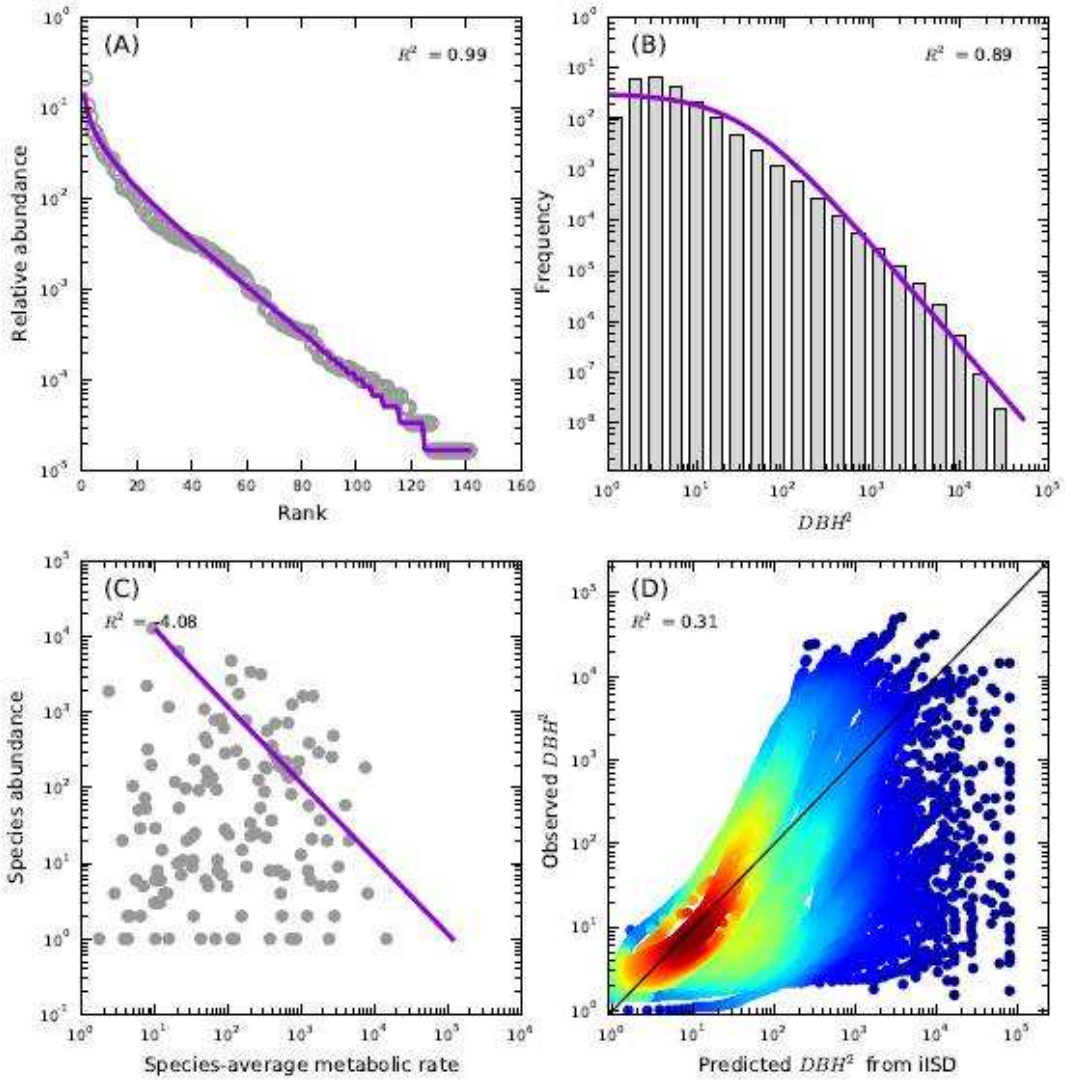
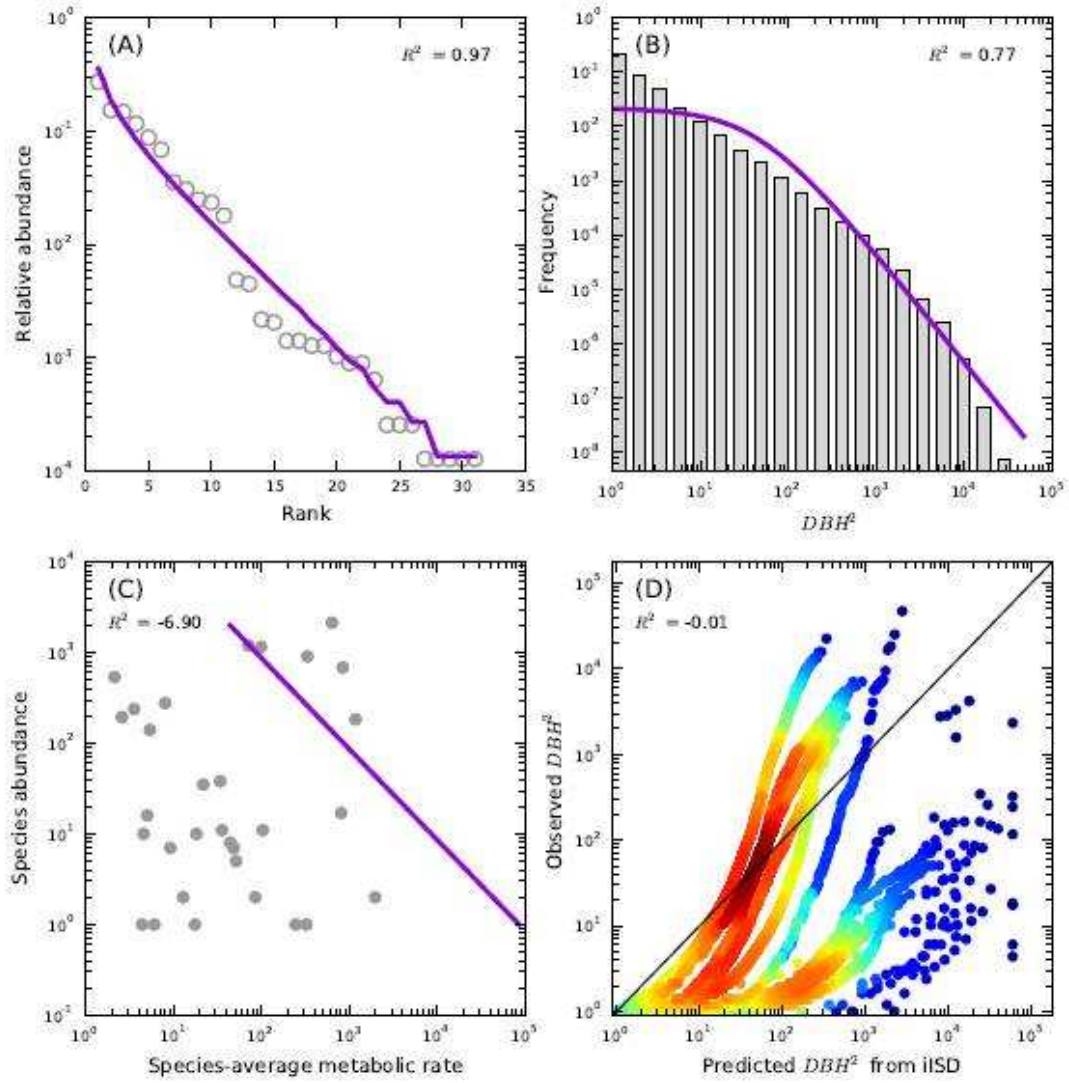
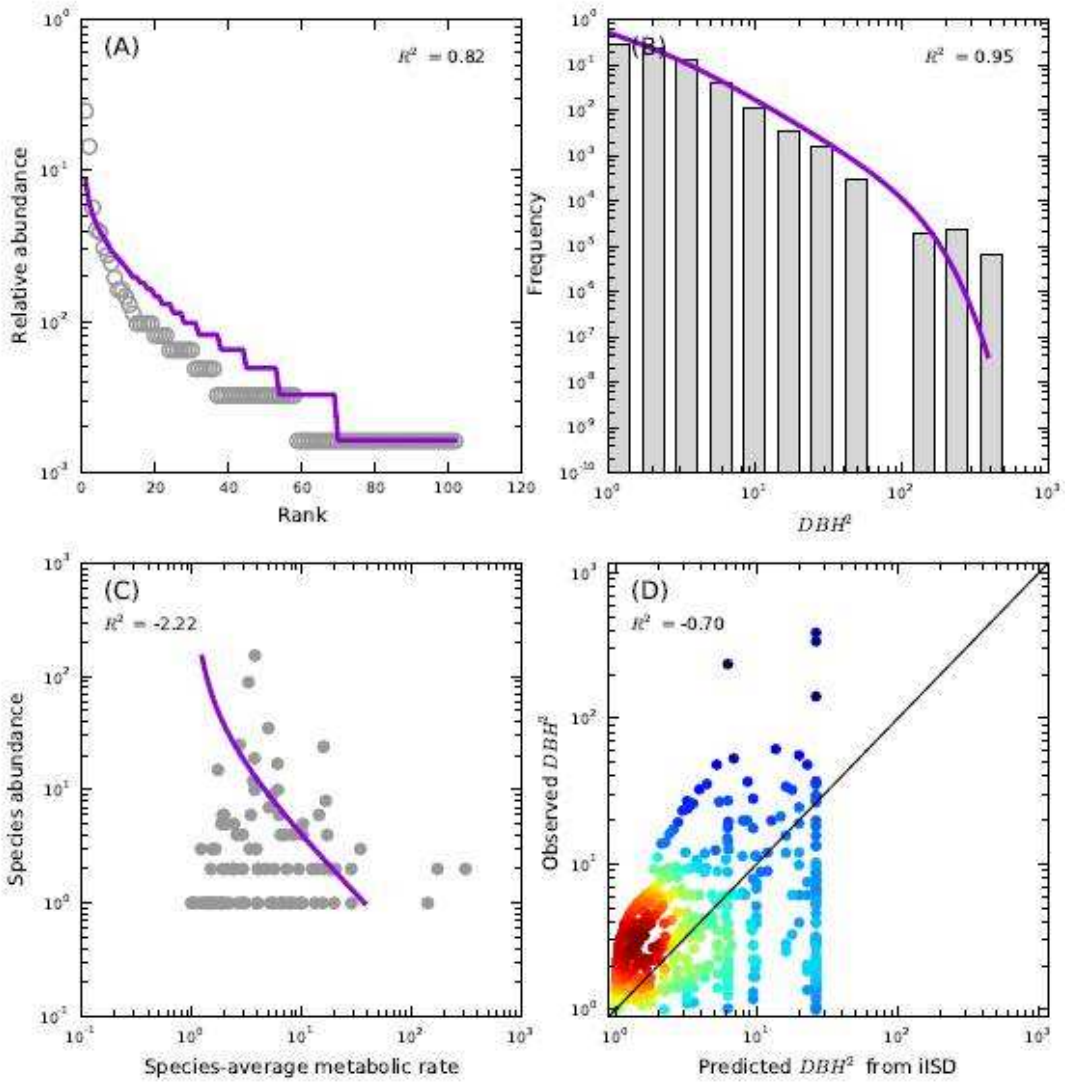


Figure D1.

FERP, FERP

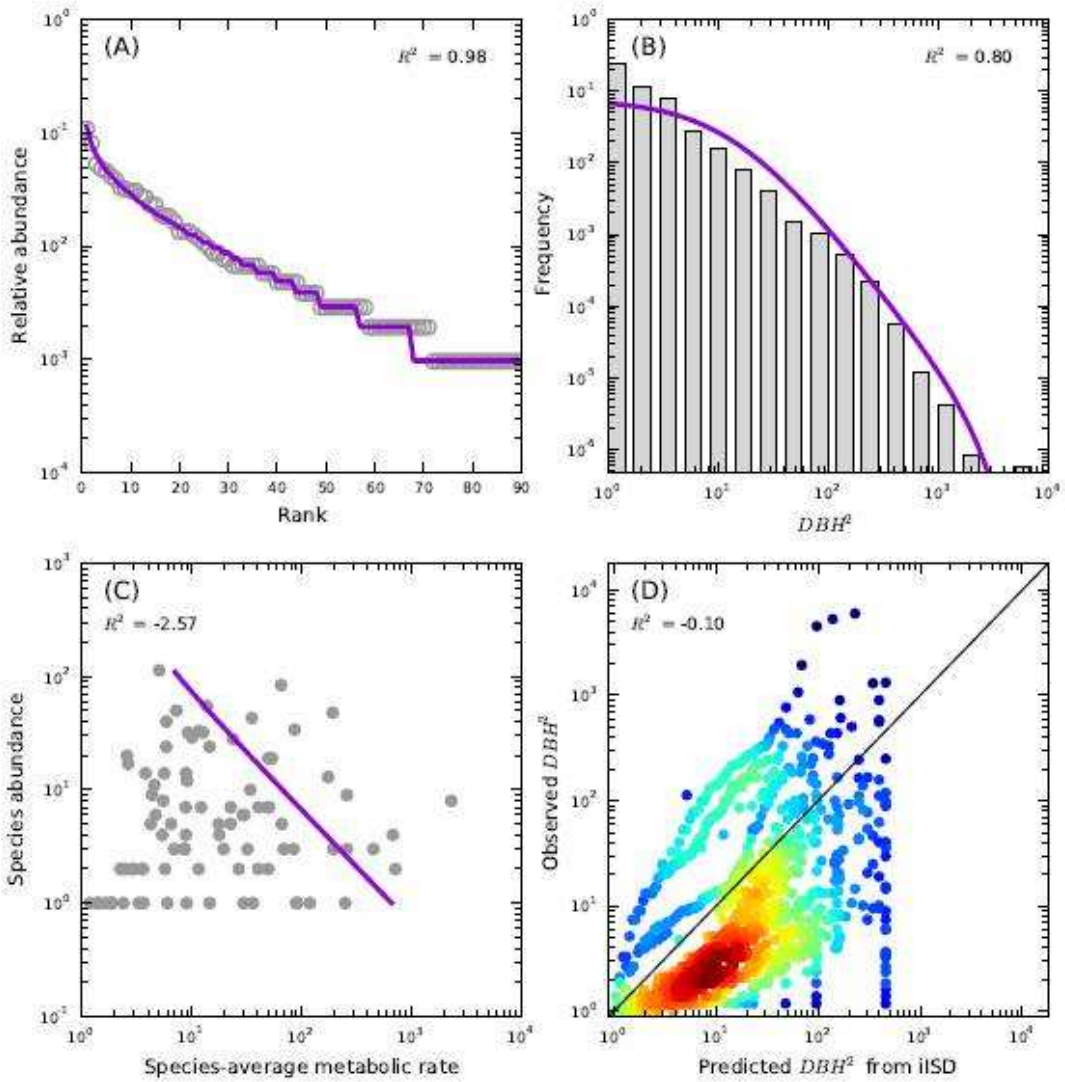


# ACA,eno-2

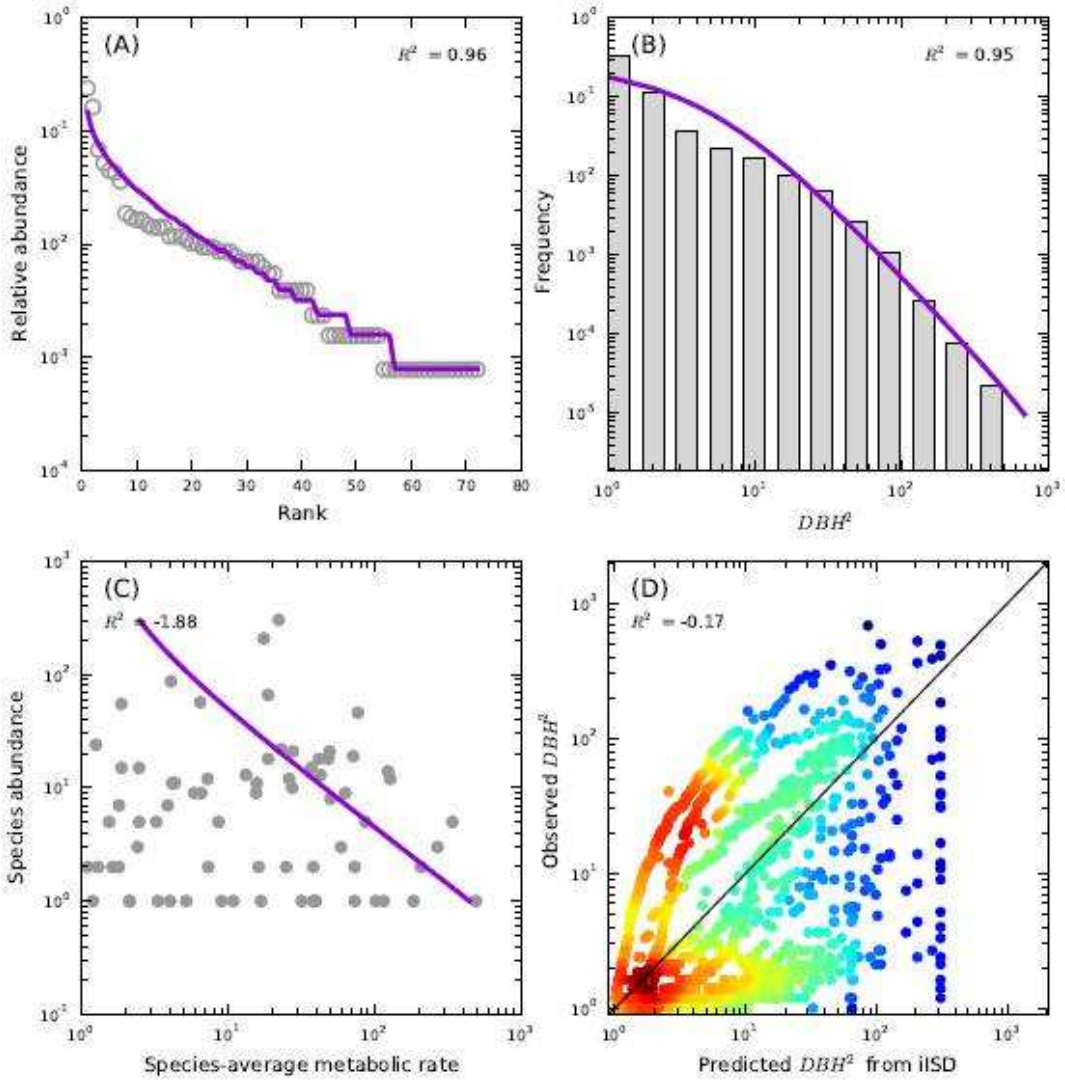




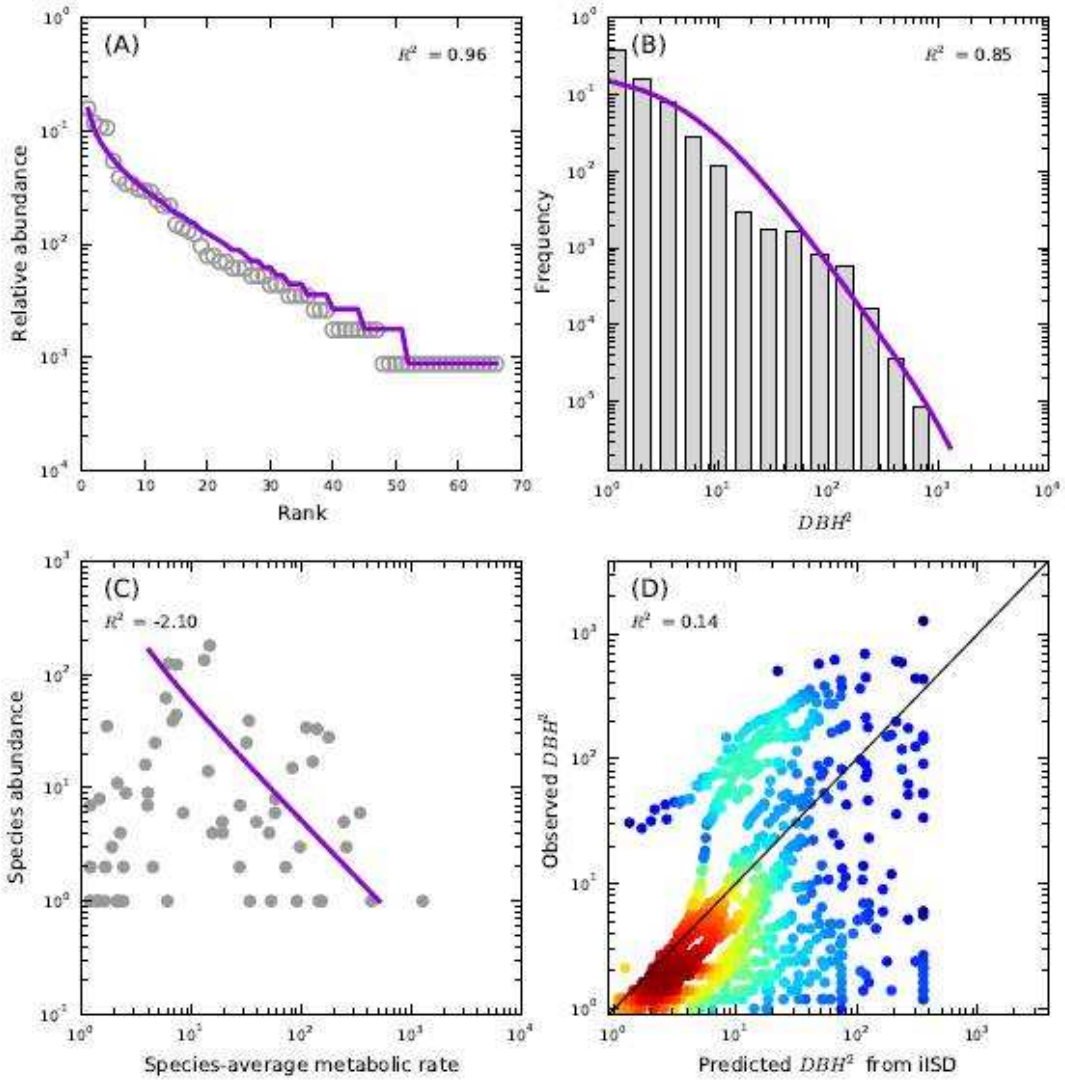
# WesternGhats,BSP104



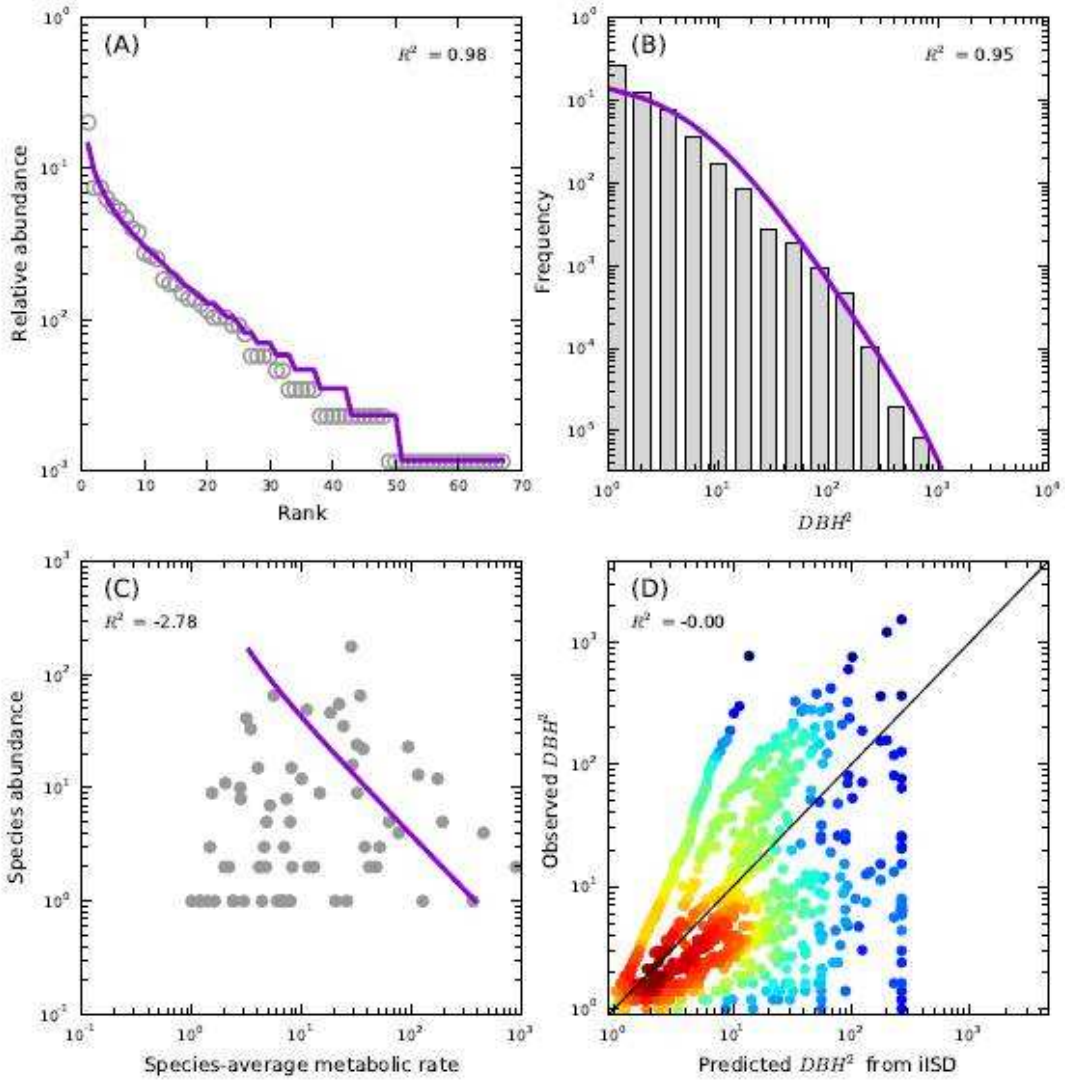
WesternGhats,BSP11



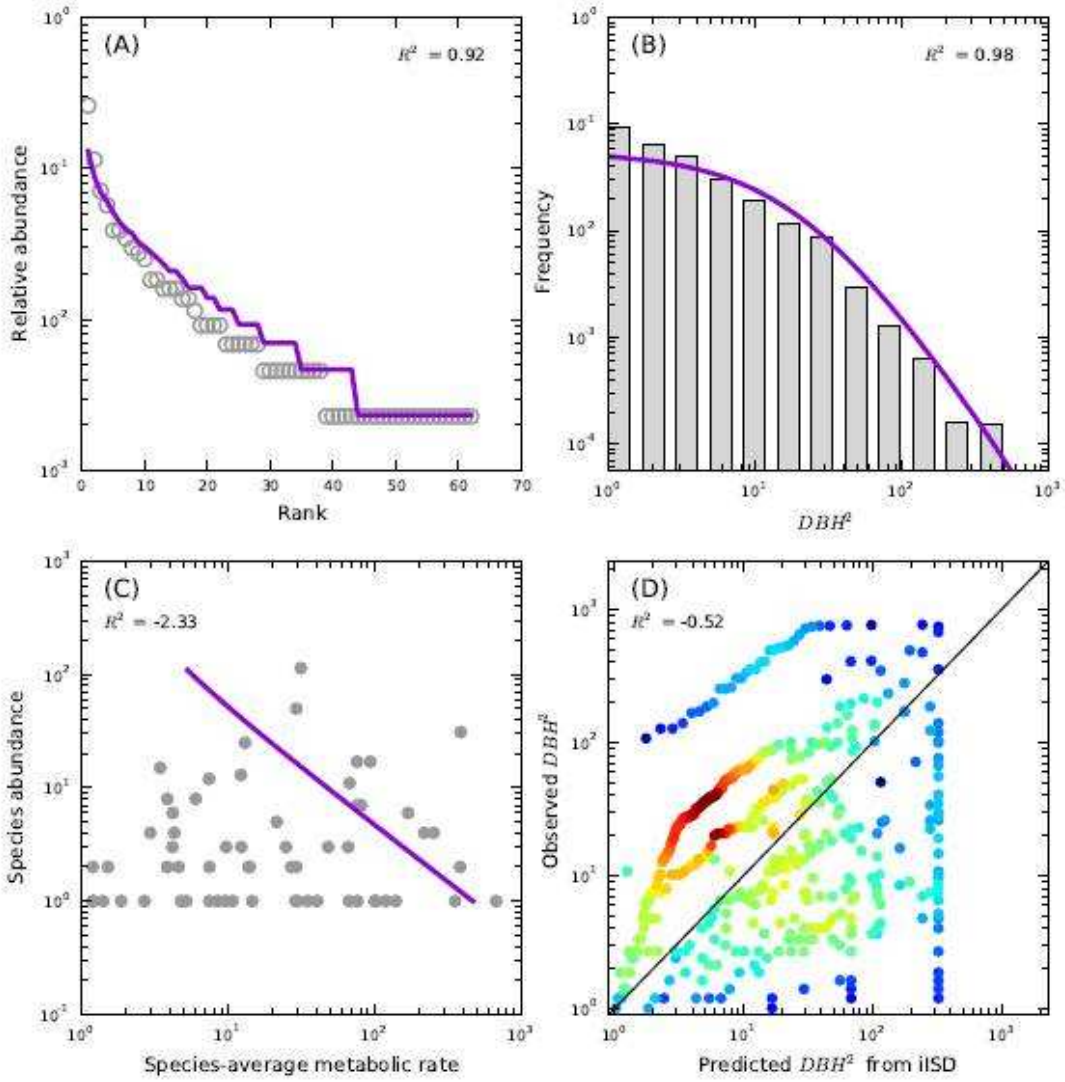
WesternGhats,BSP12



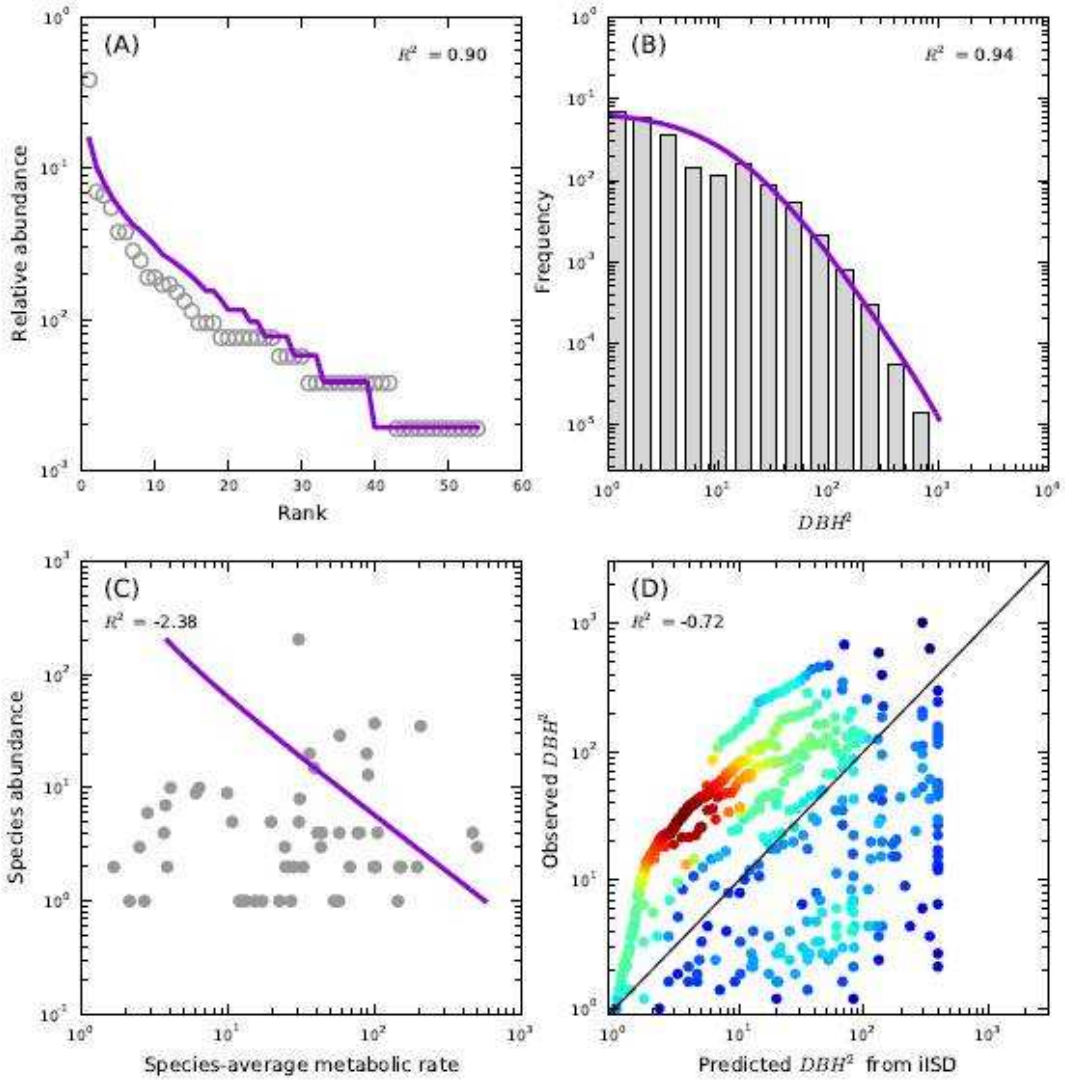
WesternGhats,BSP16



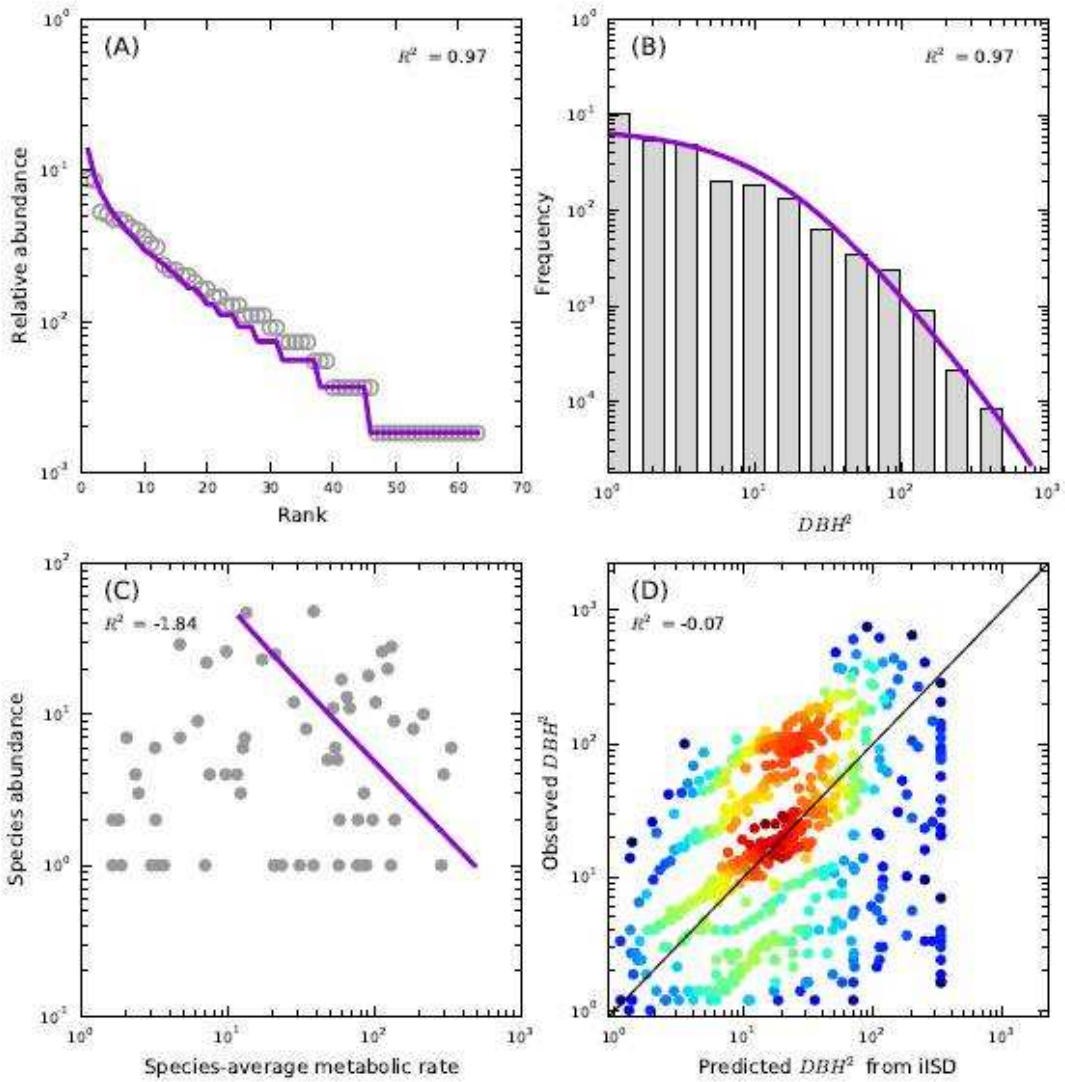
WesternGhats,BSP27



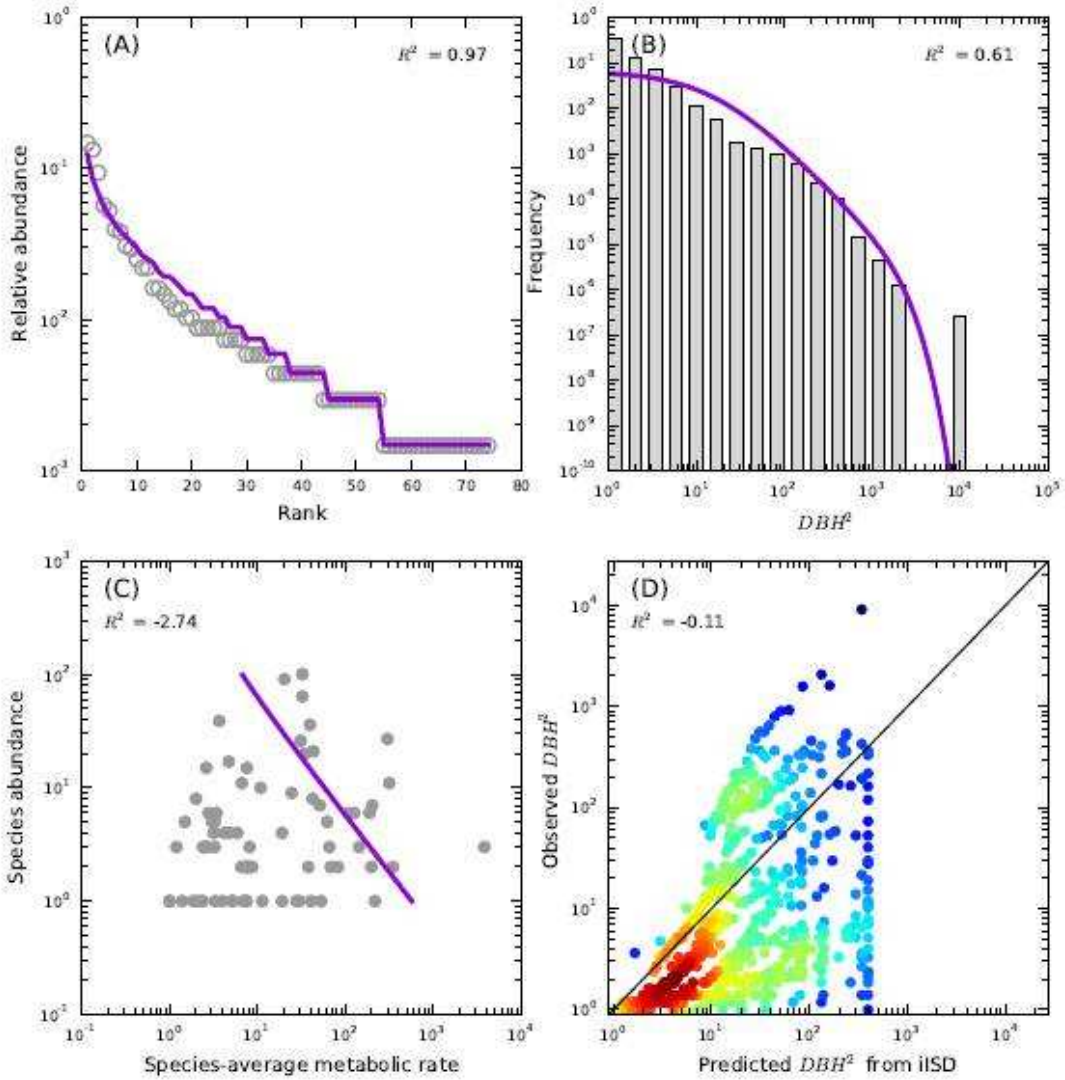
WesternGhats,BSP29



WesternGhats,BSP30

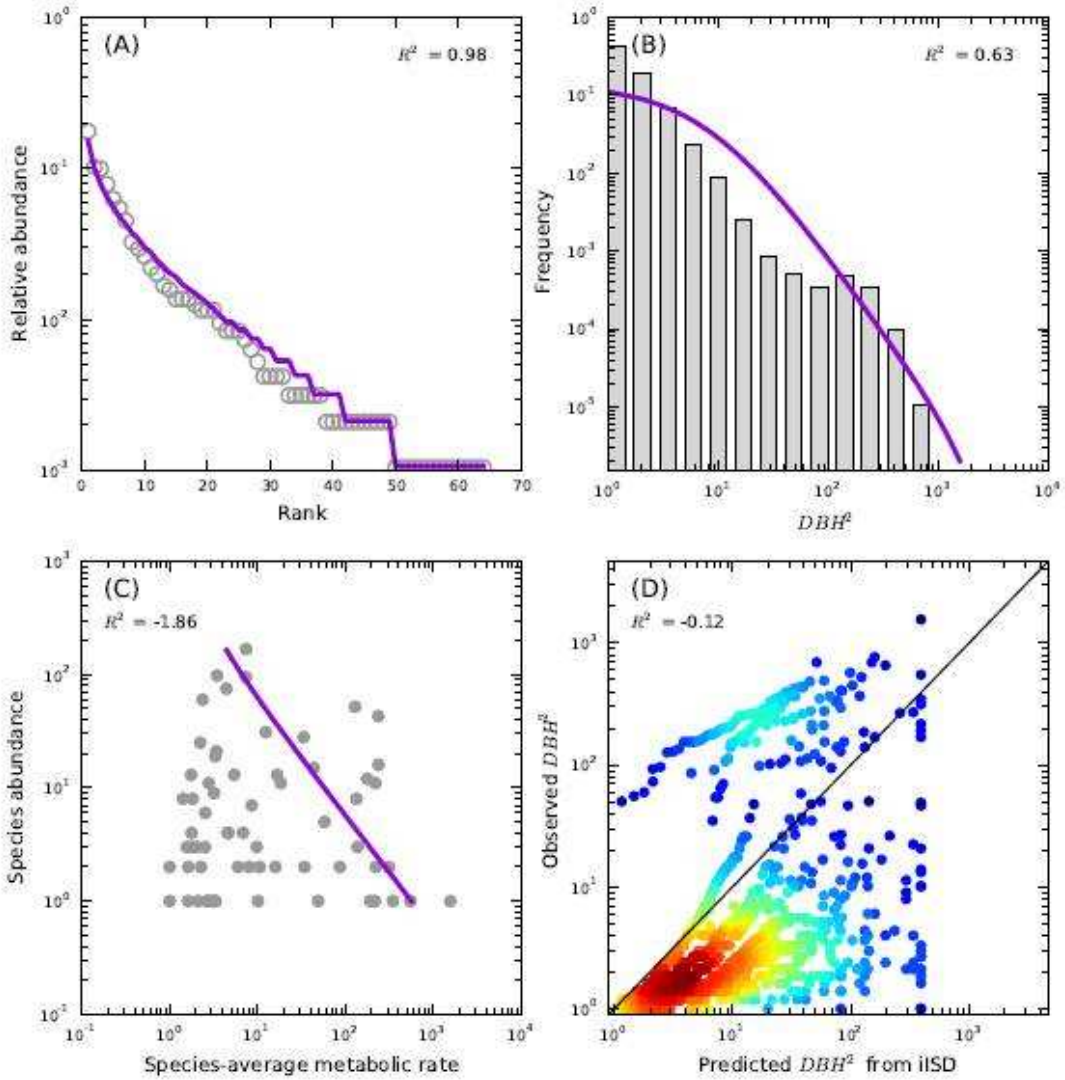


WesternGhats,BSP36

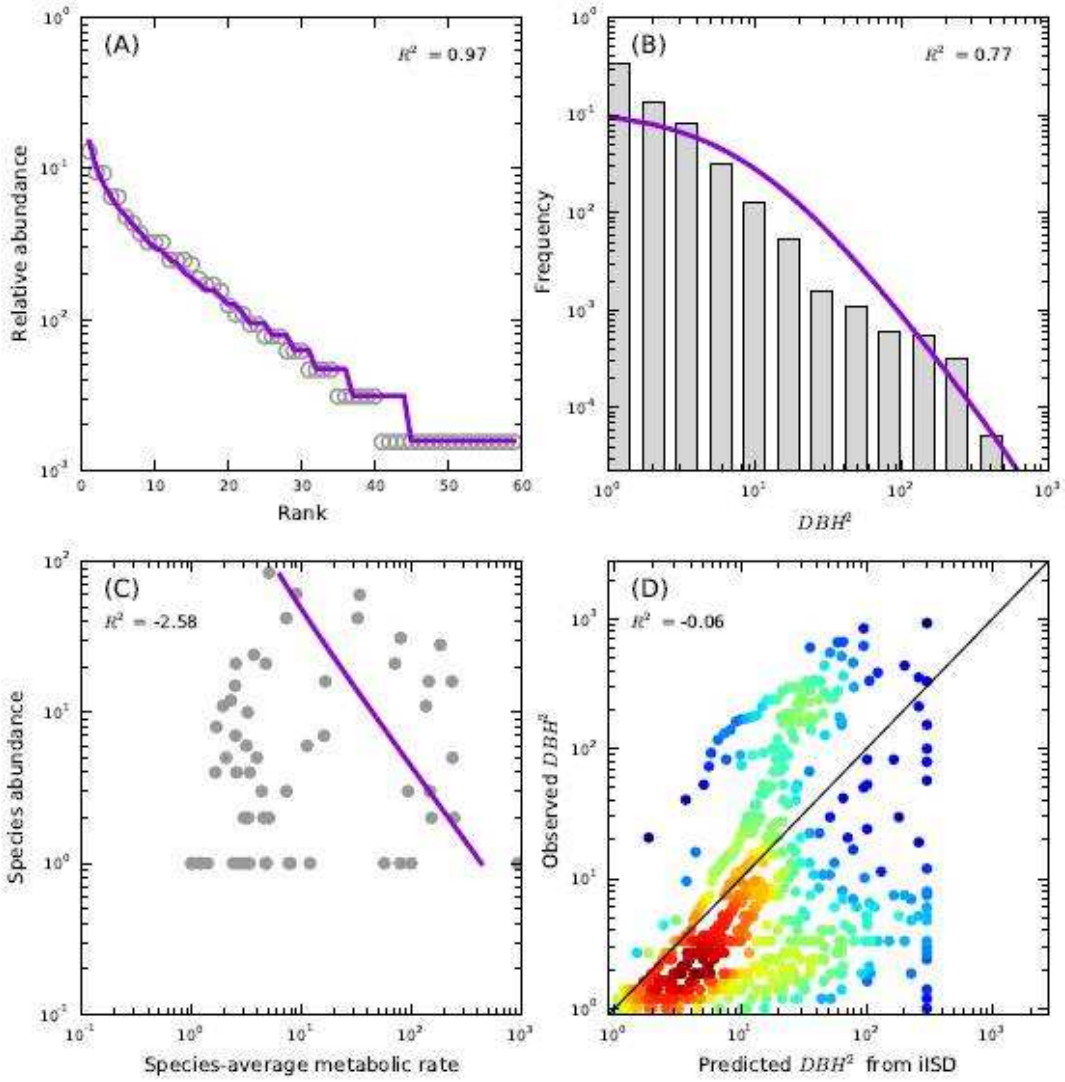




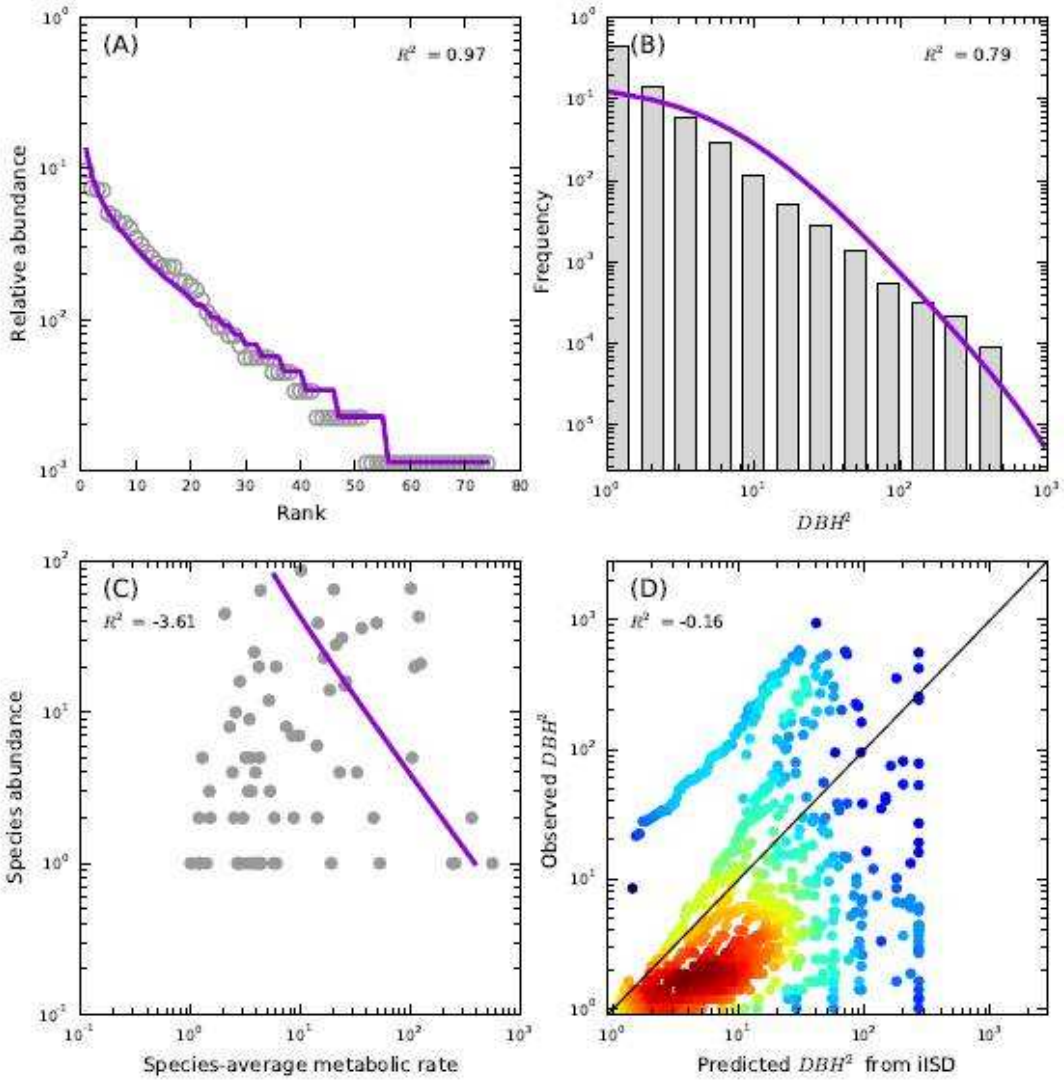
WesternGhats,BSP37



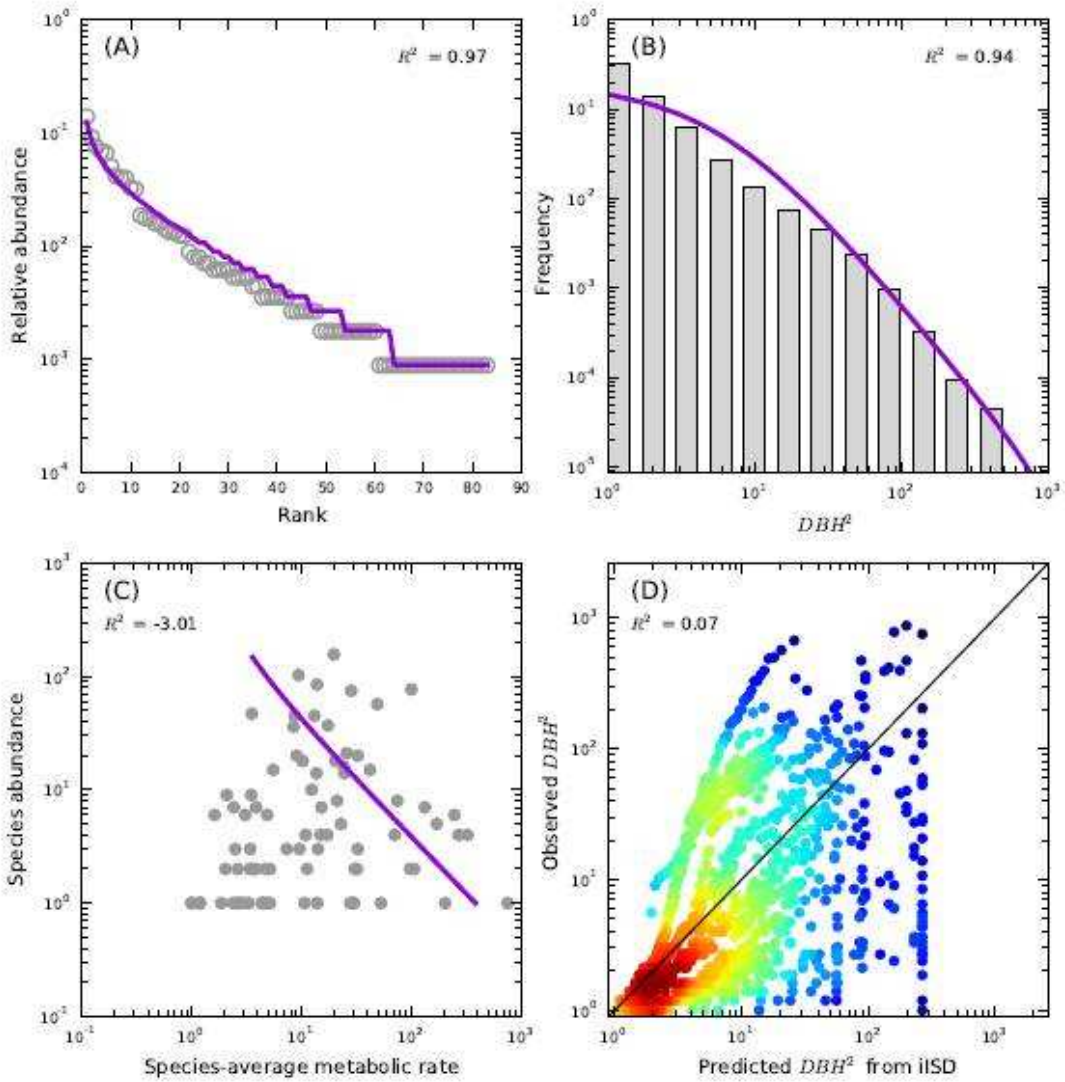
WesternGhats,BSP42



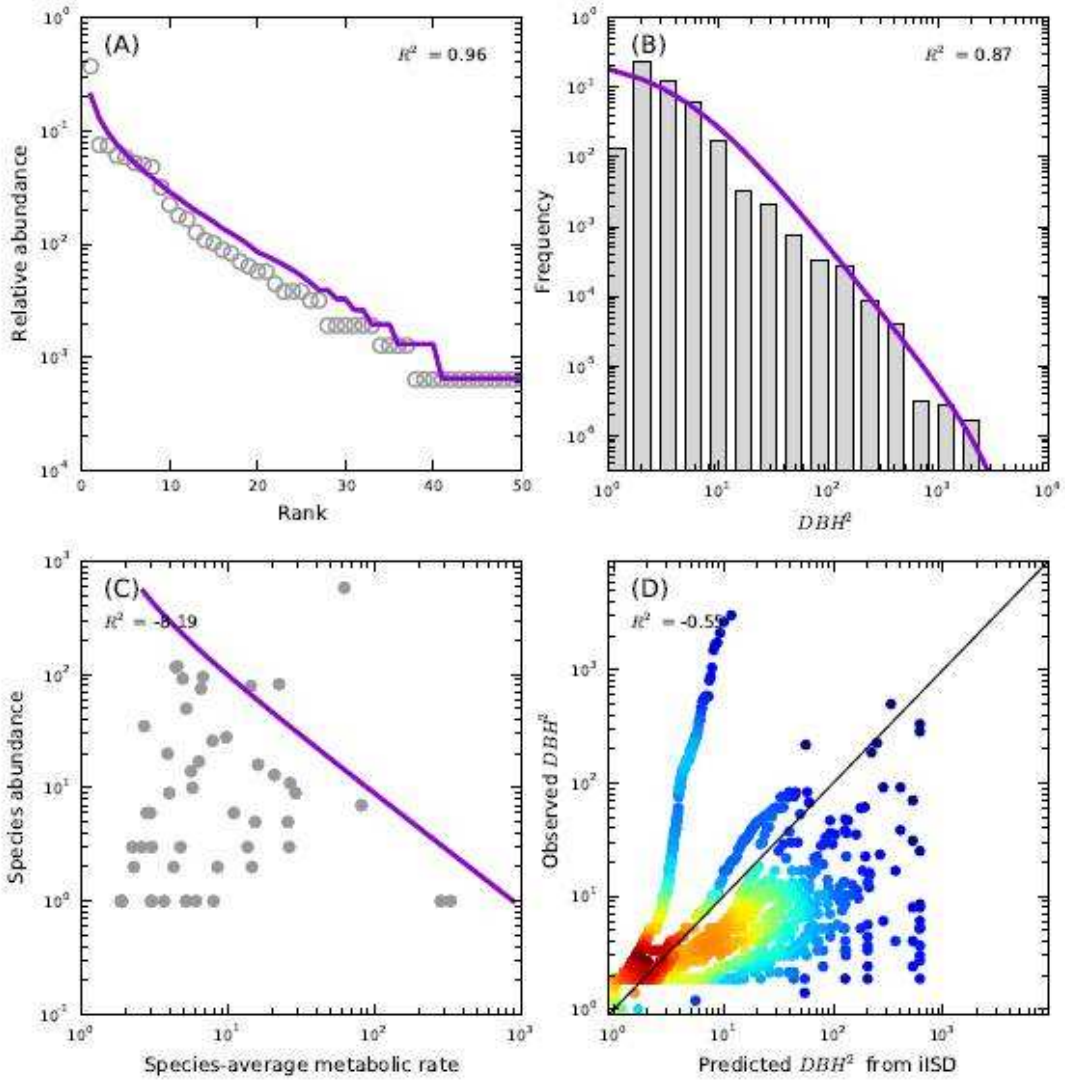
WesternGhats,BSP5



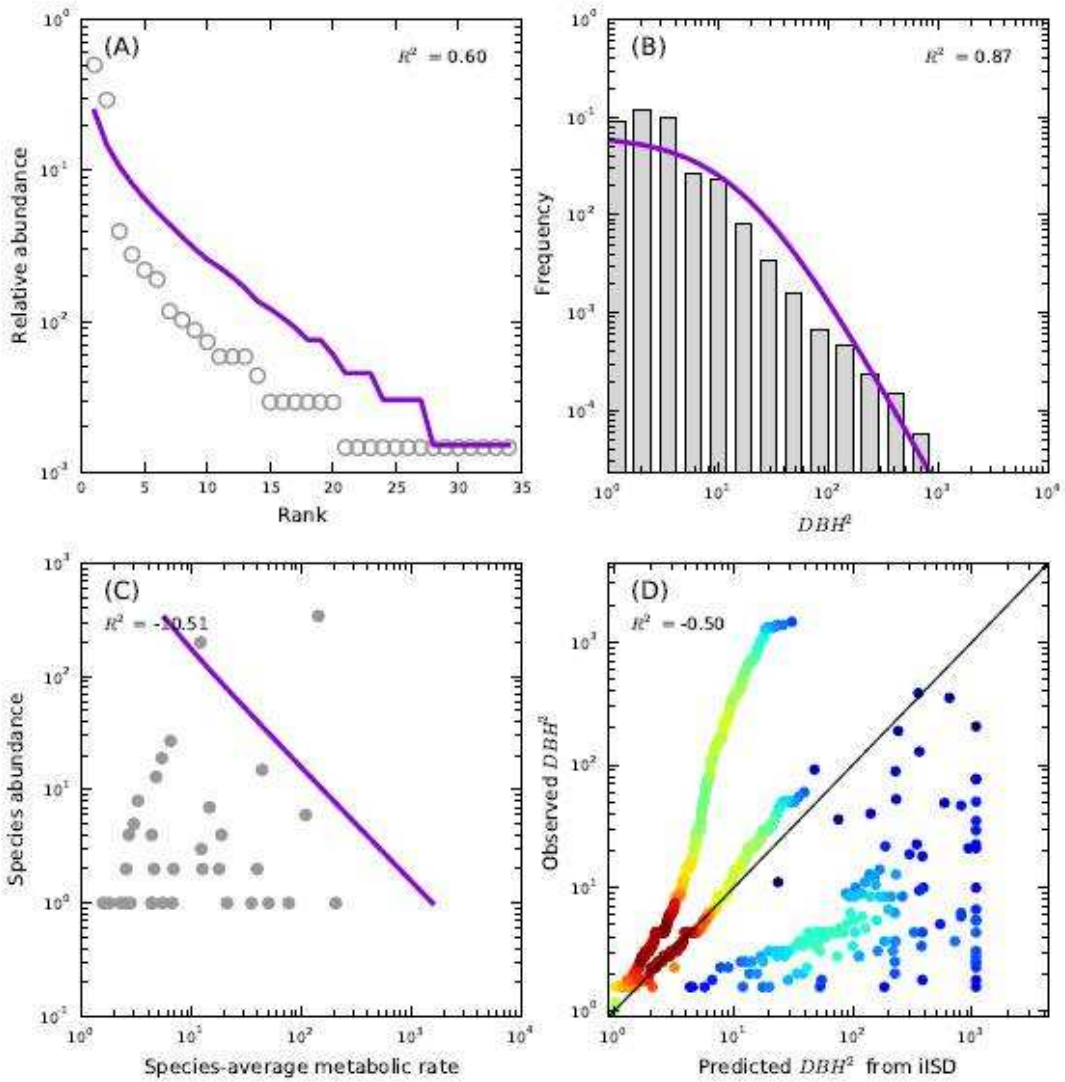
# WesternGhats,BSP6



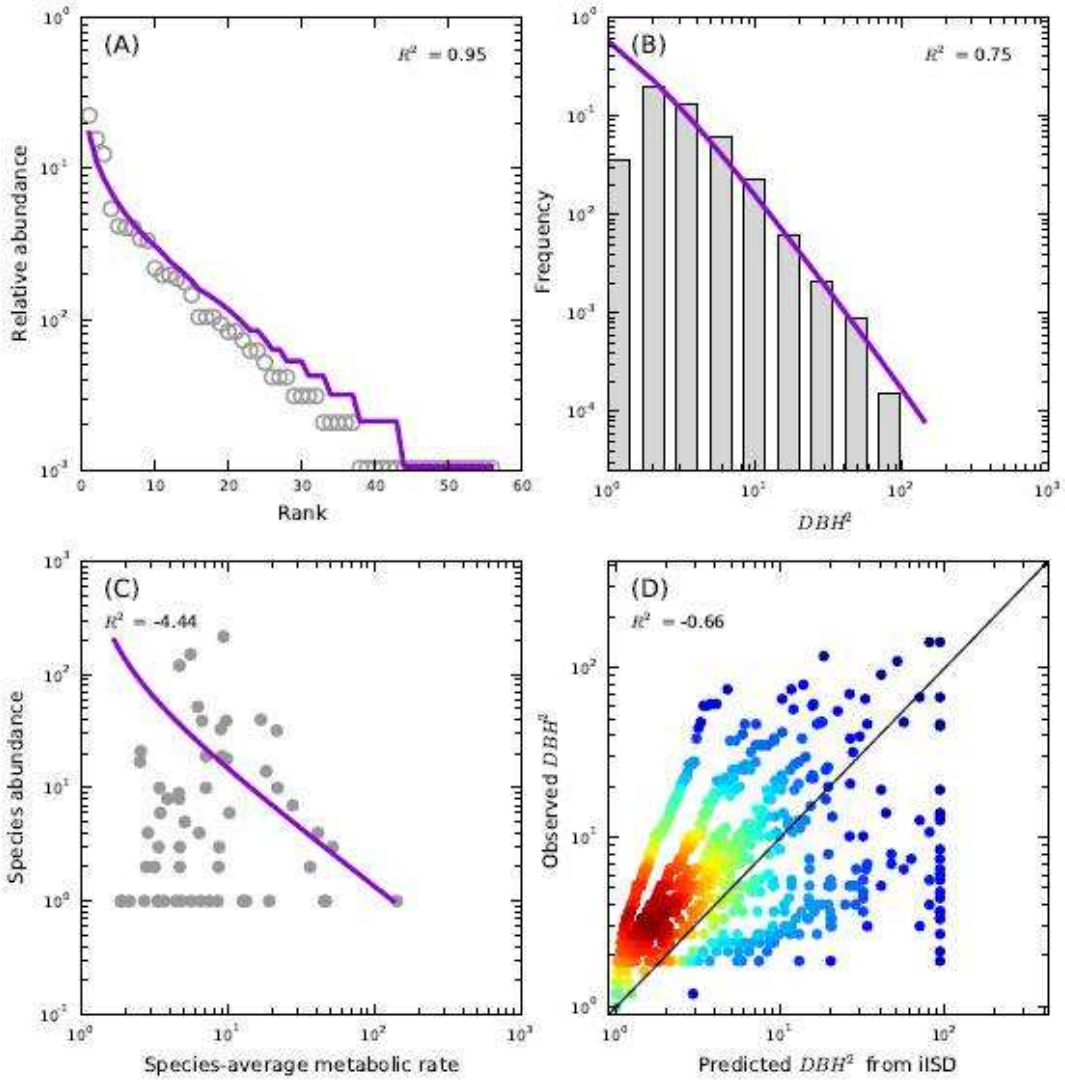
WesternGhats,BSP65



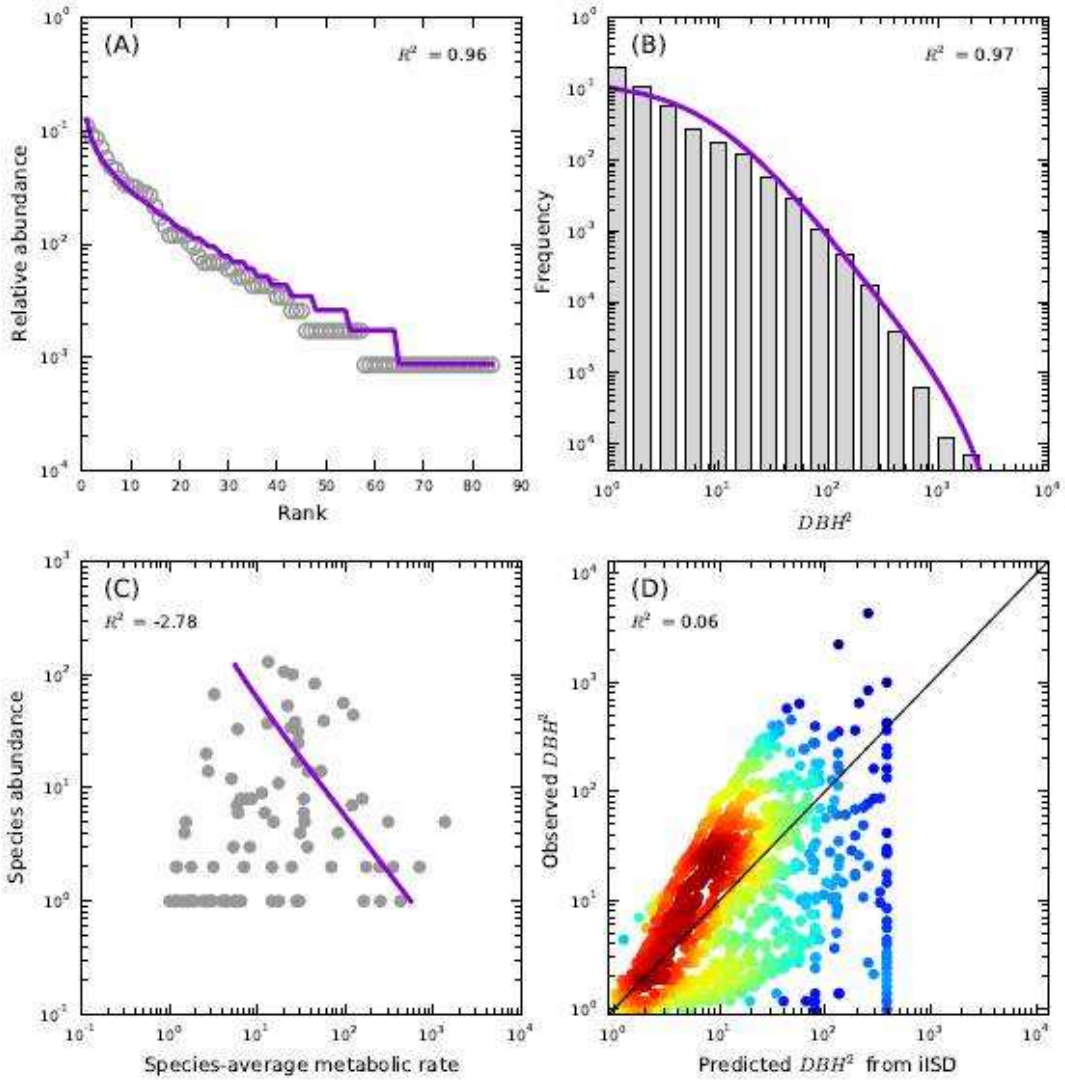
WesternGhats,BSP66



WesternGhats,BSP67

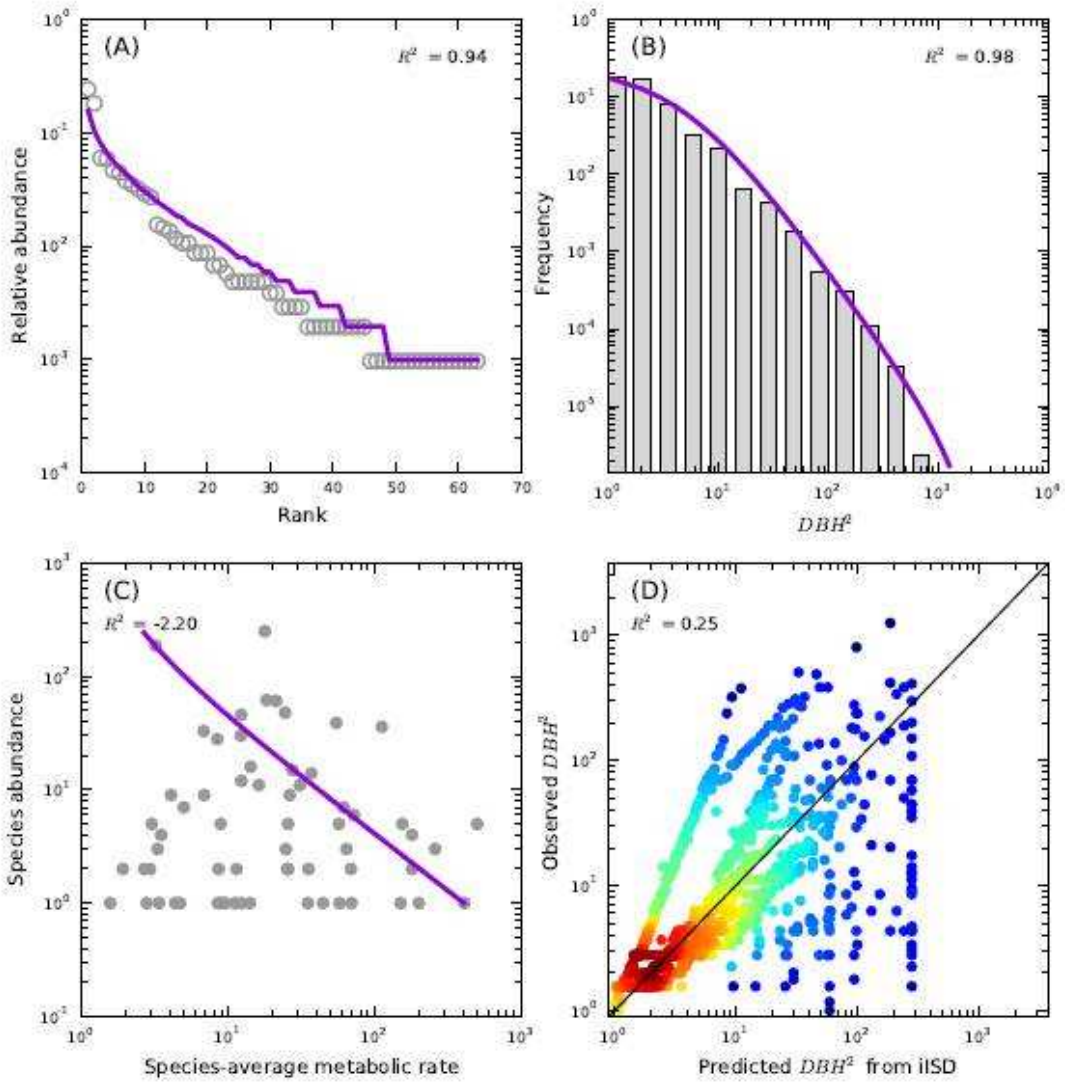


WesternGhats,BSP69

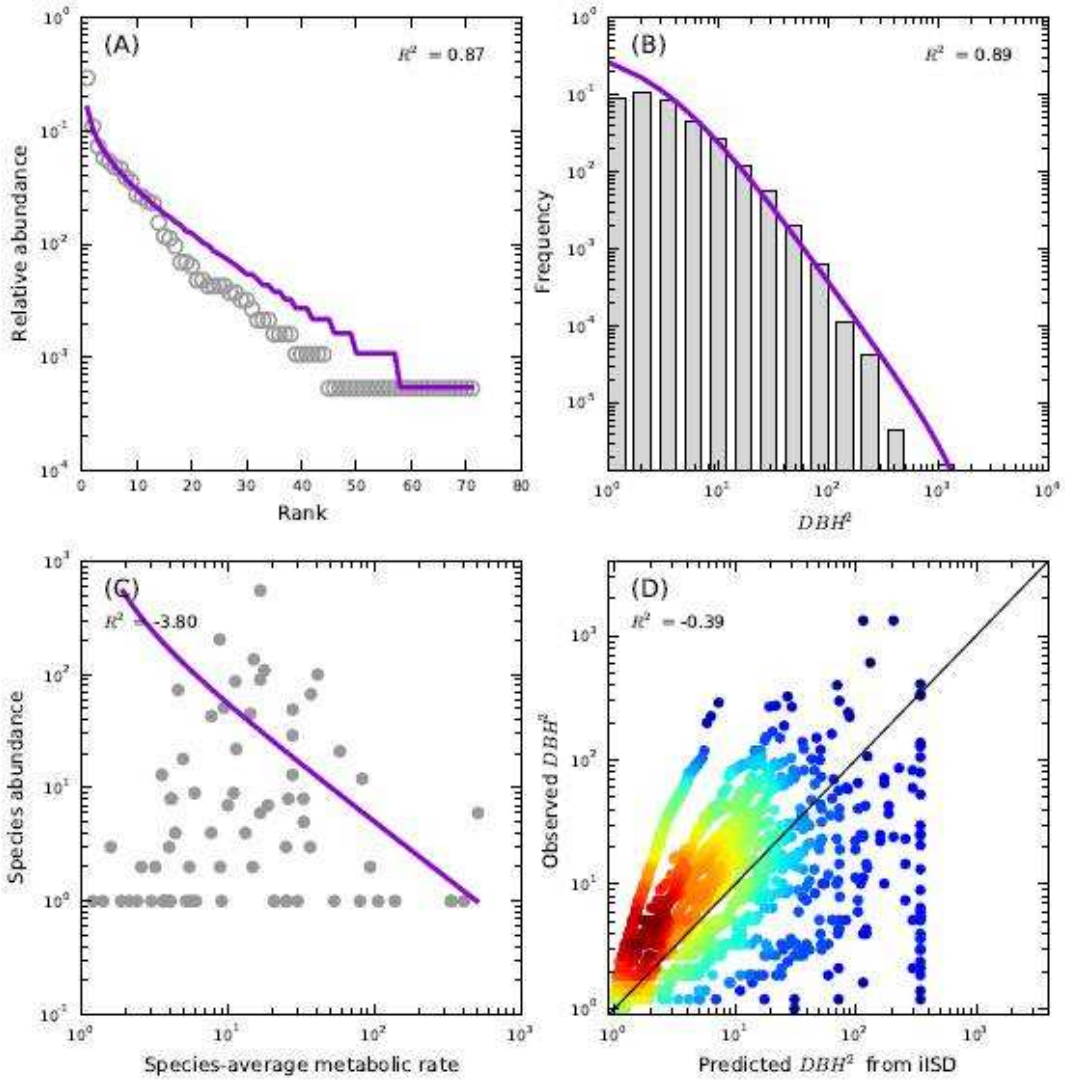




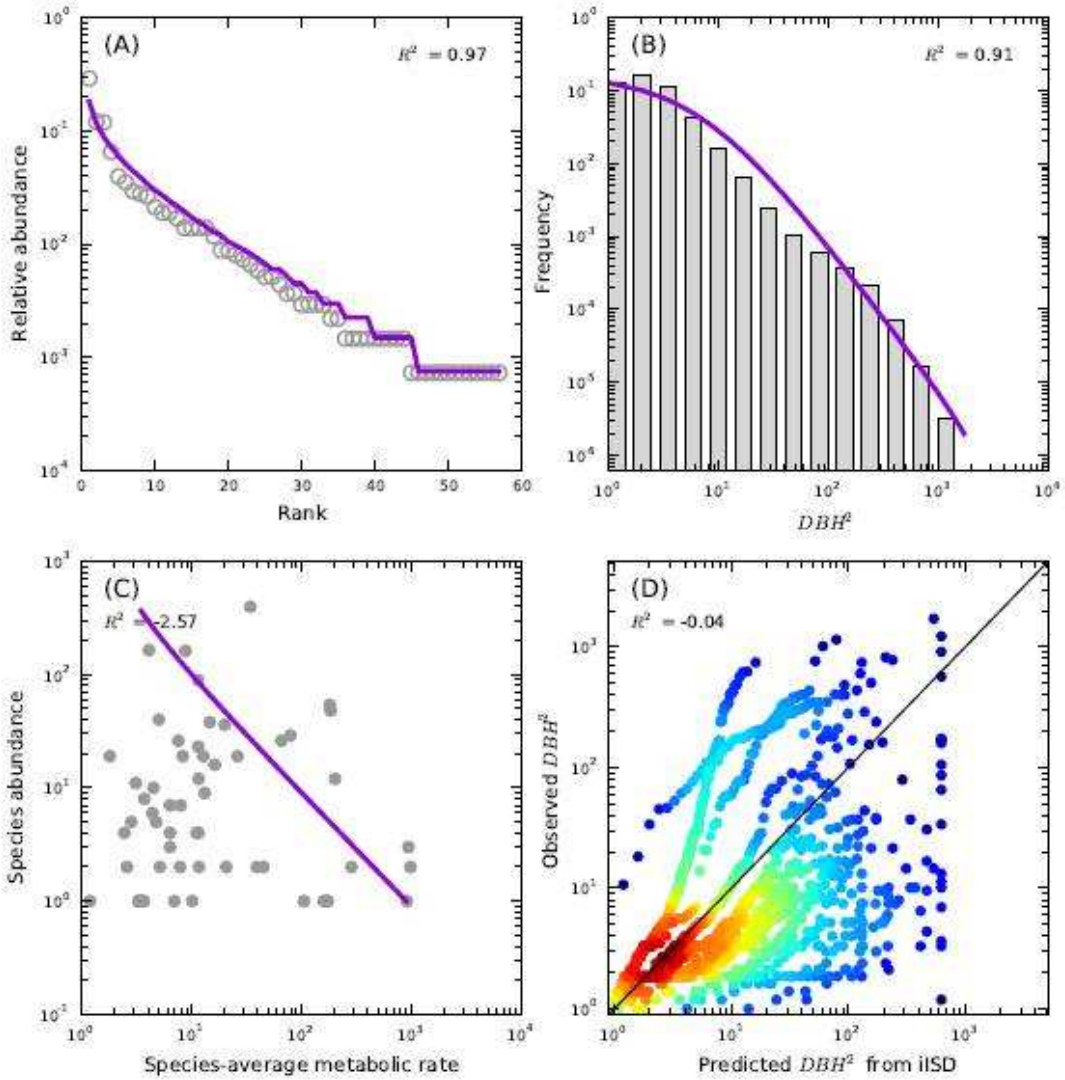
WesternGhats,BSP70



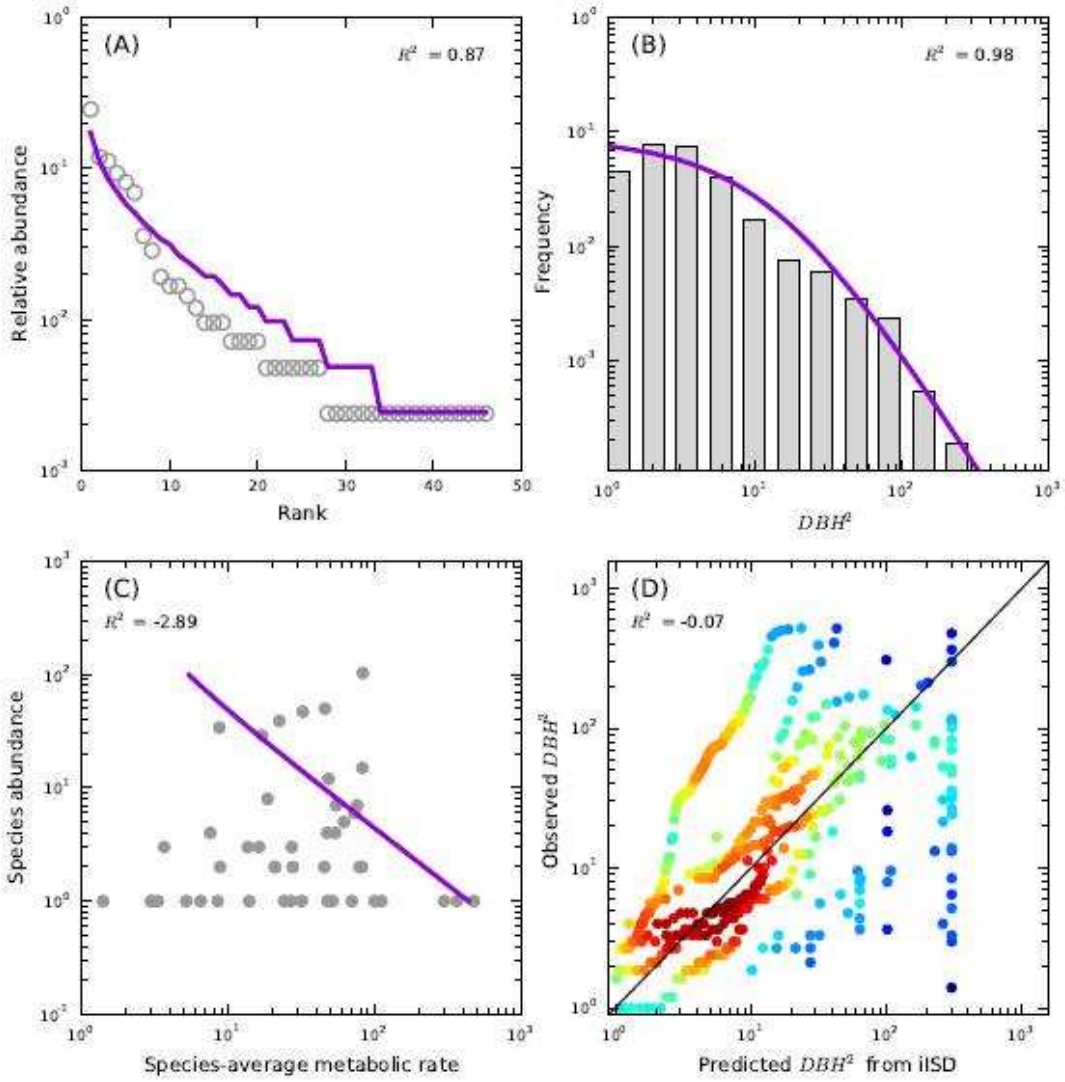
WesternGhats,BSP73



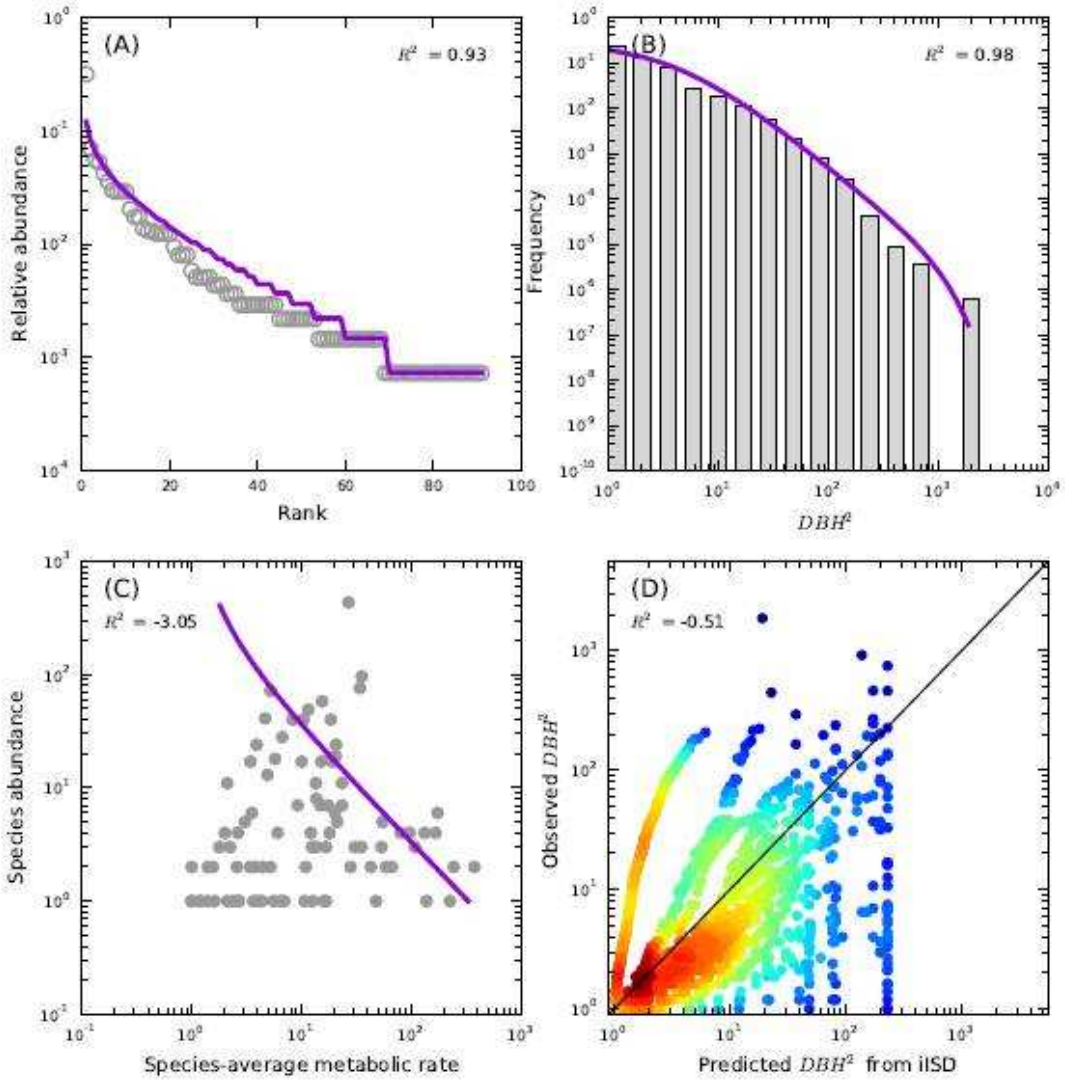
WesternGhats,BSP74



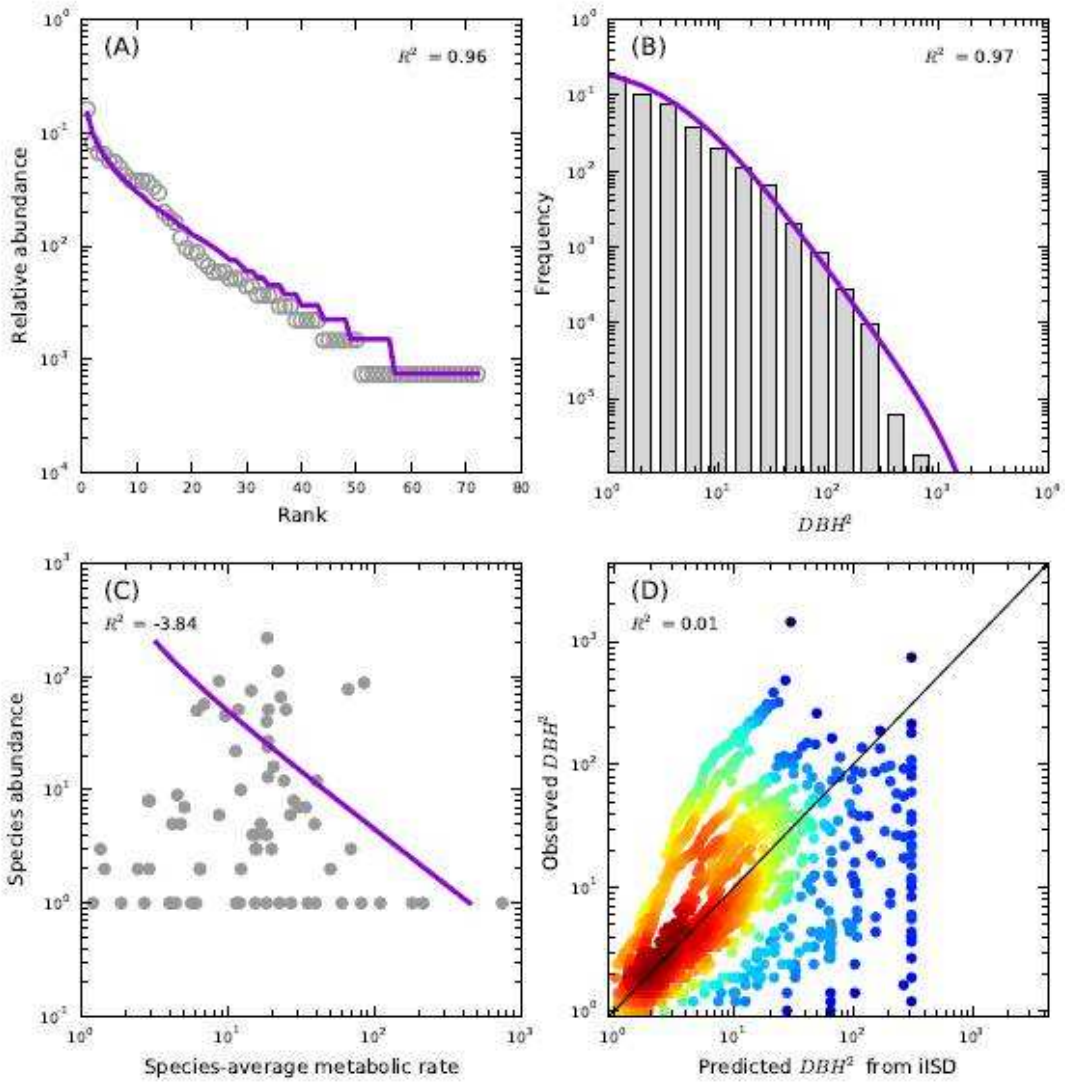
WesternGhats,BSP75



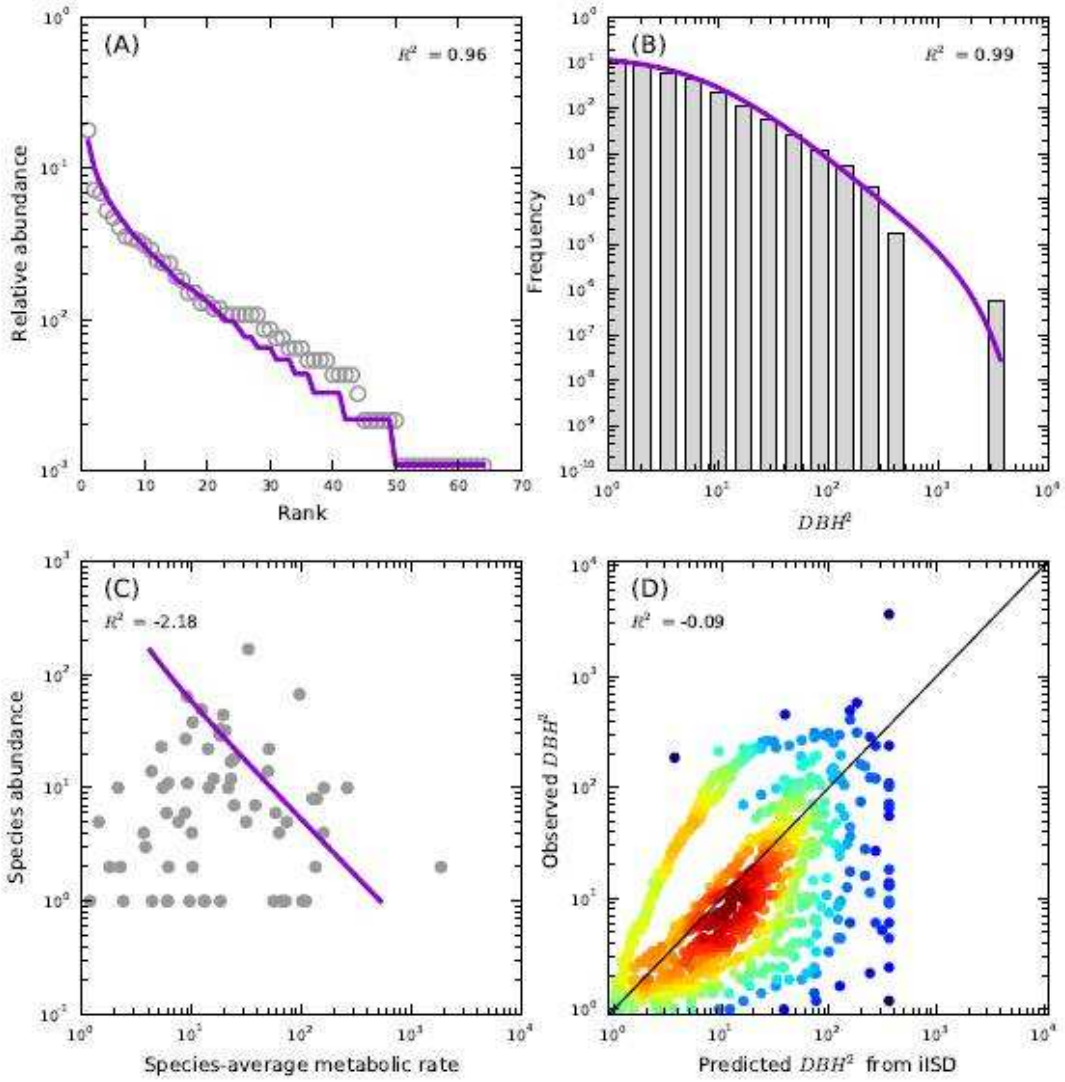
WesternGhats,BSP79



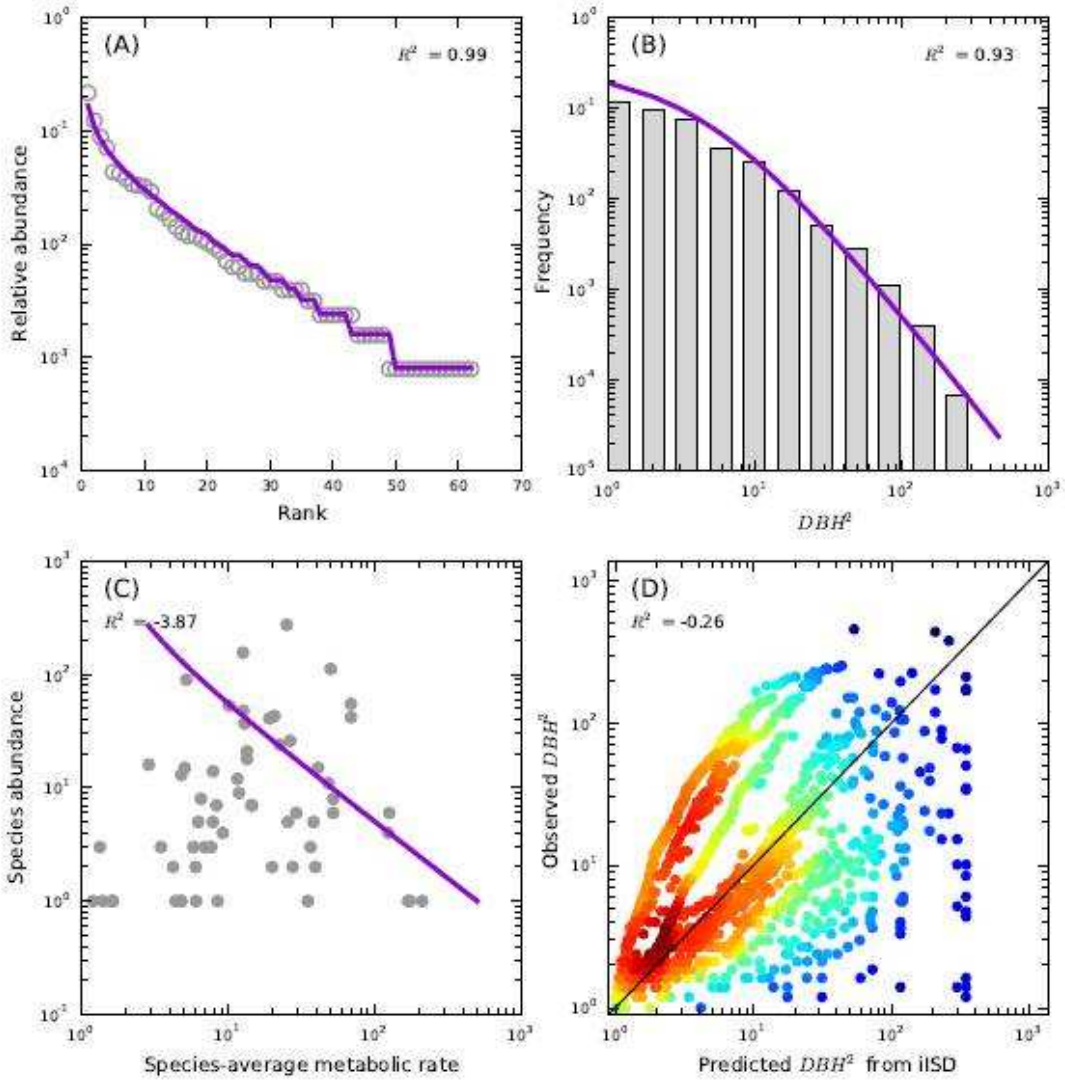
WesternGhats,BSP80



WesternGhats,BSP82

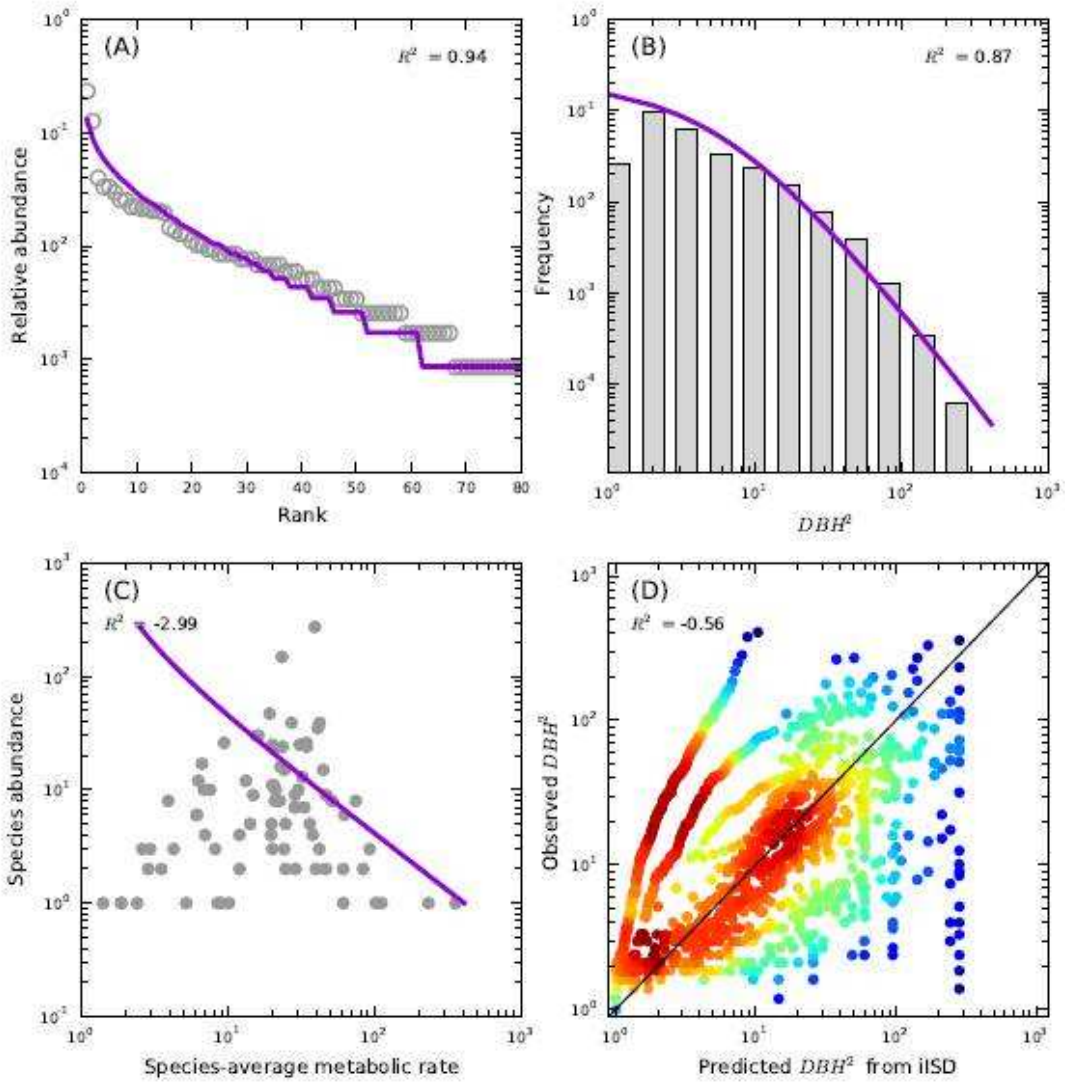


WesternGhats,BSP83

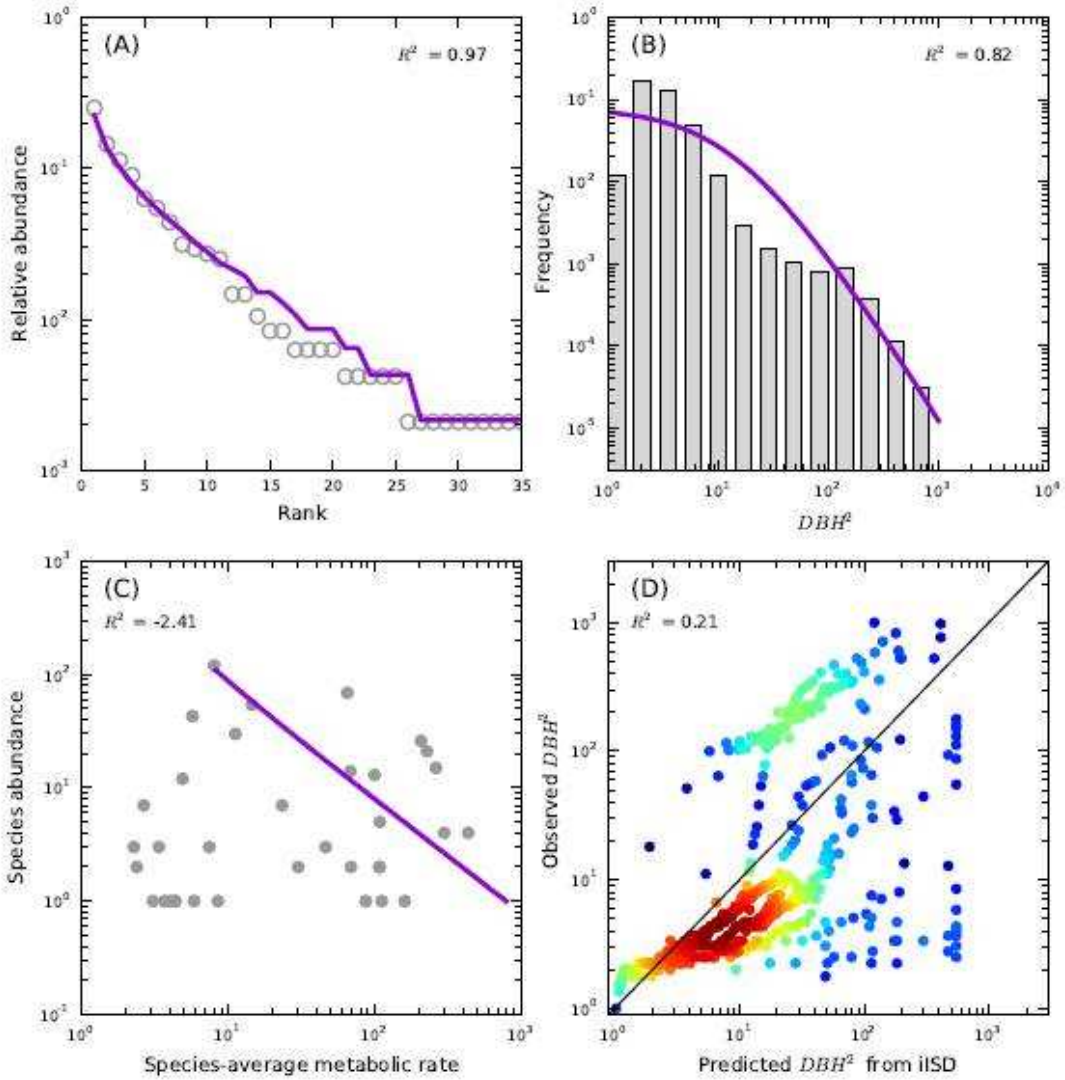




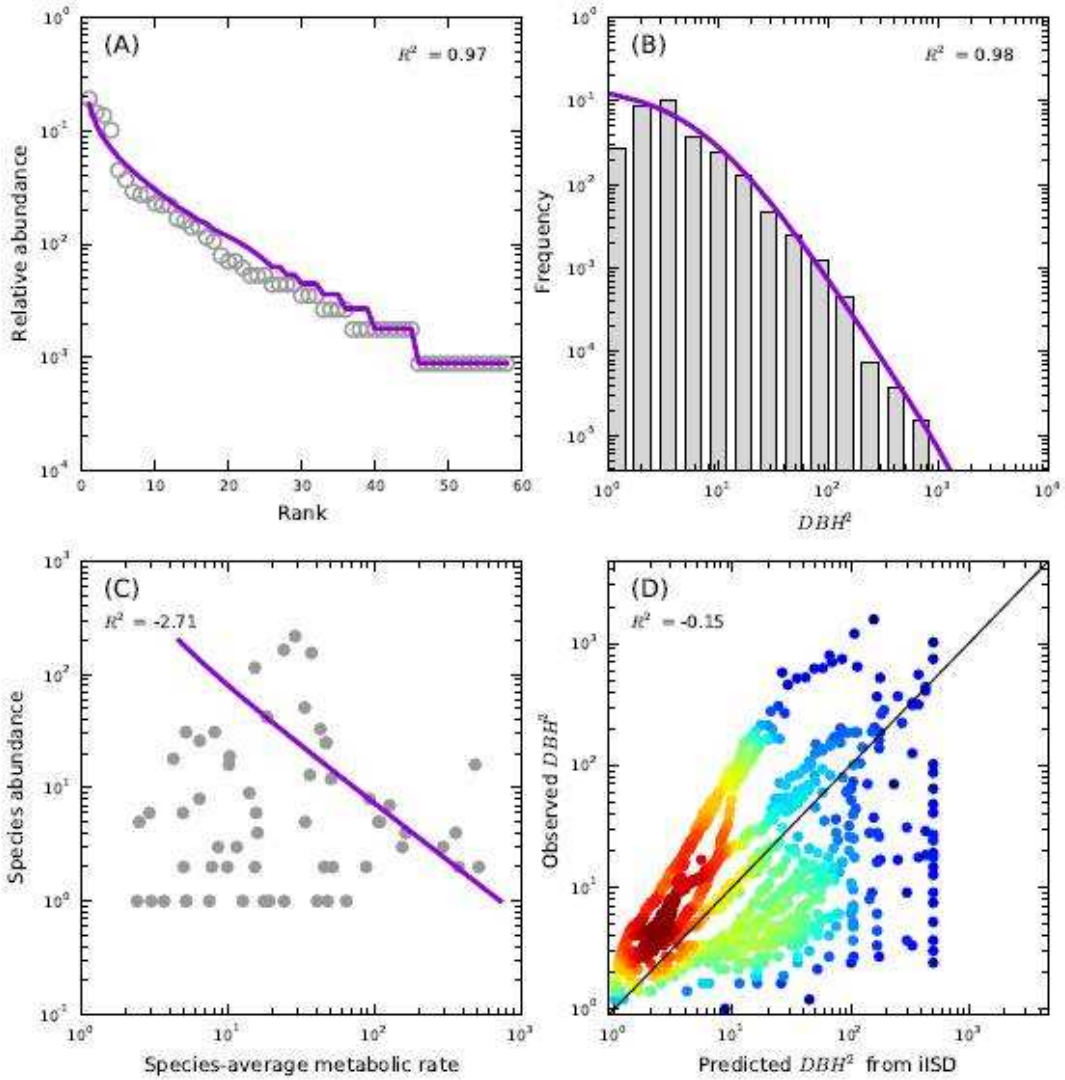
WesternGhats,BSP84



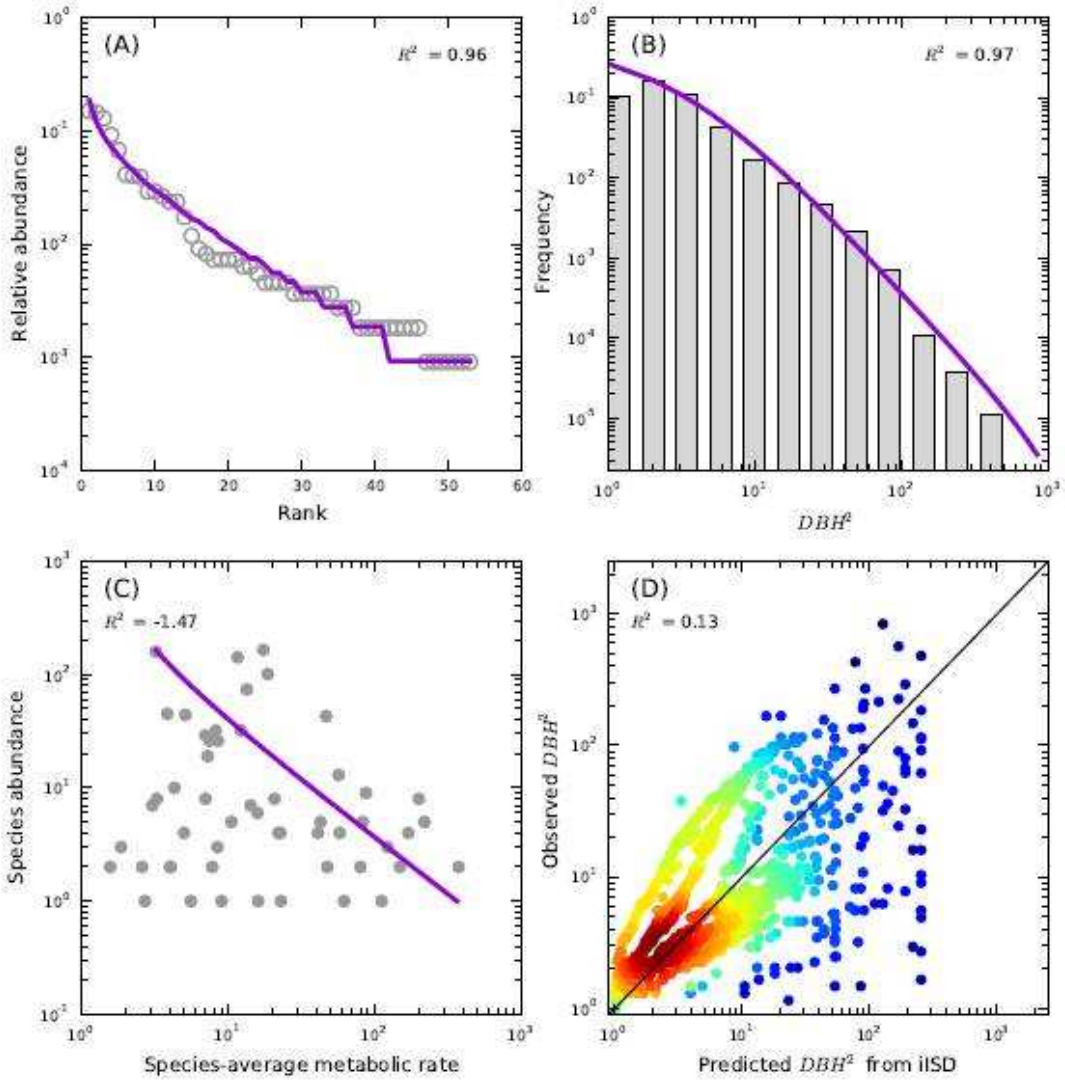
WesternGhats,BSP85



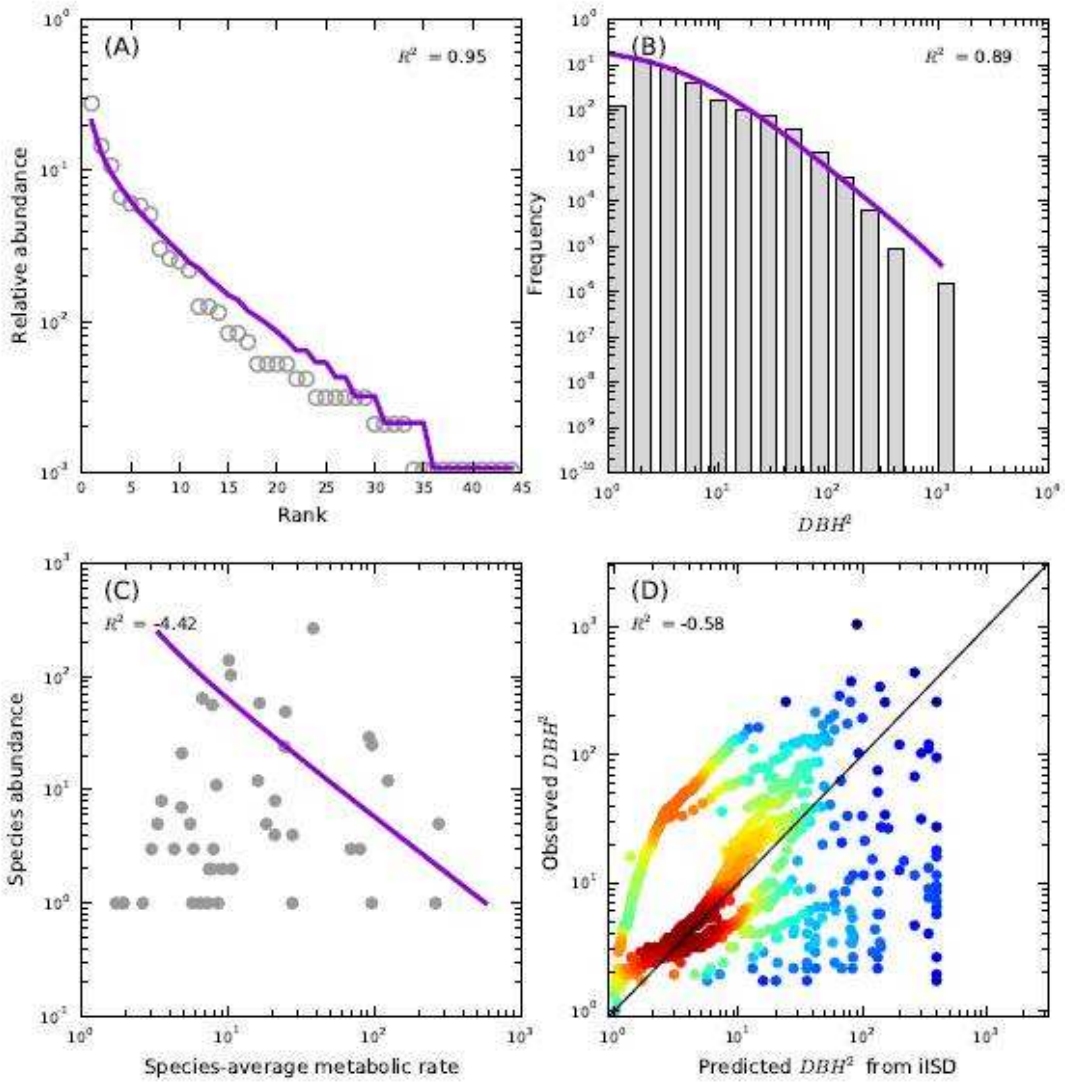
WesternGhats,BSP88



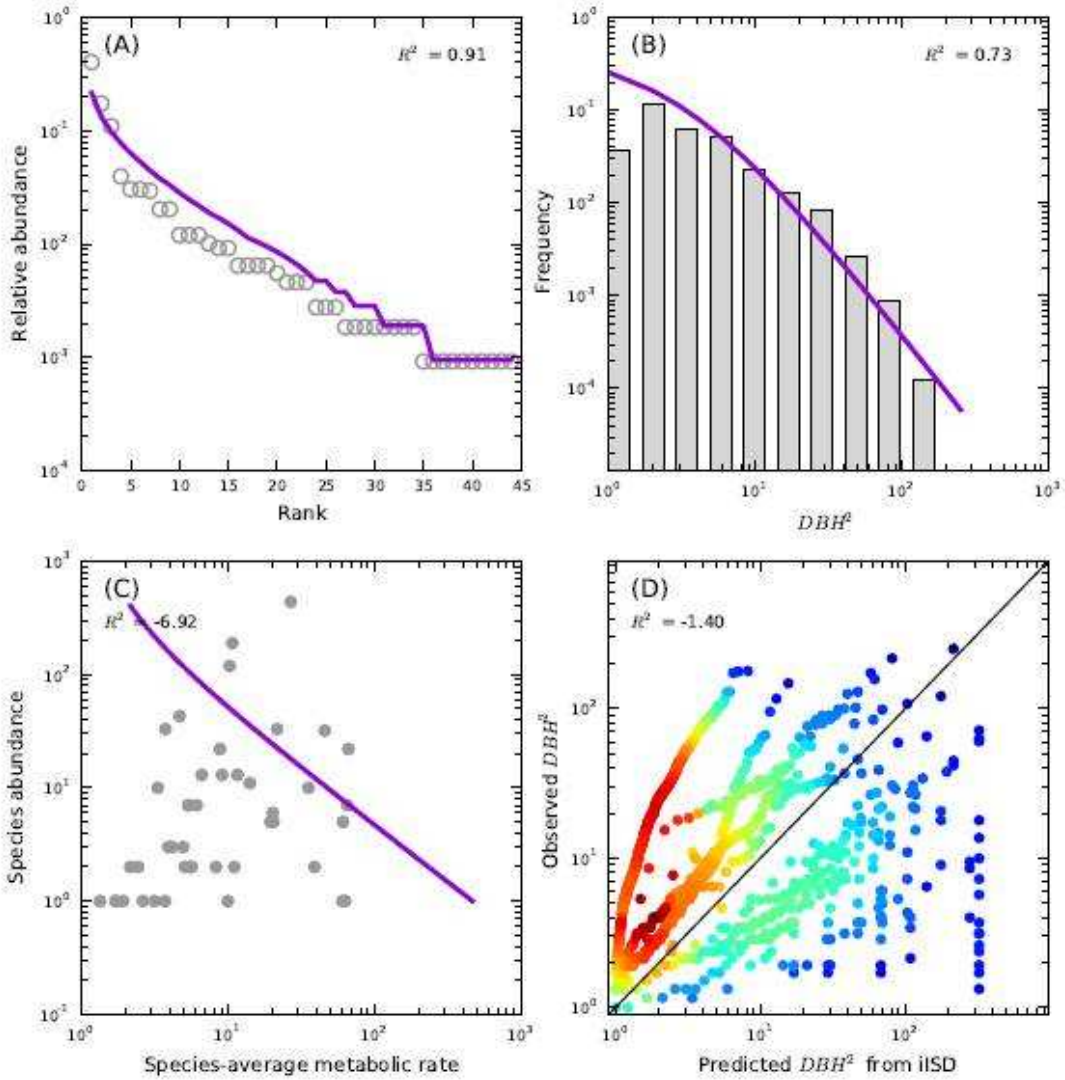
WesternGhats,BSP89



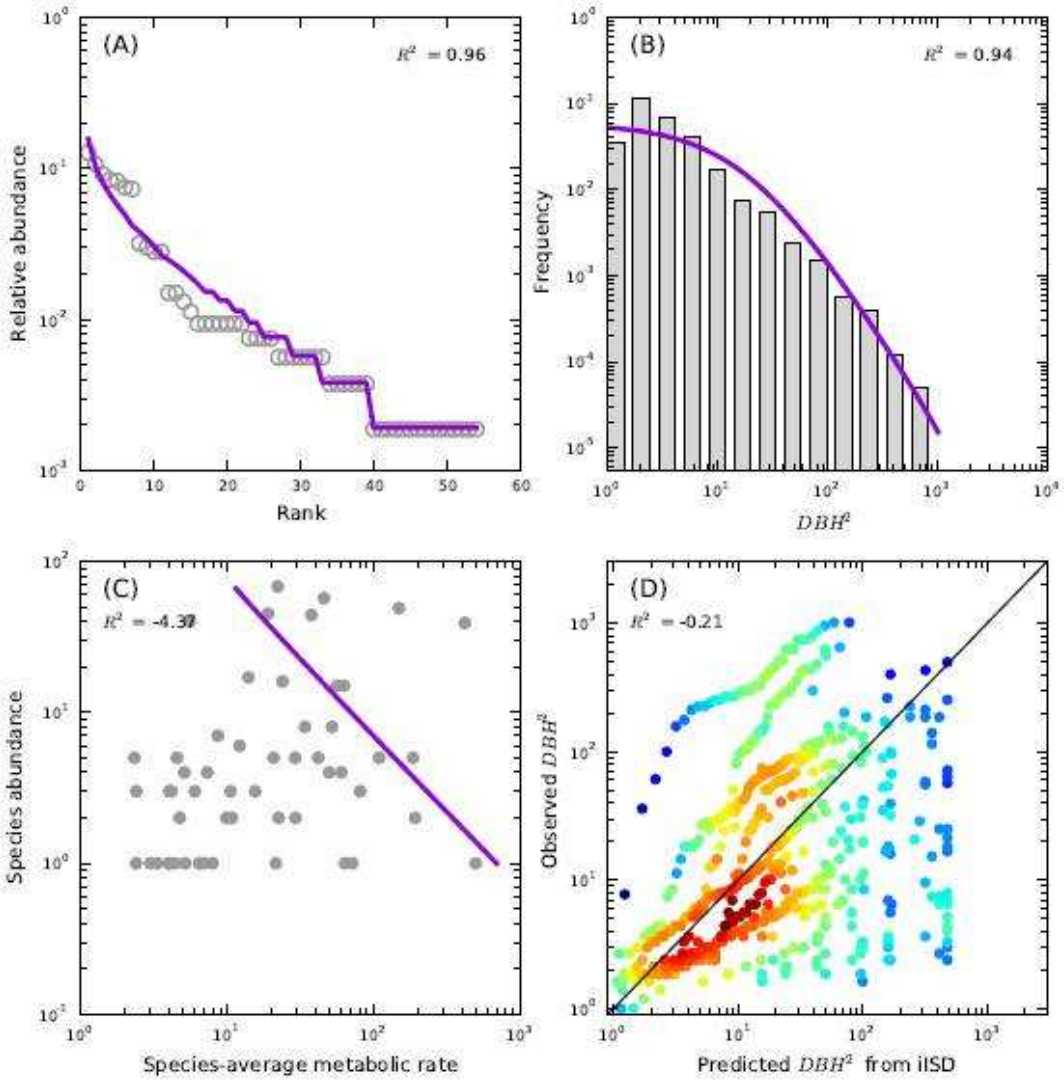
WesternGhats,BSP90



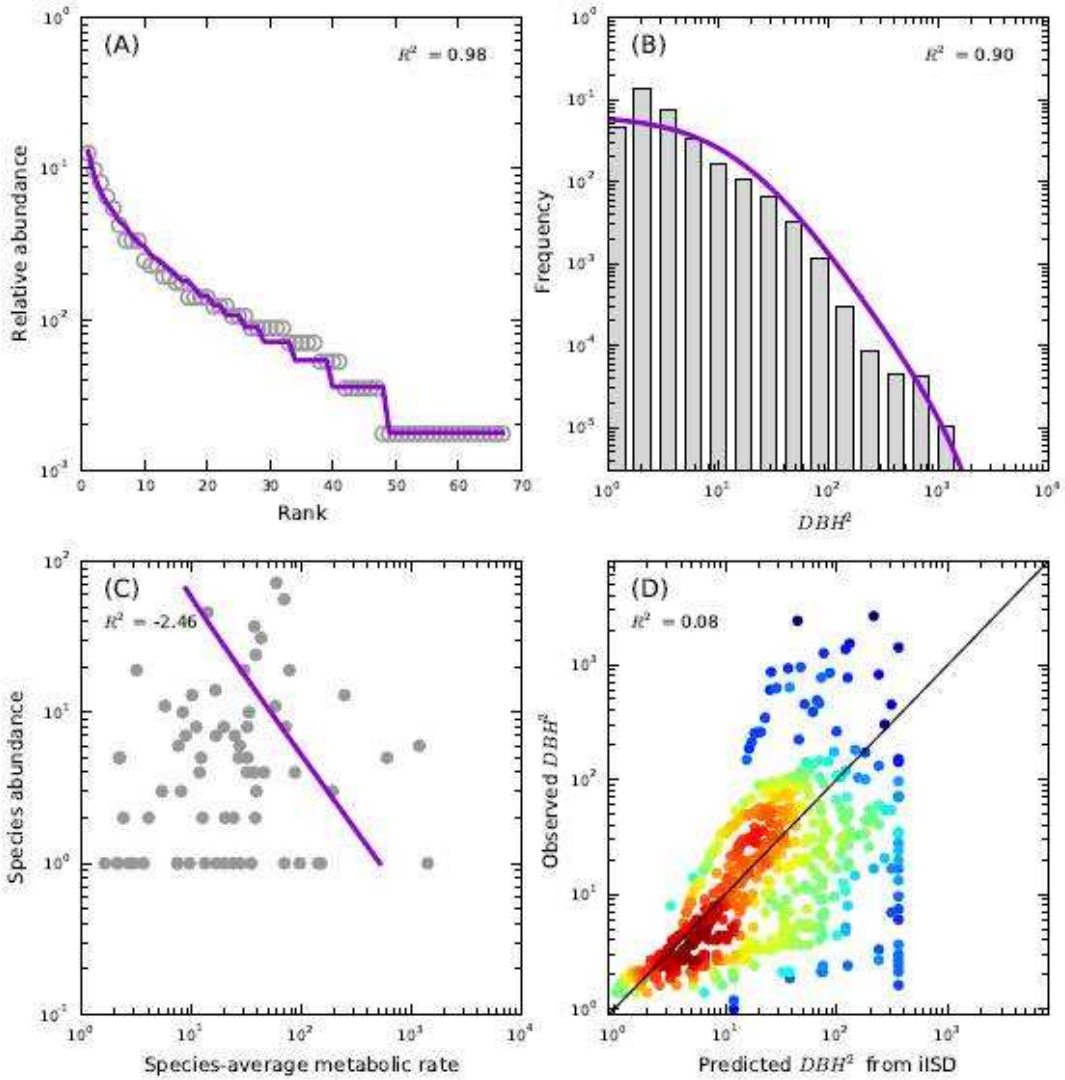
WesternGhats,BSP91



WesternGhats,BSP92

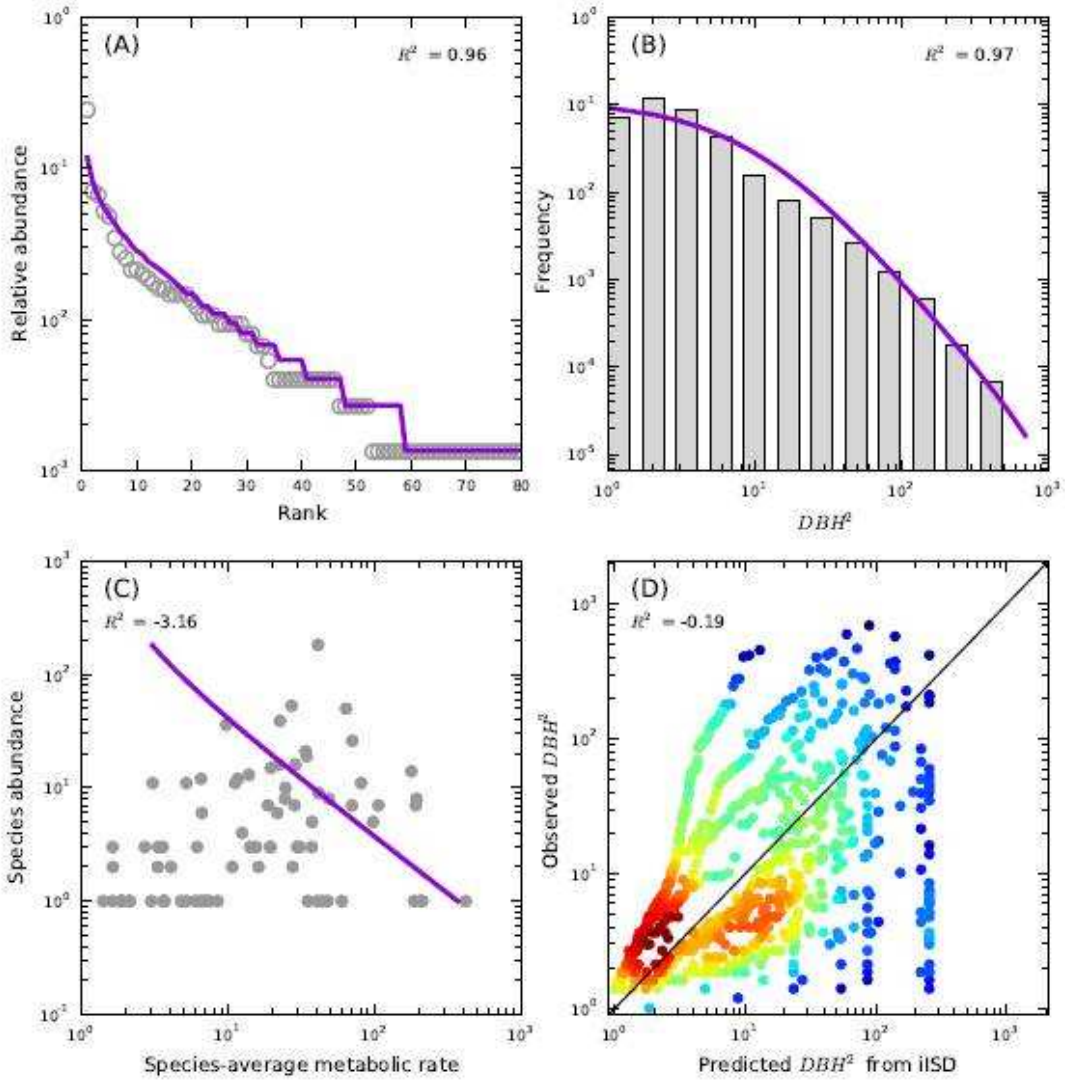


WesternGhats,BSP94

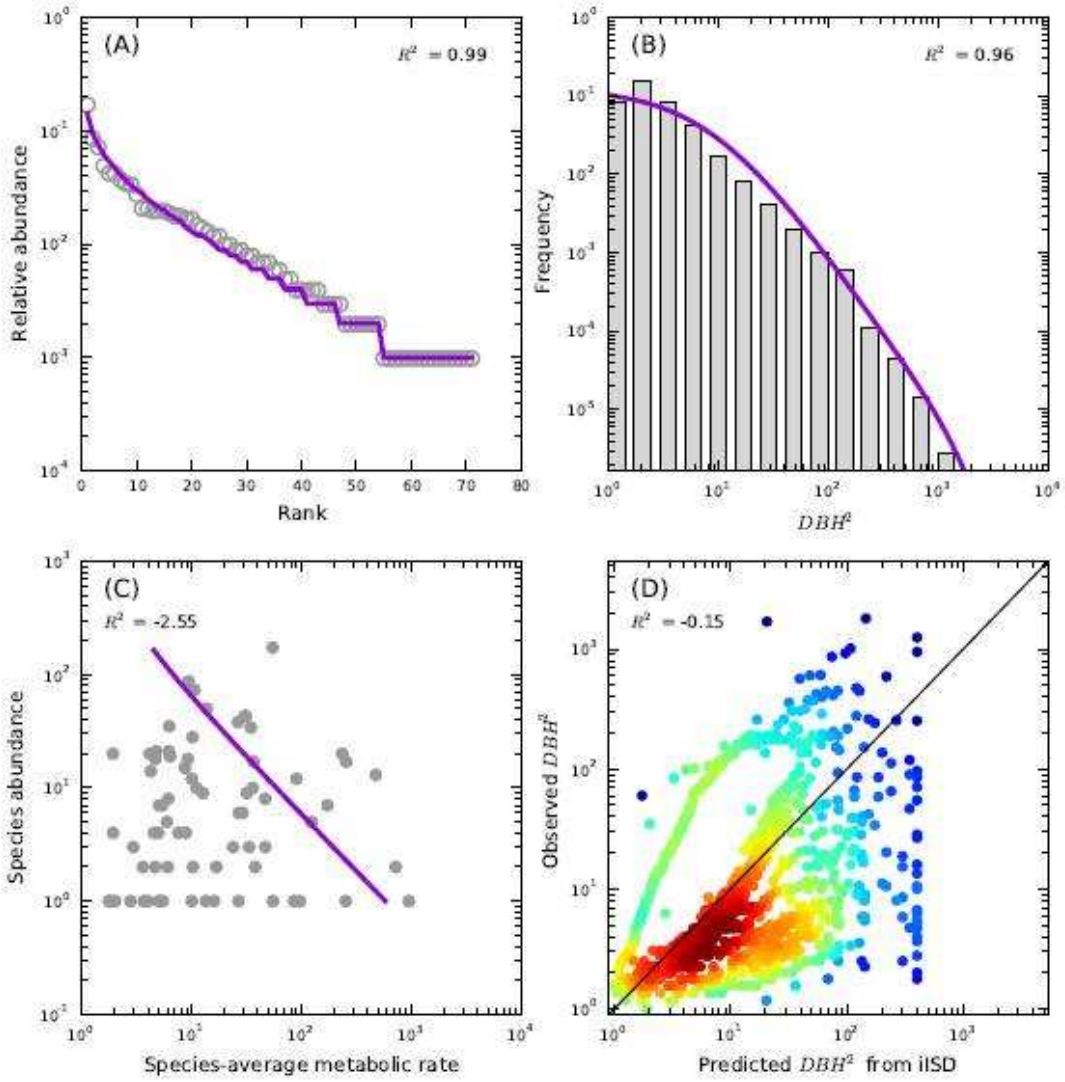




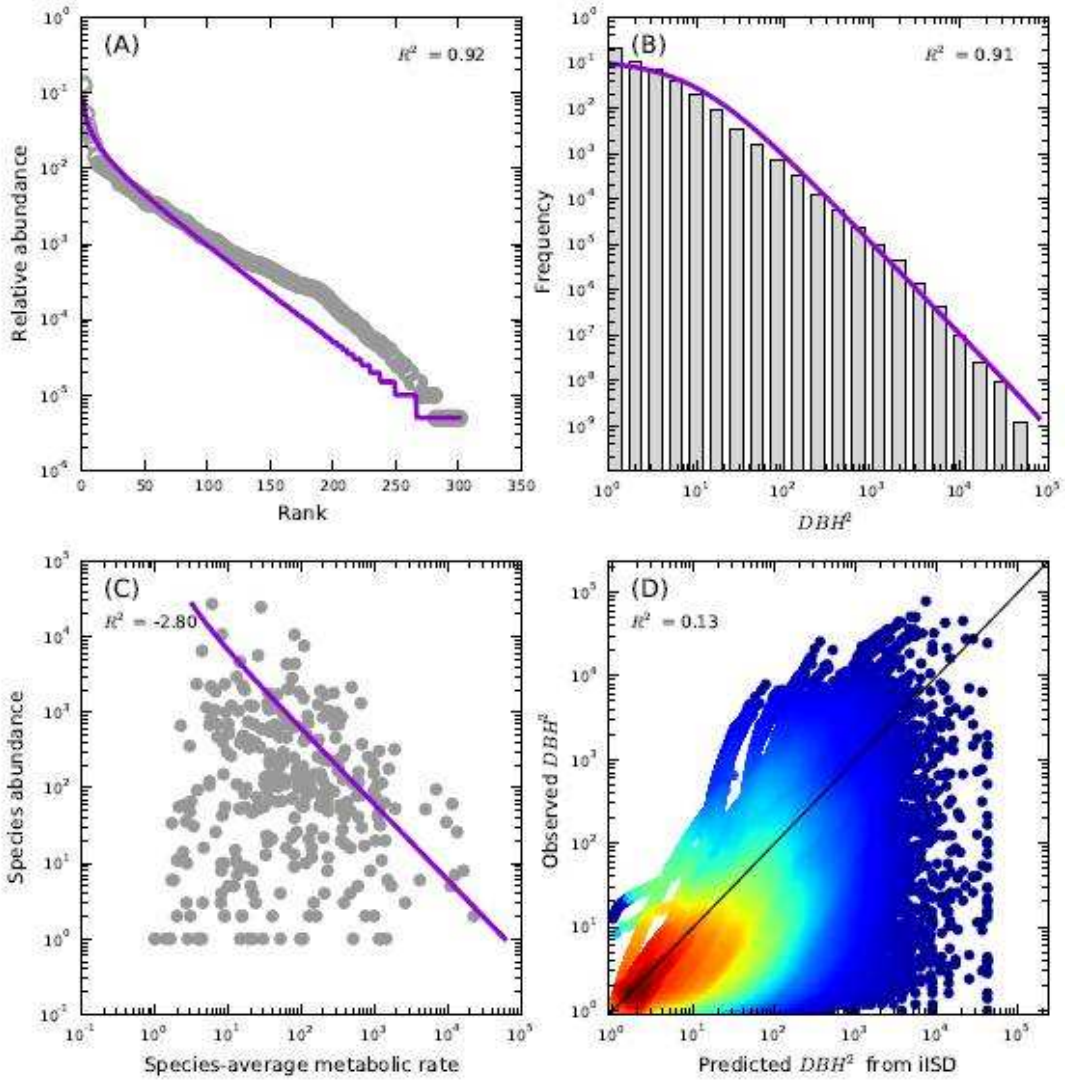
WesternGhats,BSP98



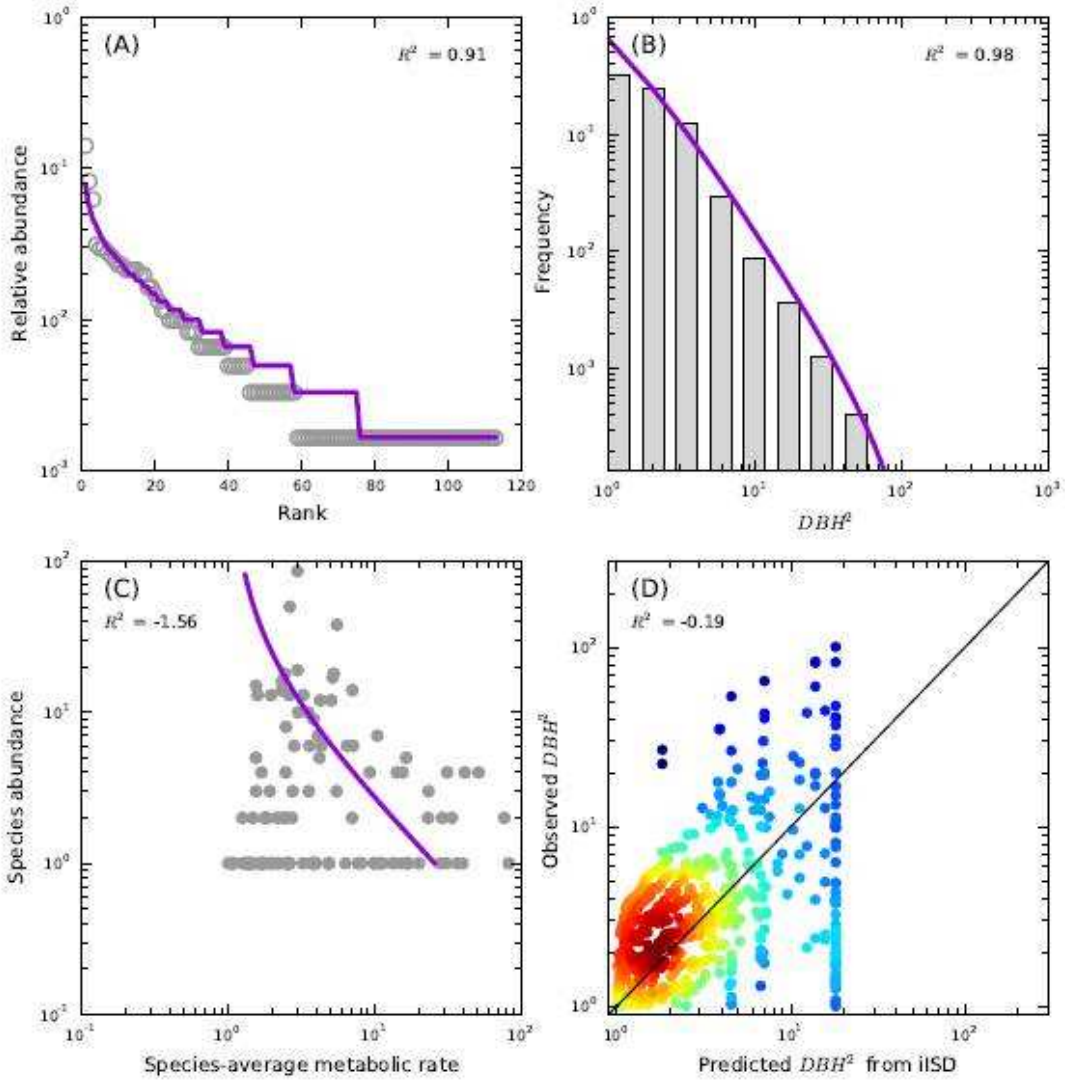
WesternGhats,BSP99



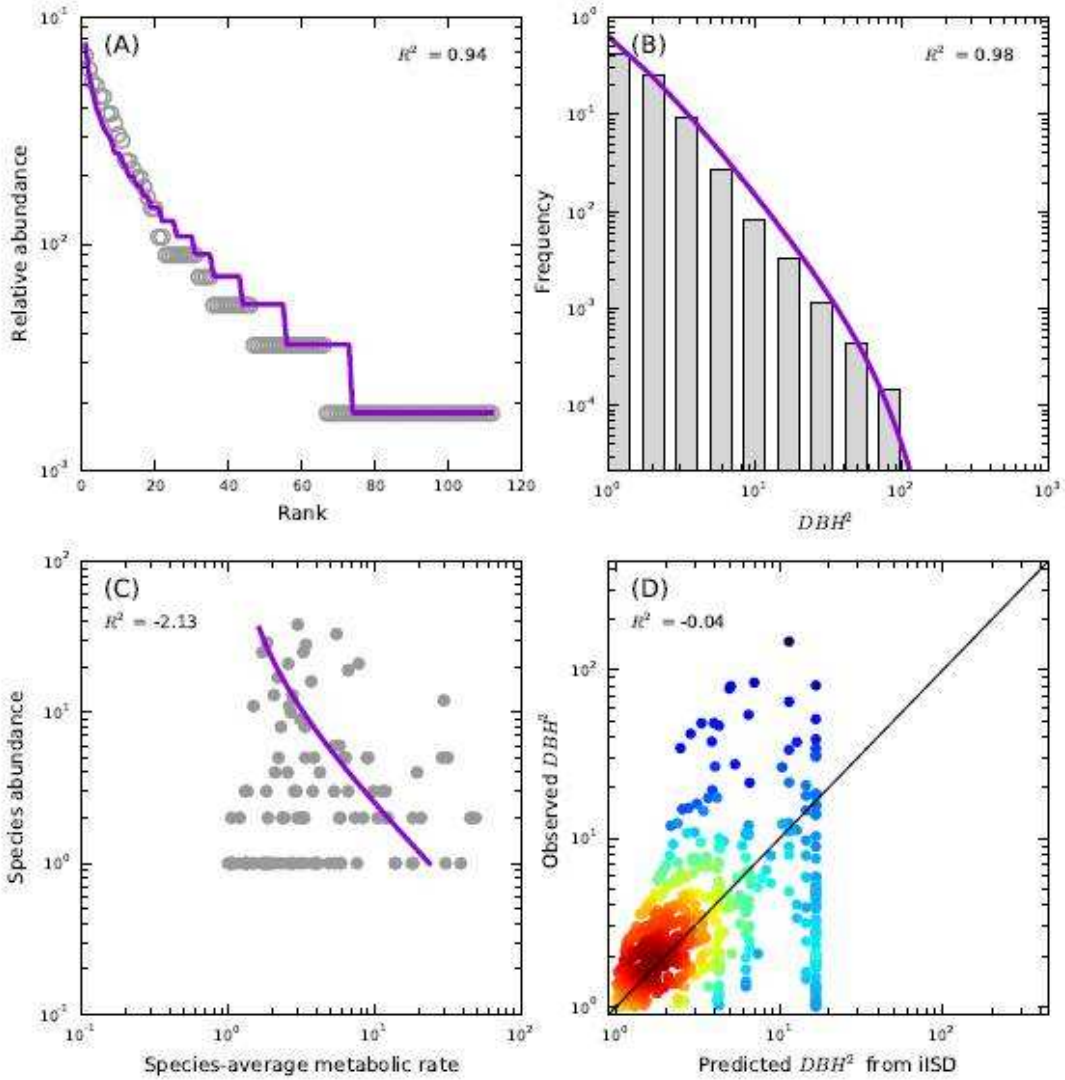
BCI,bci



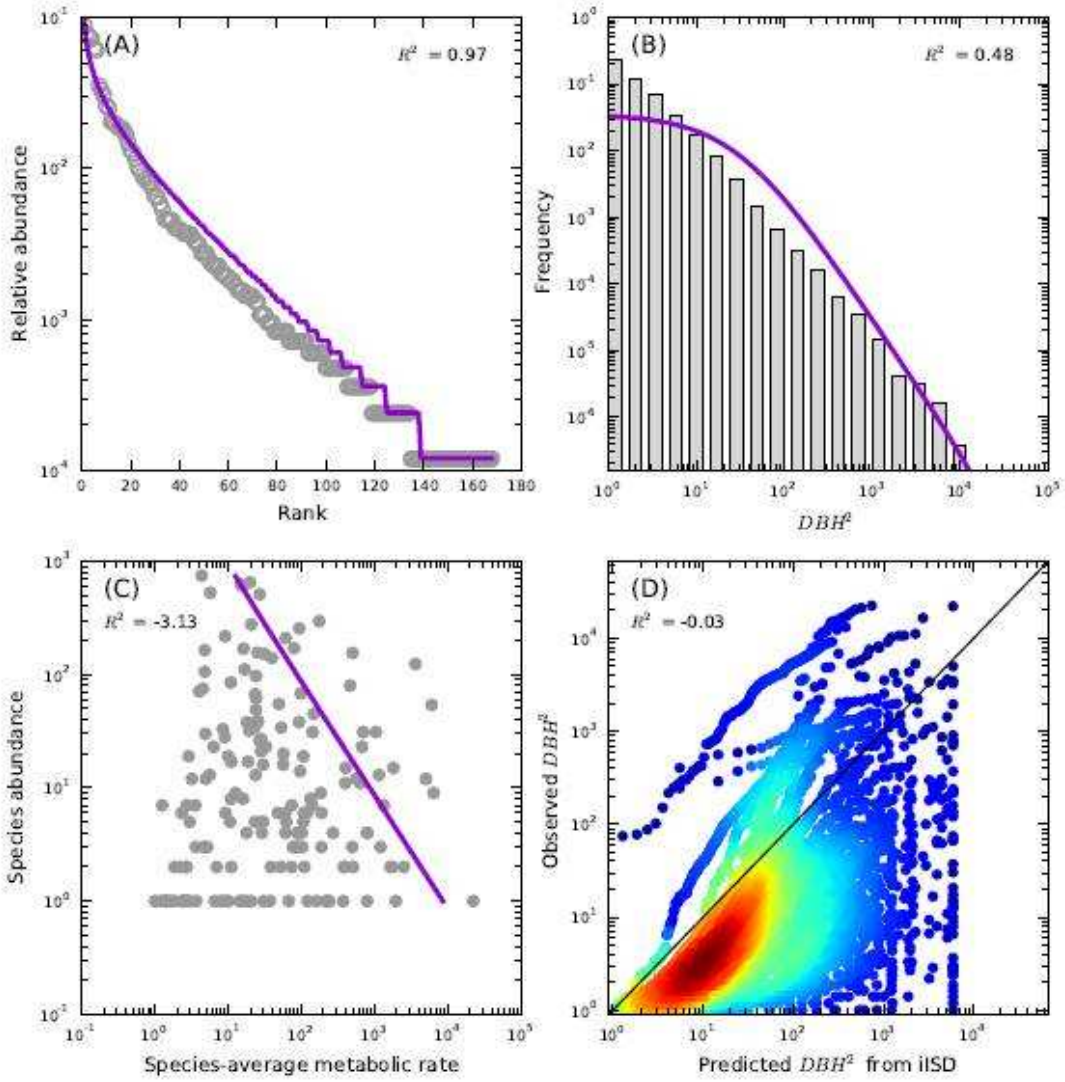
# BVSF, BVPlot



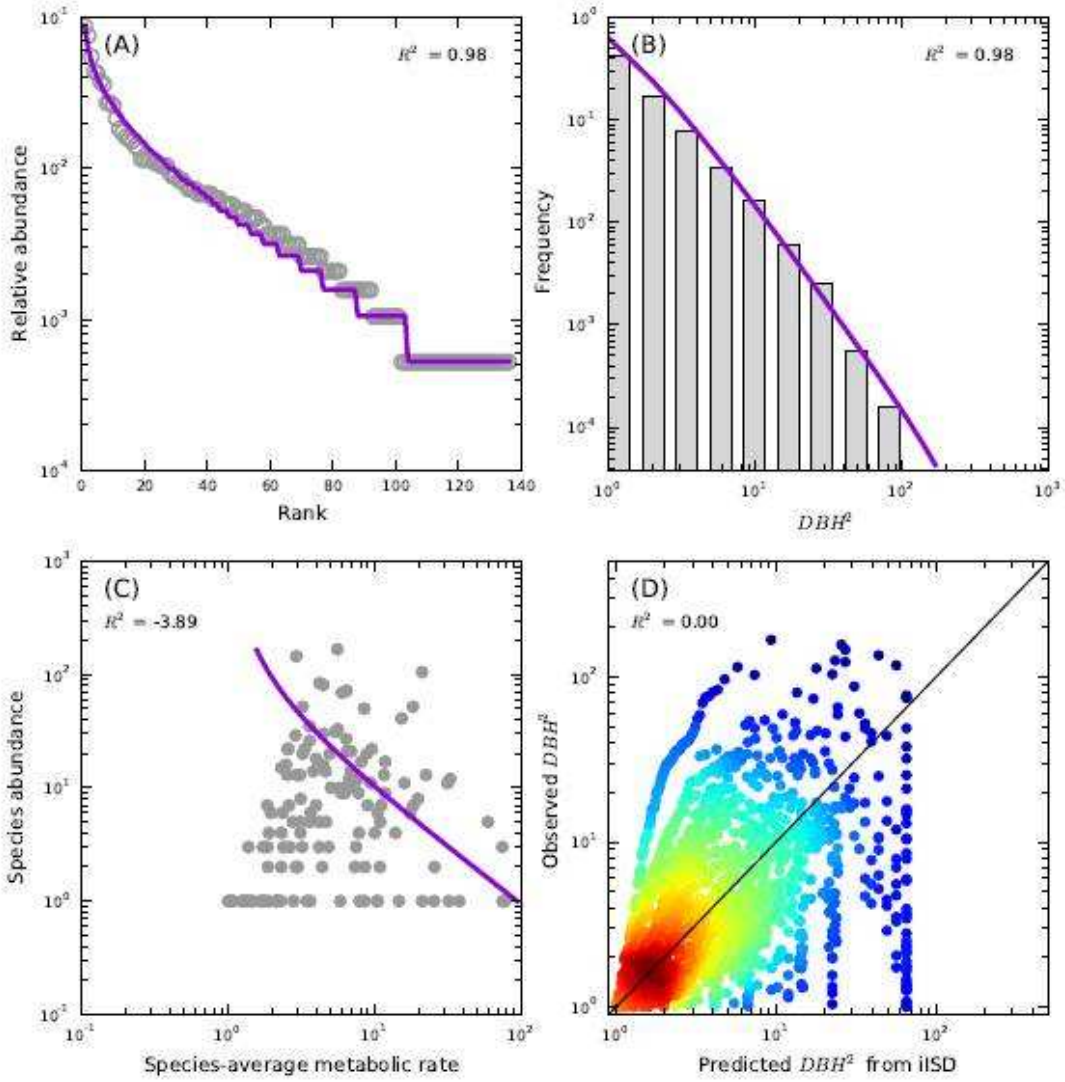
# BVSF,SFPlot



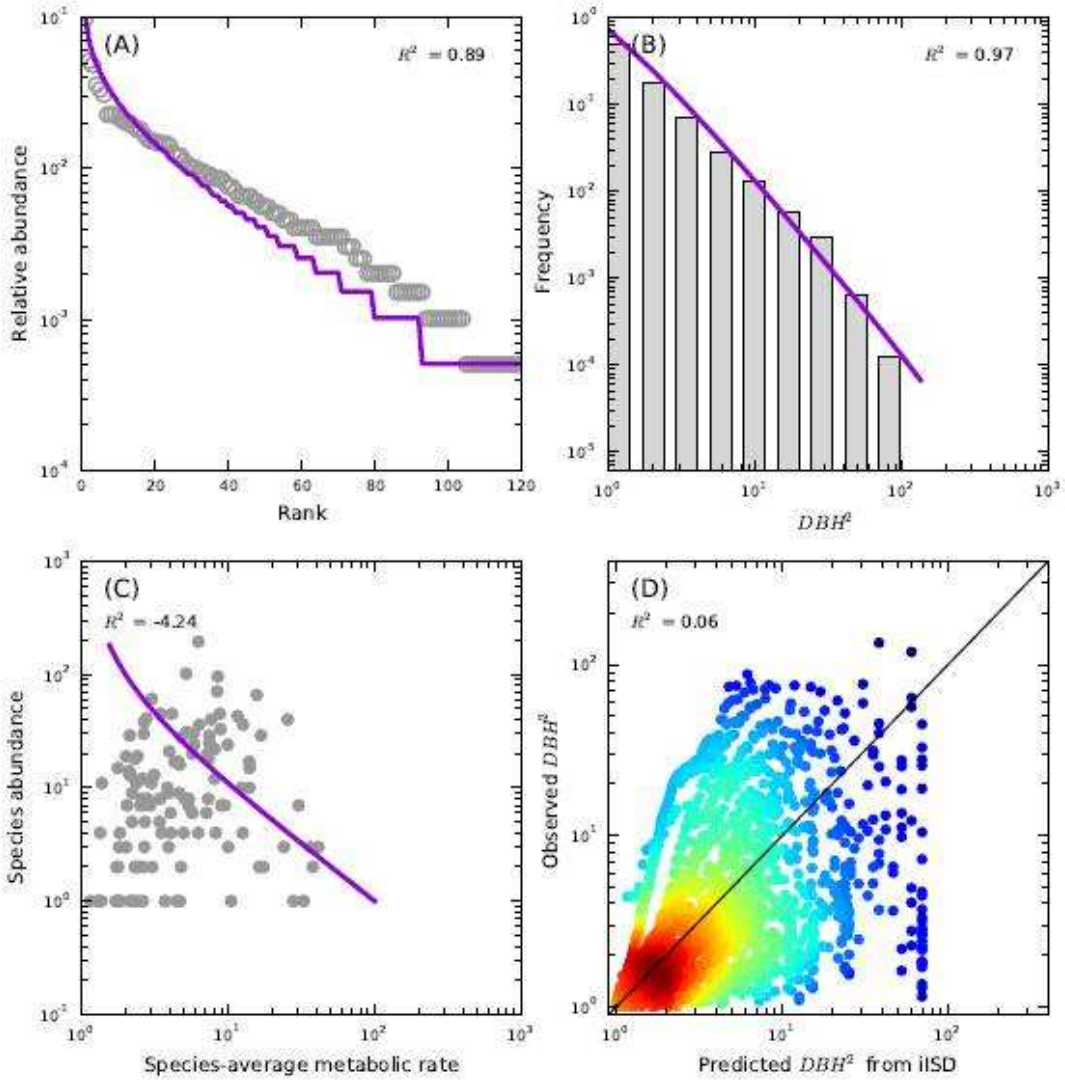
# Cocoli,cocoli



Lahei,heath1

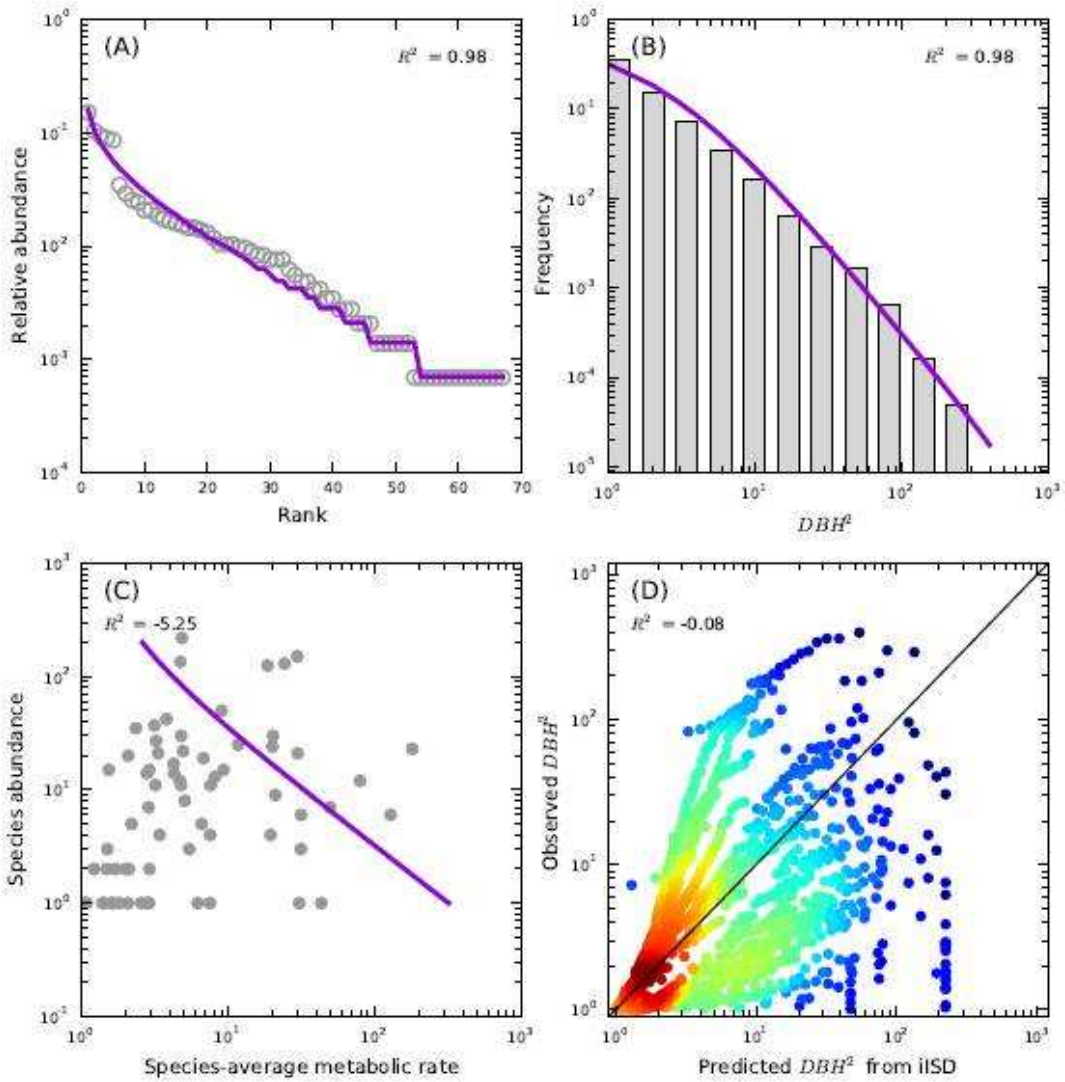


Lahei,heath2

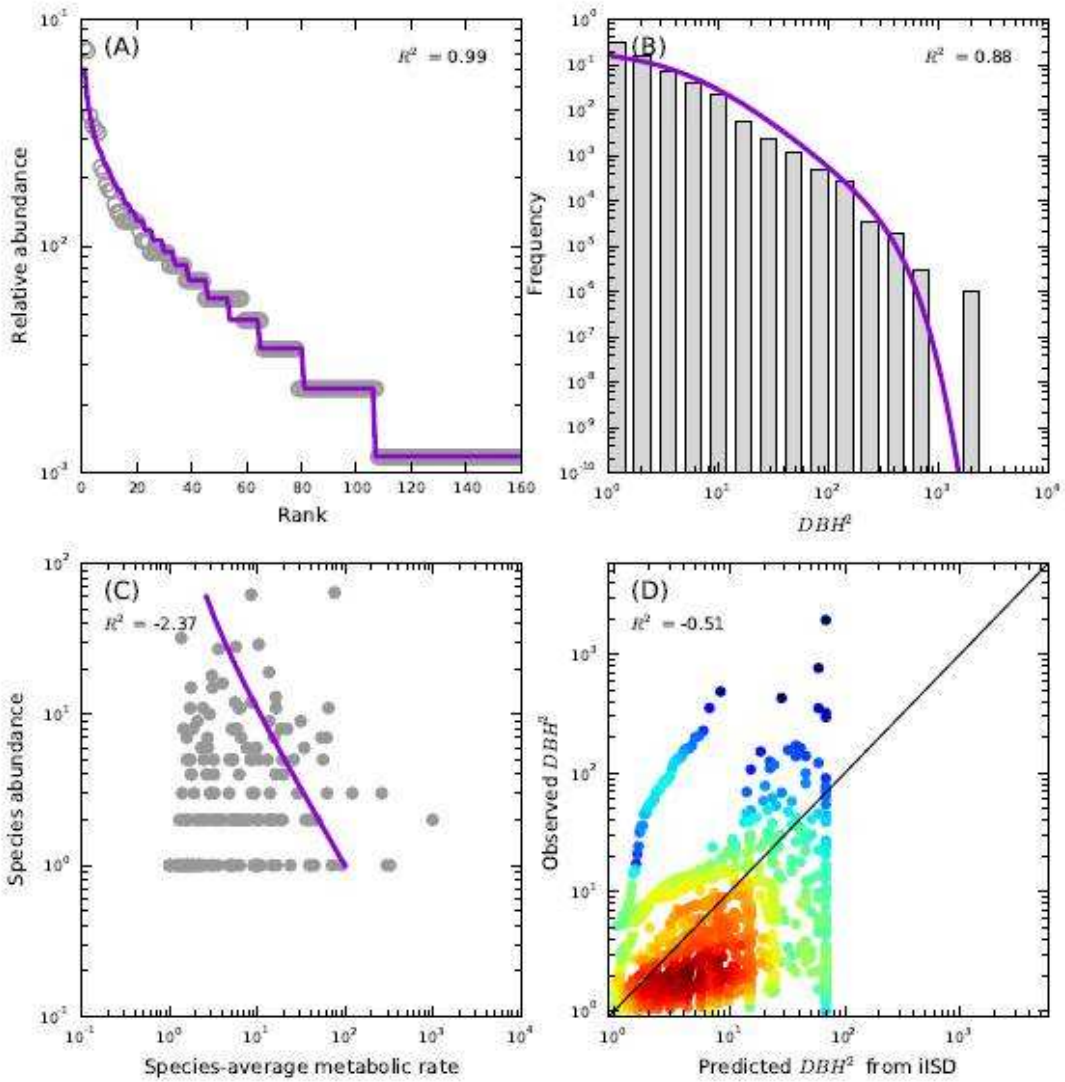




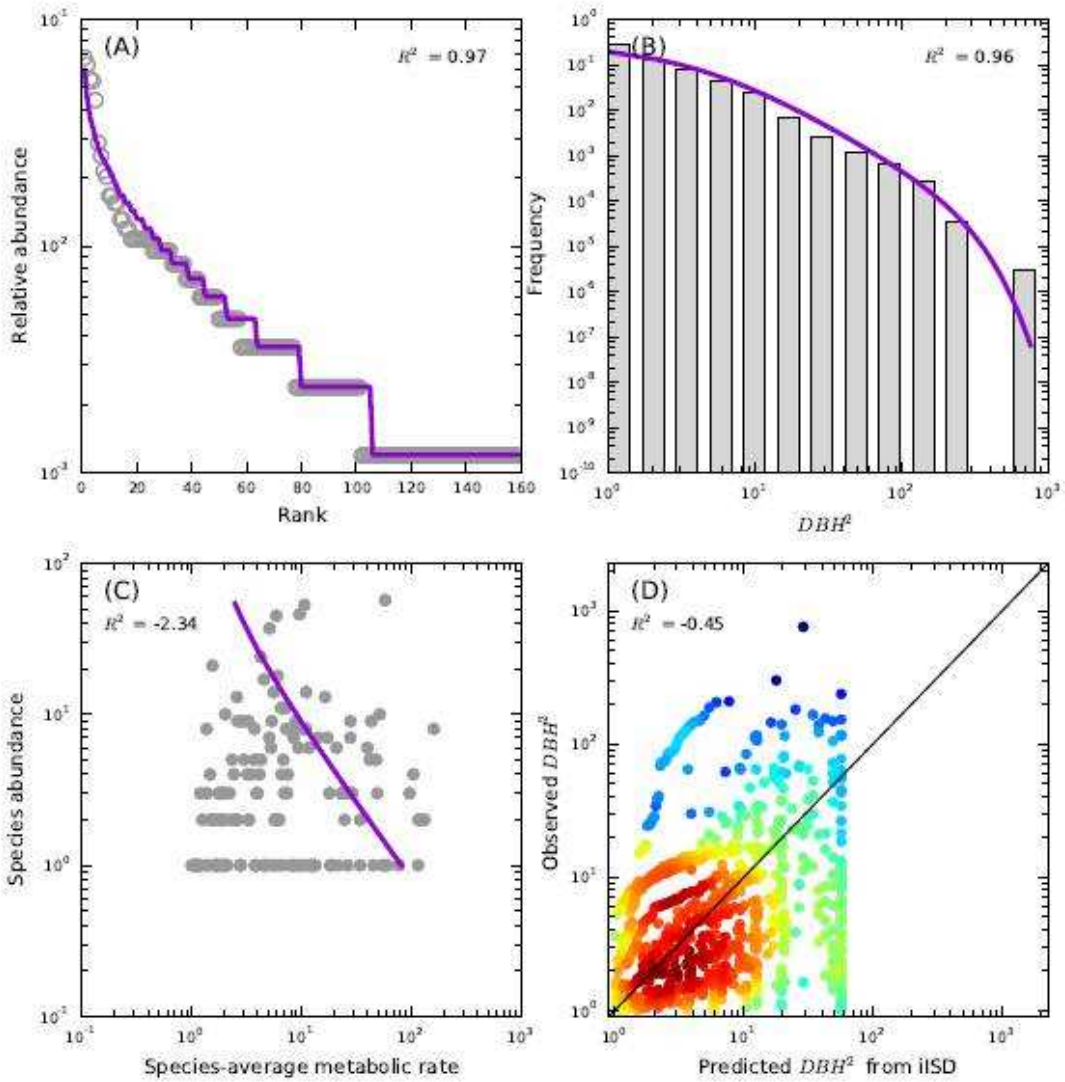
# Lahei,peat



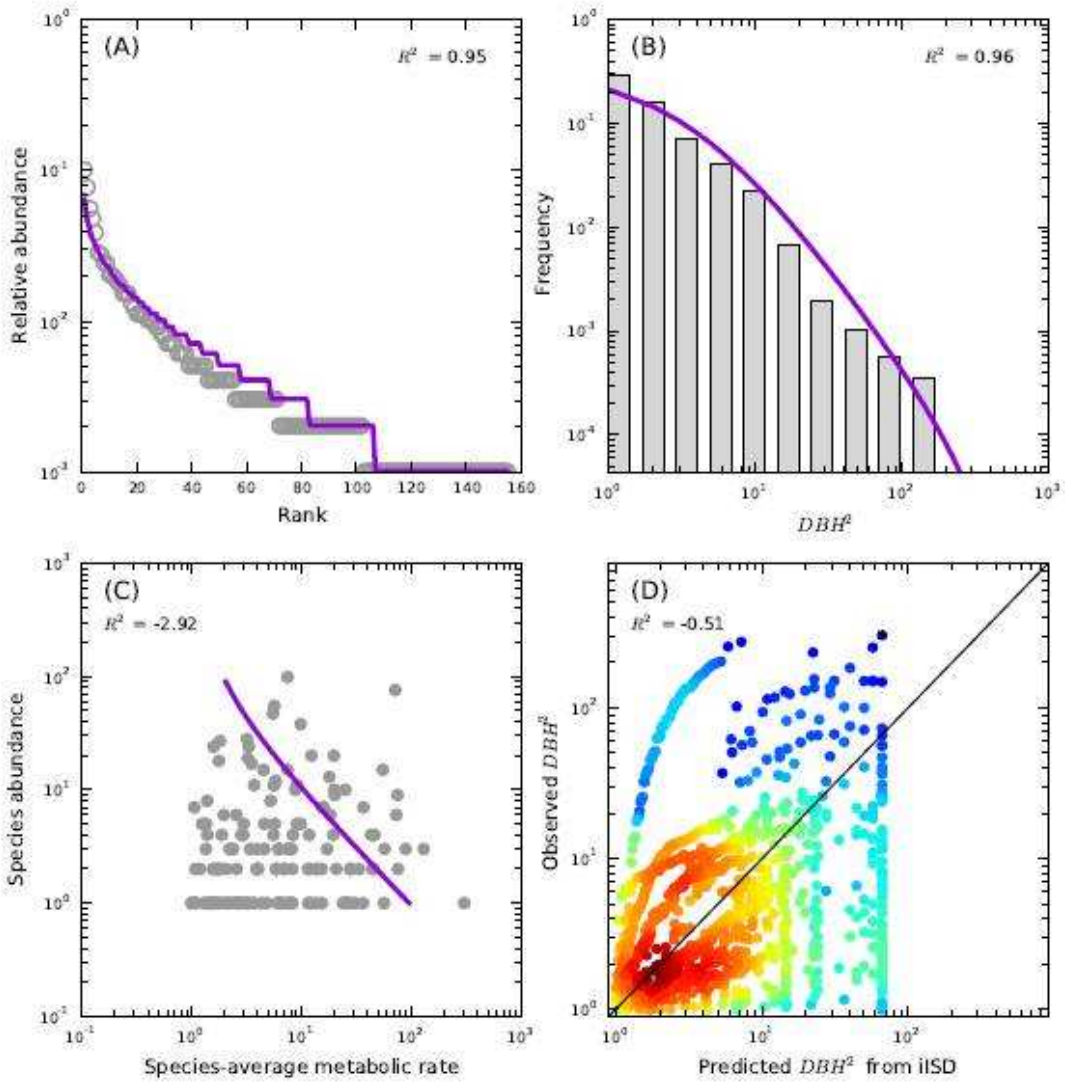
# LaSelva,1



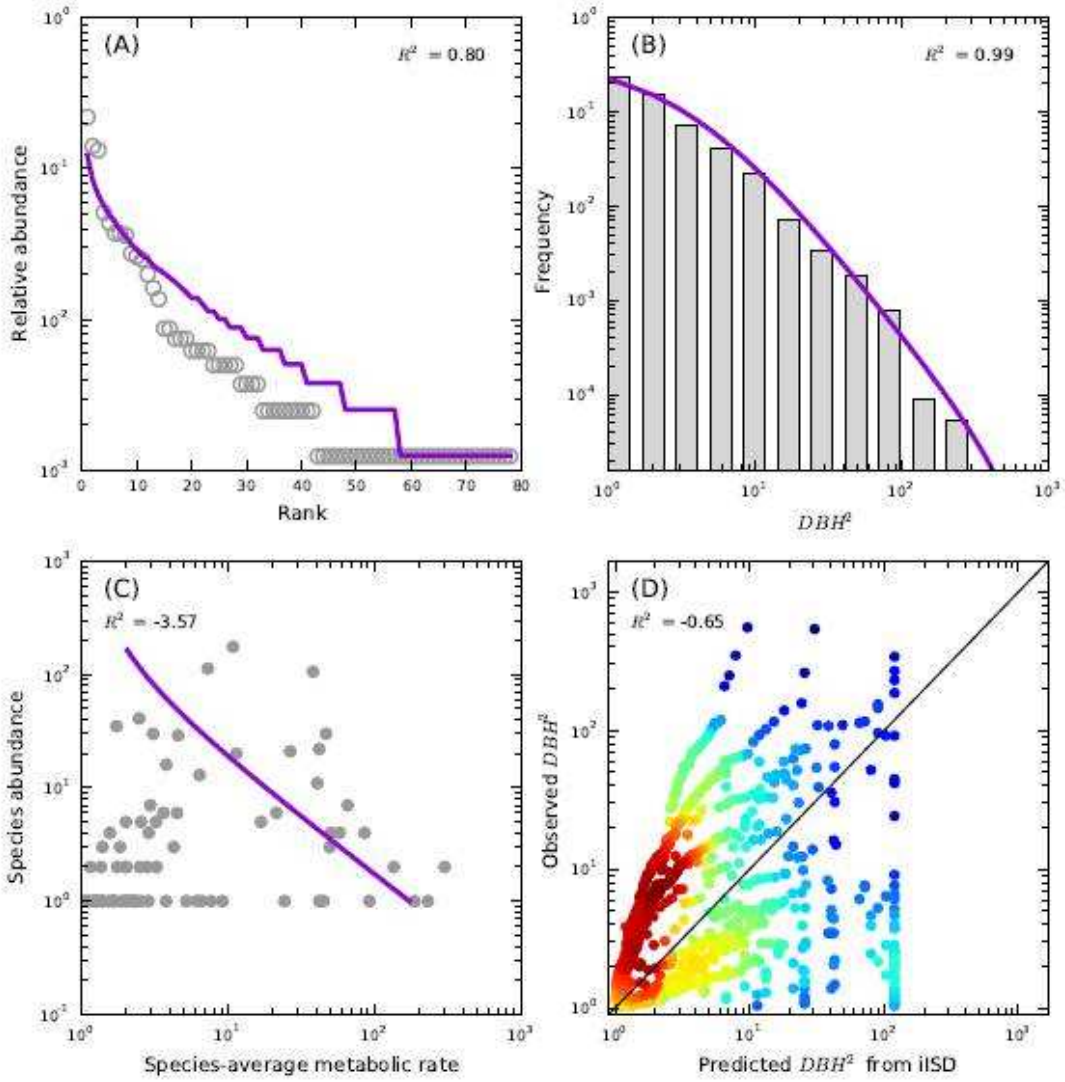
# LaSelva,2



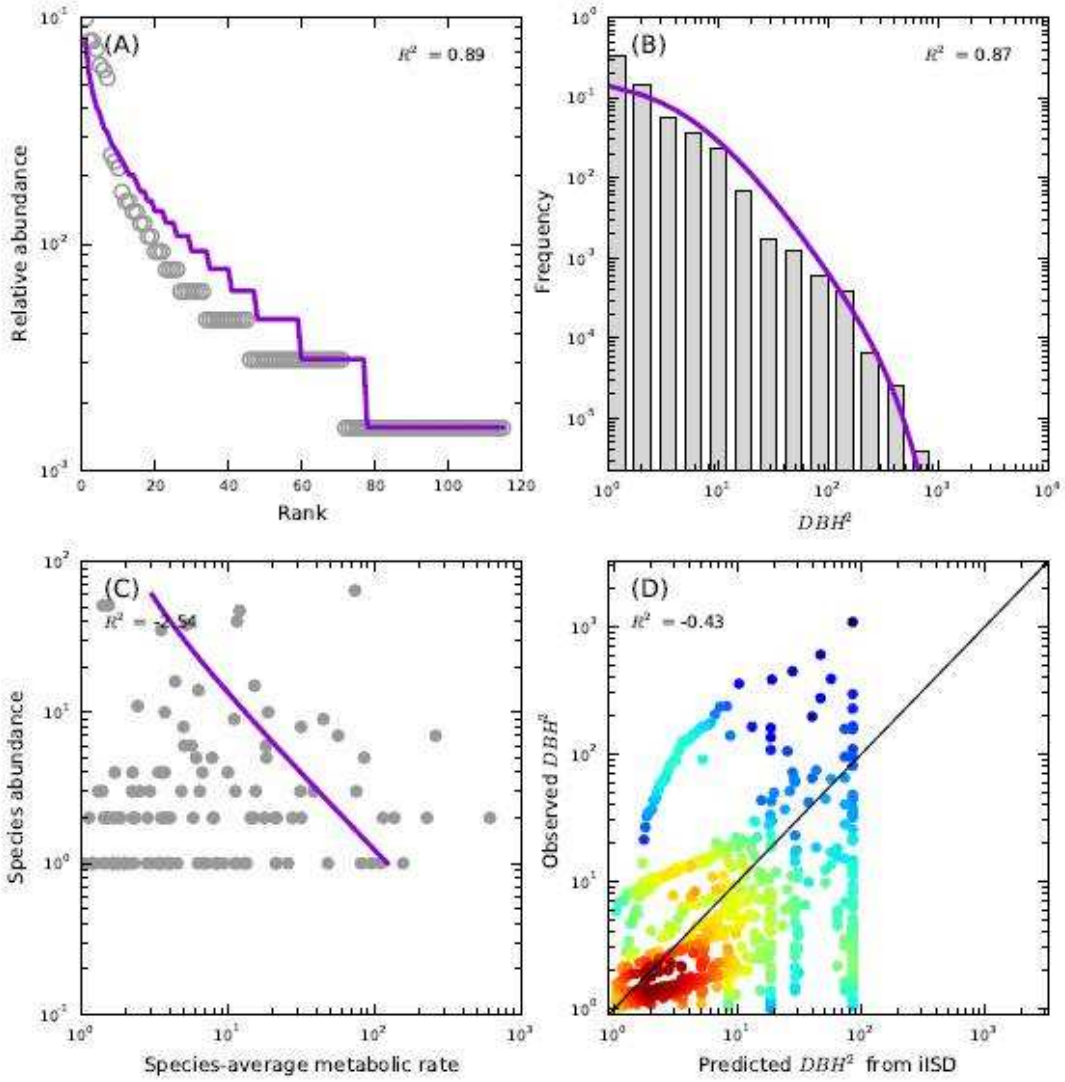
# LaSelva,3



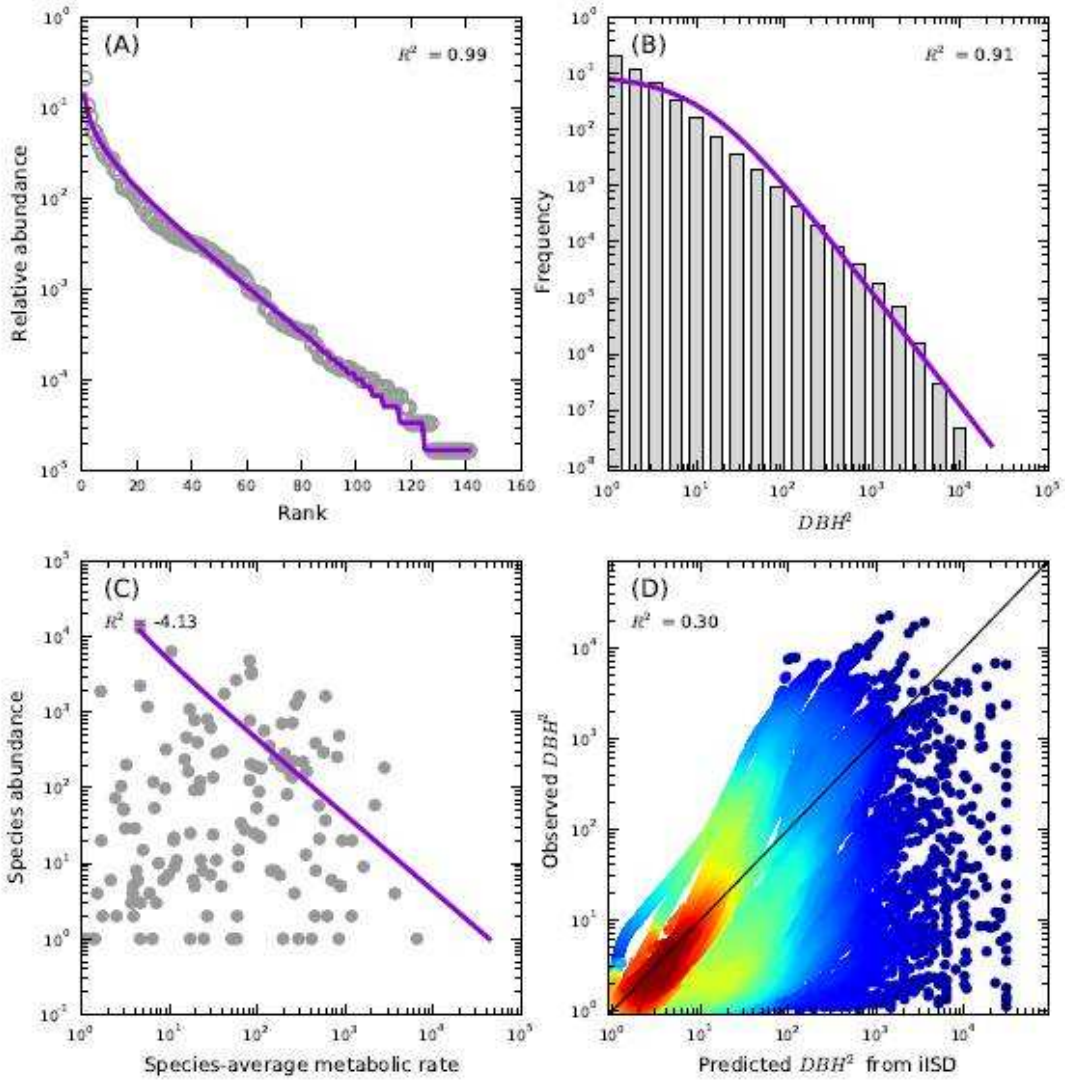
# LaSelva,4



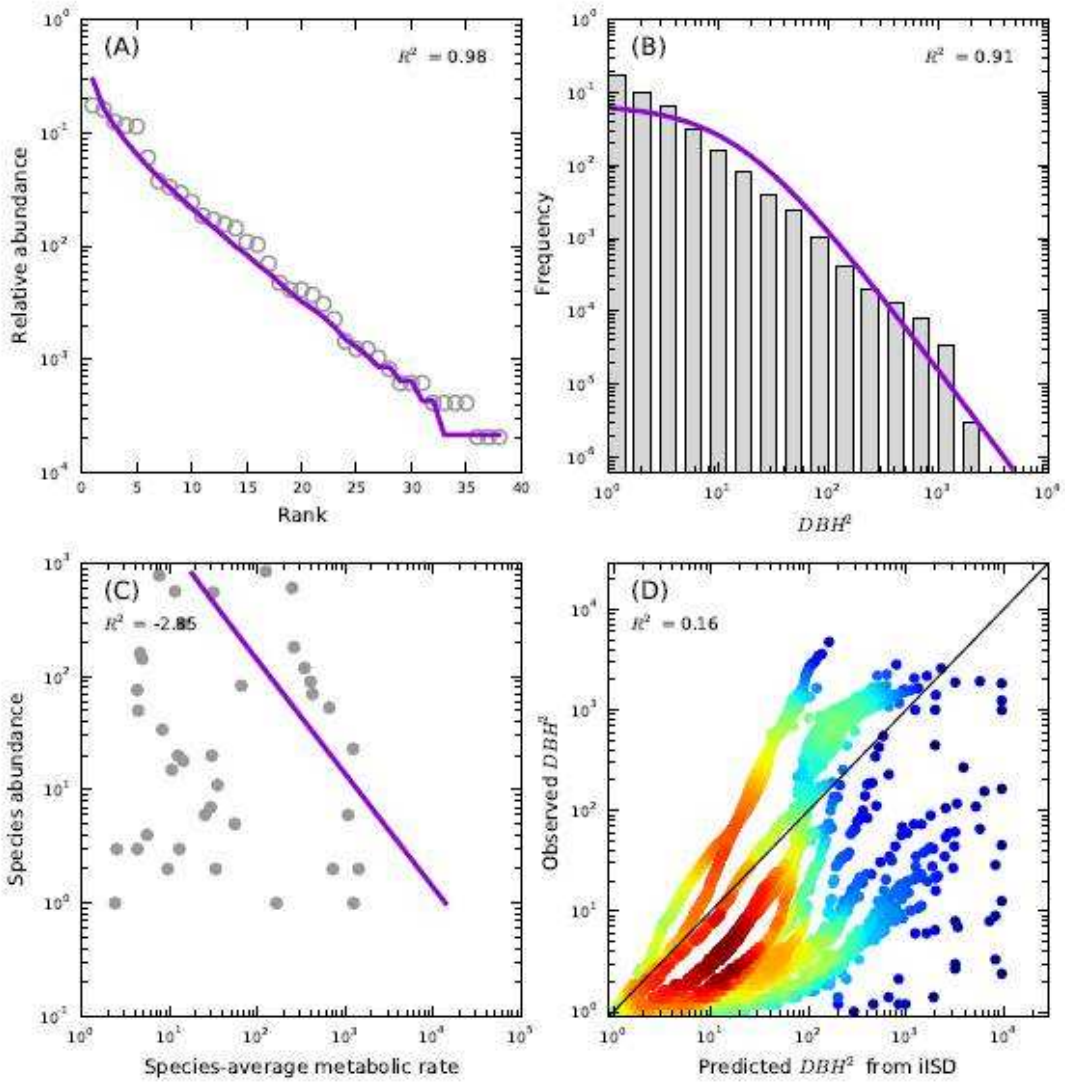
# LaSelva,5



Luquillo, lfdp

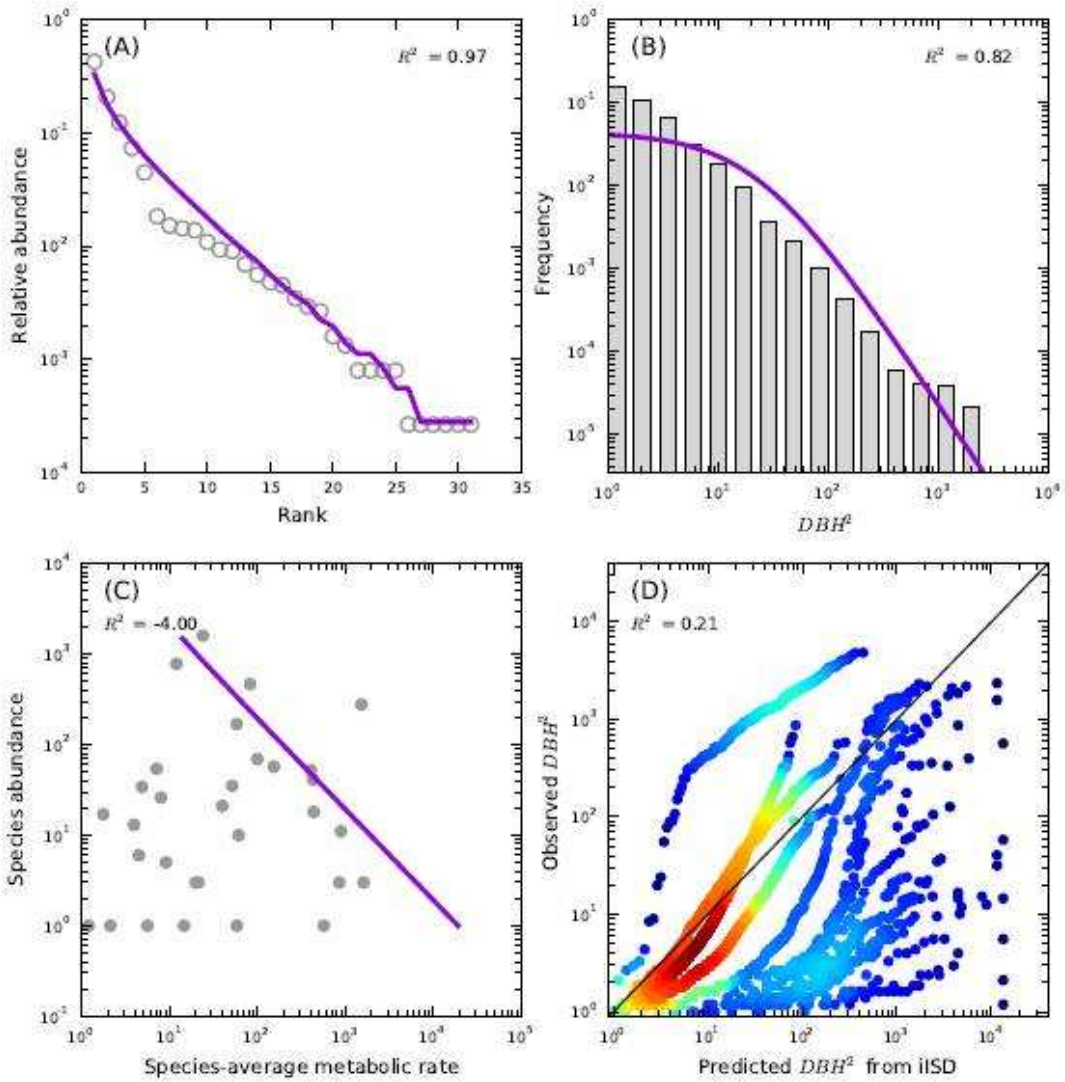


NC,12

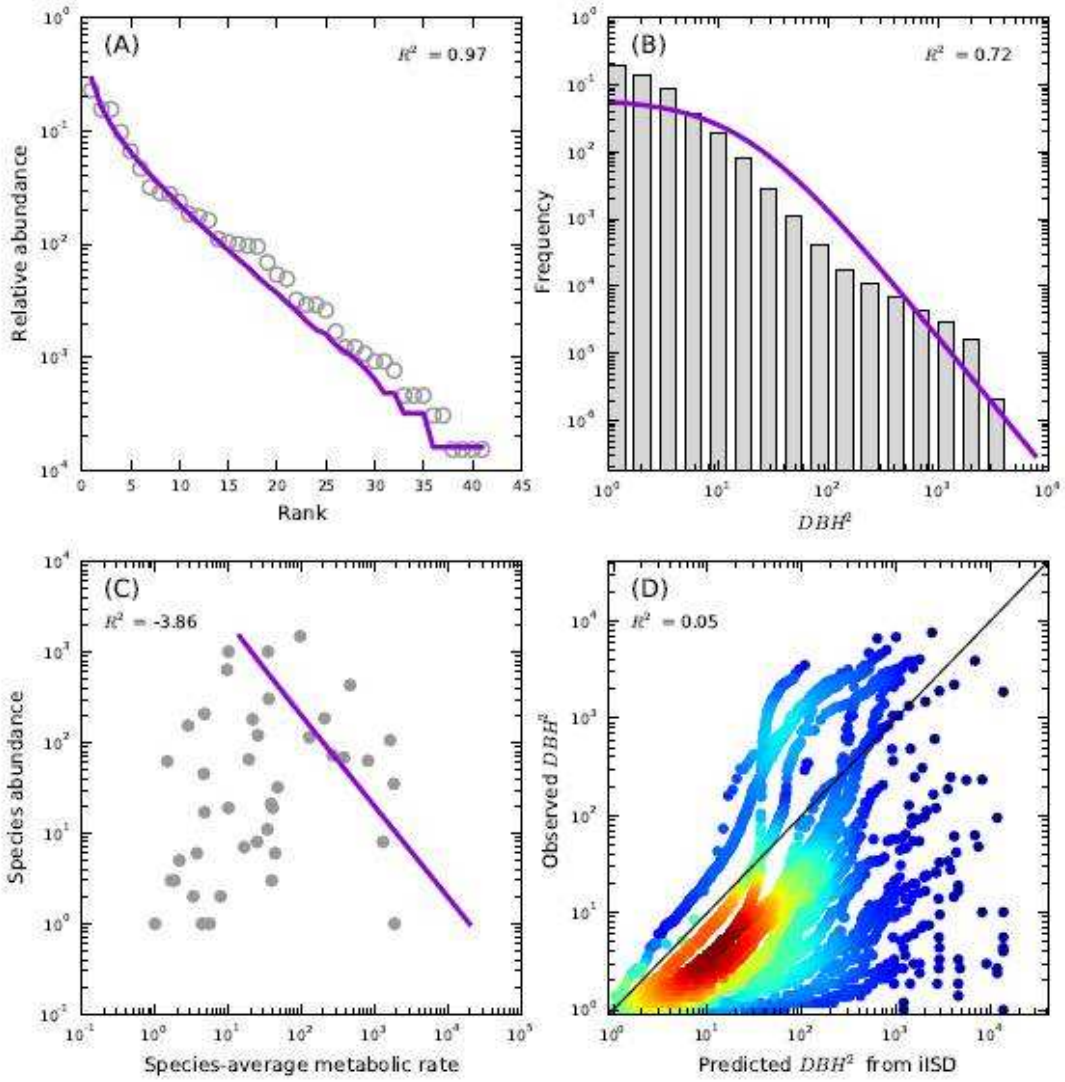




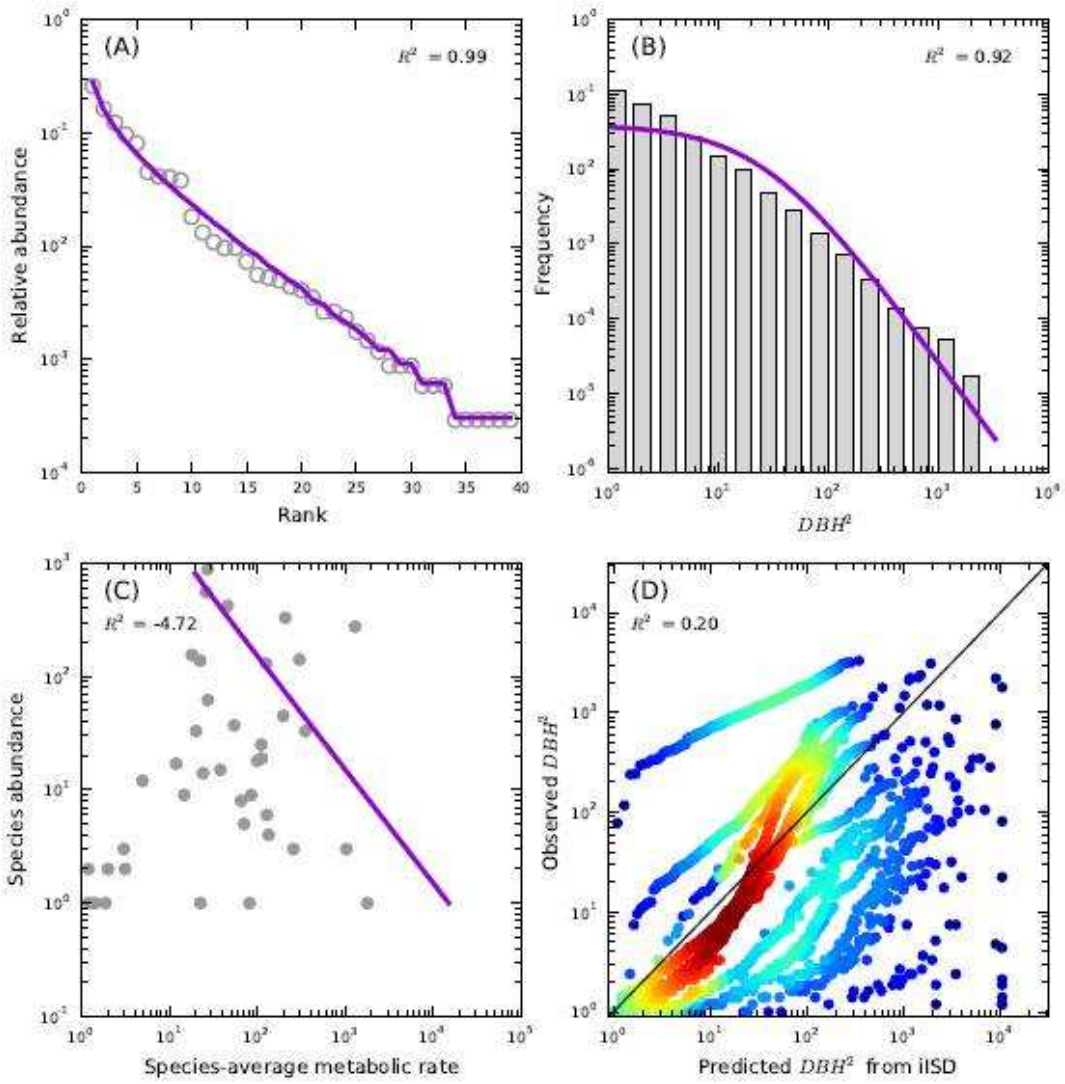
NC,13



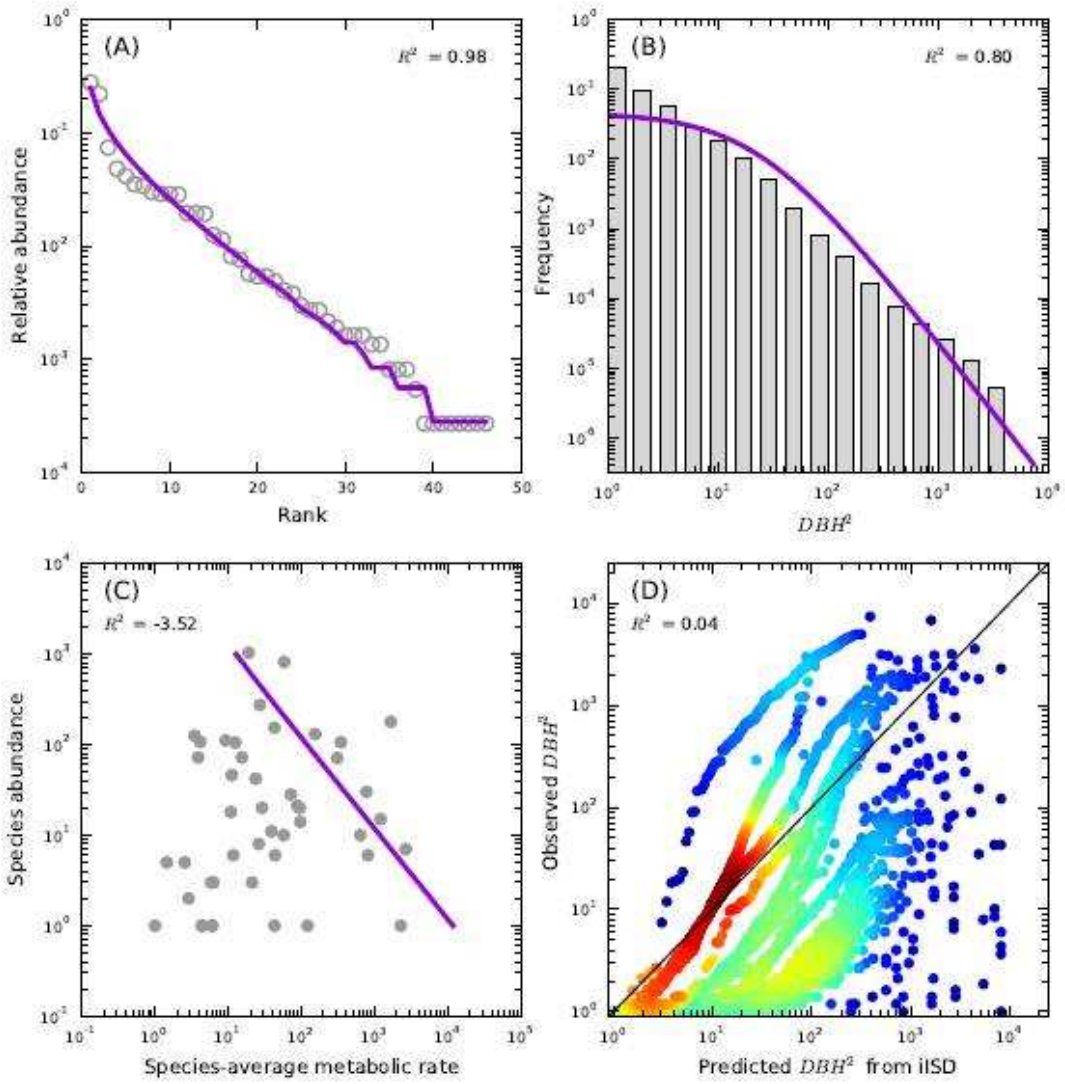
NC,14



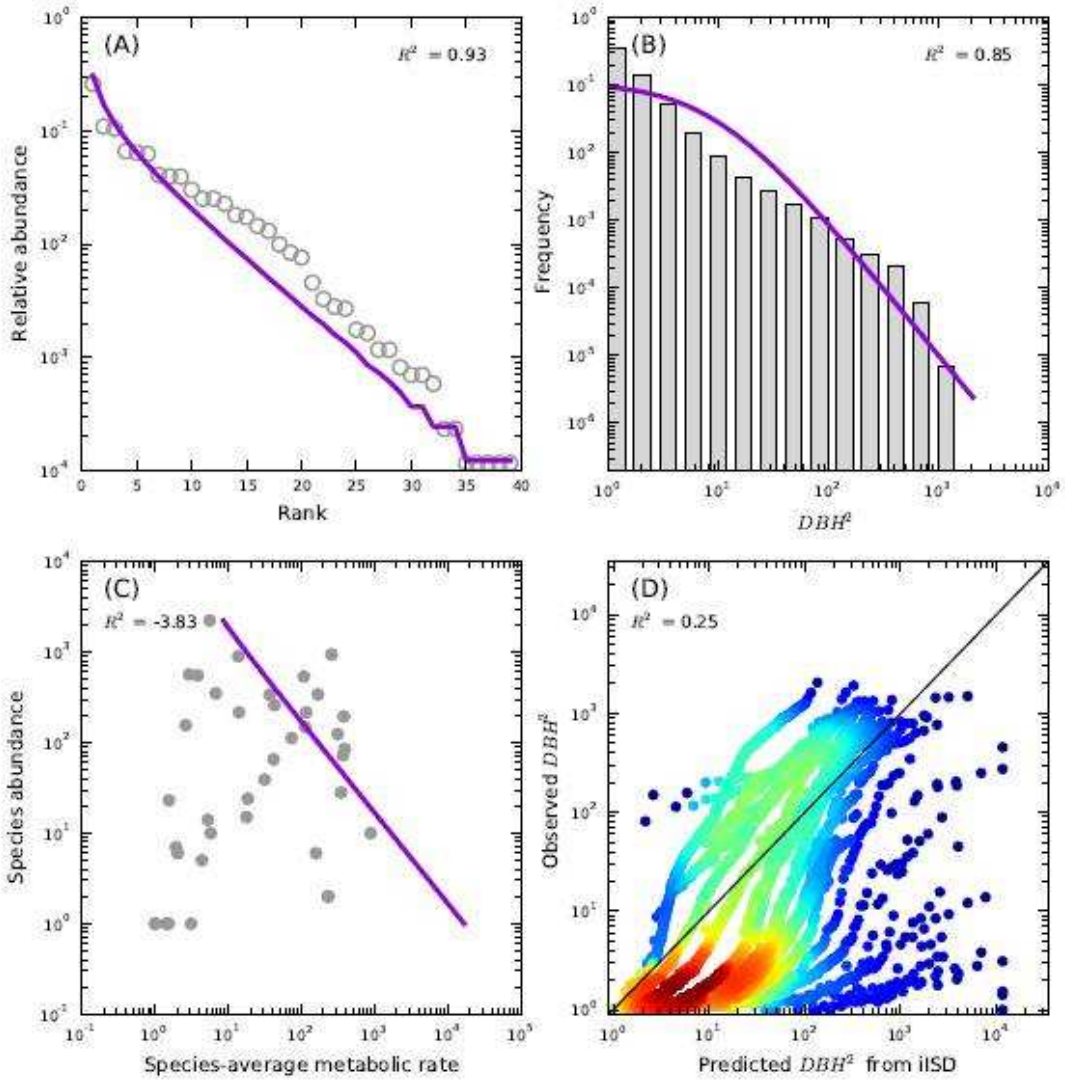
# NC,4



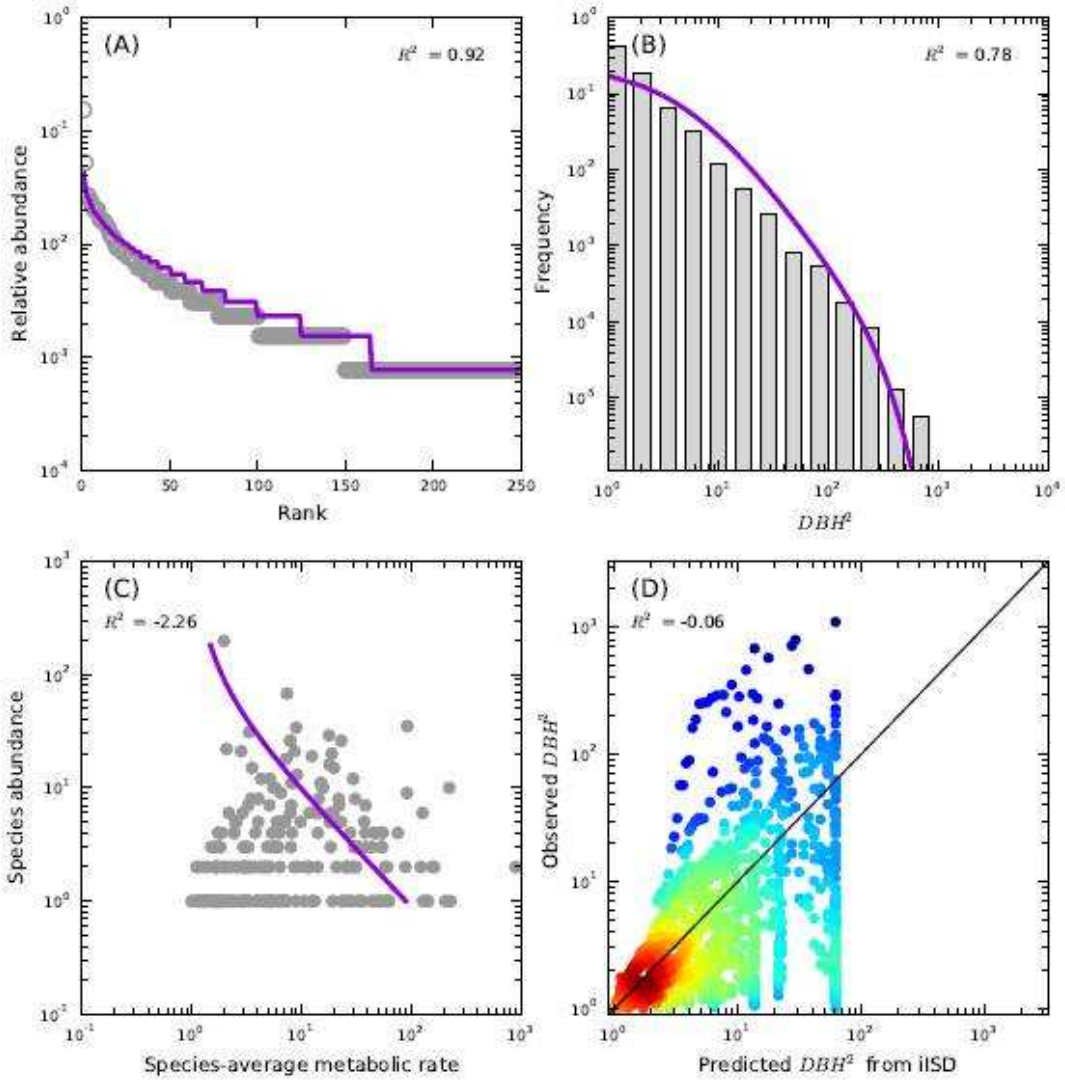
NC,93



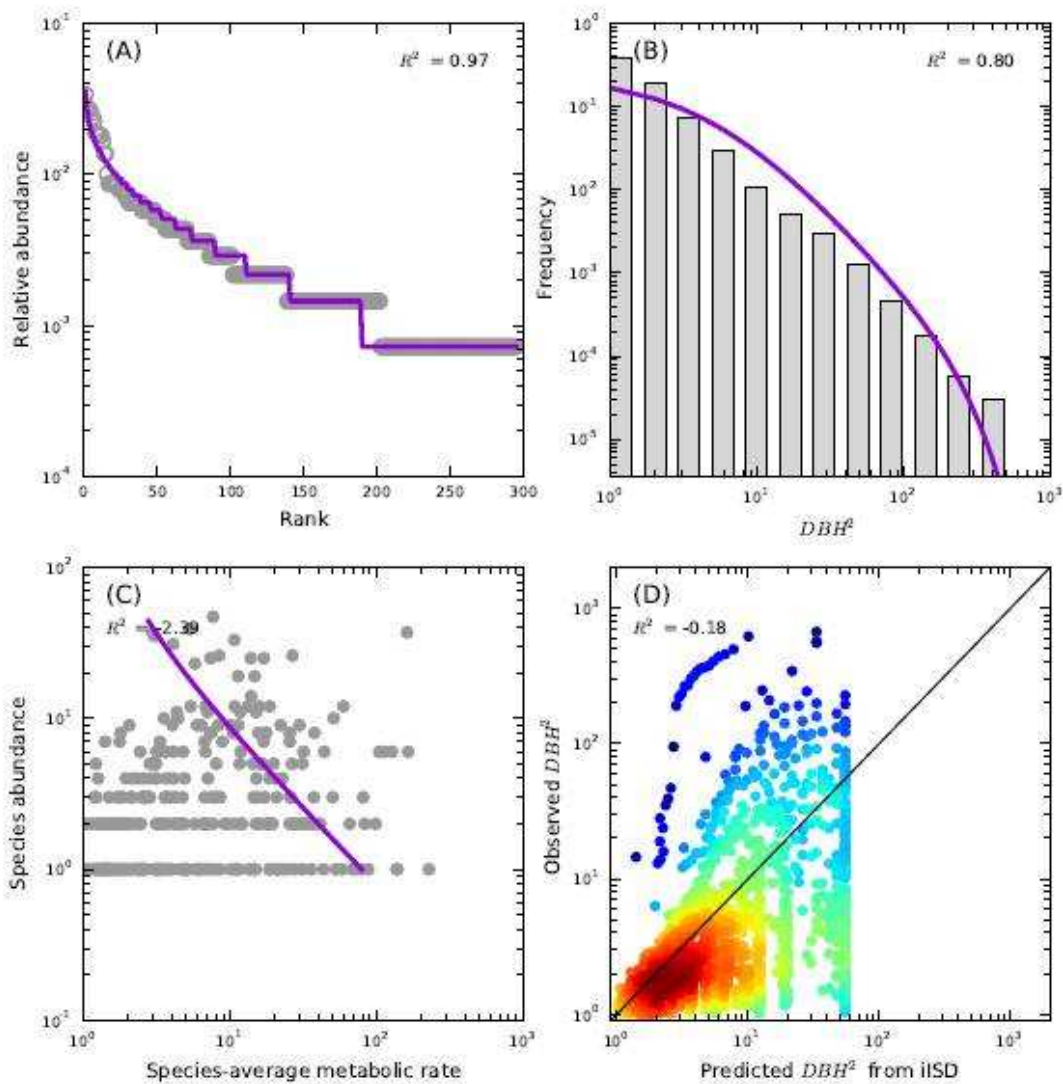
# Oosting, Oosting



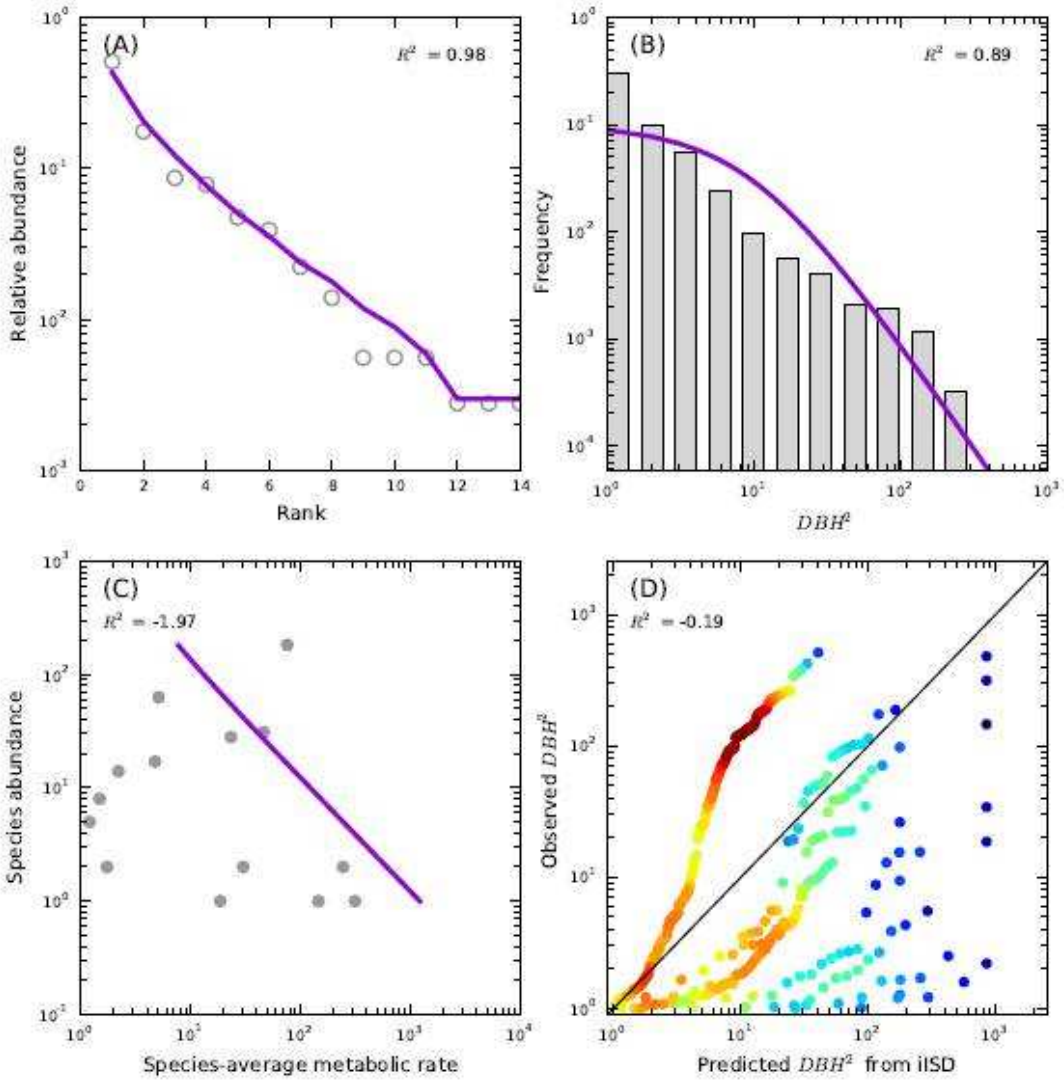
Serimbu, S-1



Serimbu,S-2

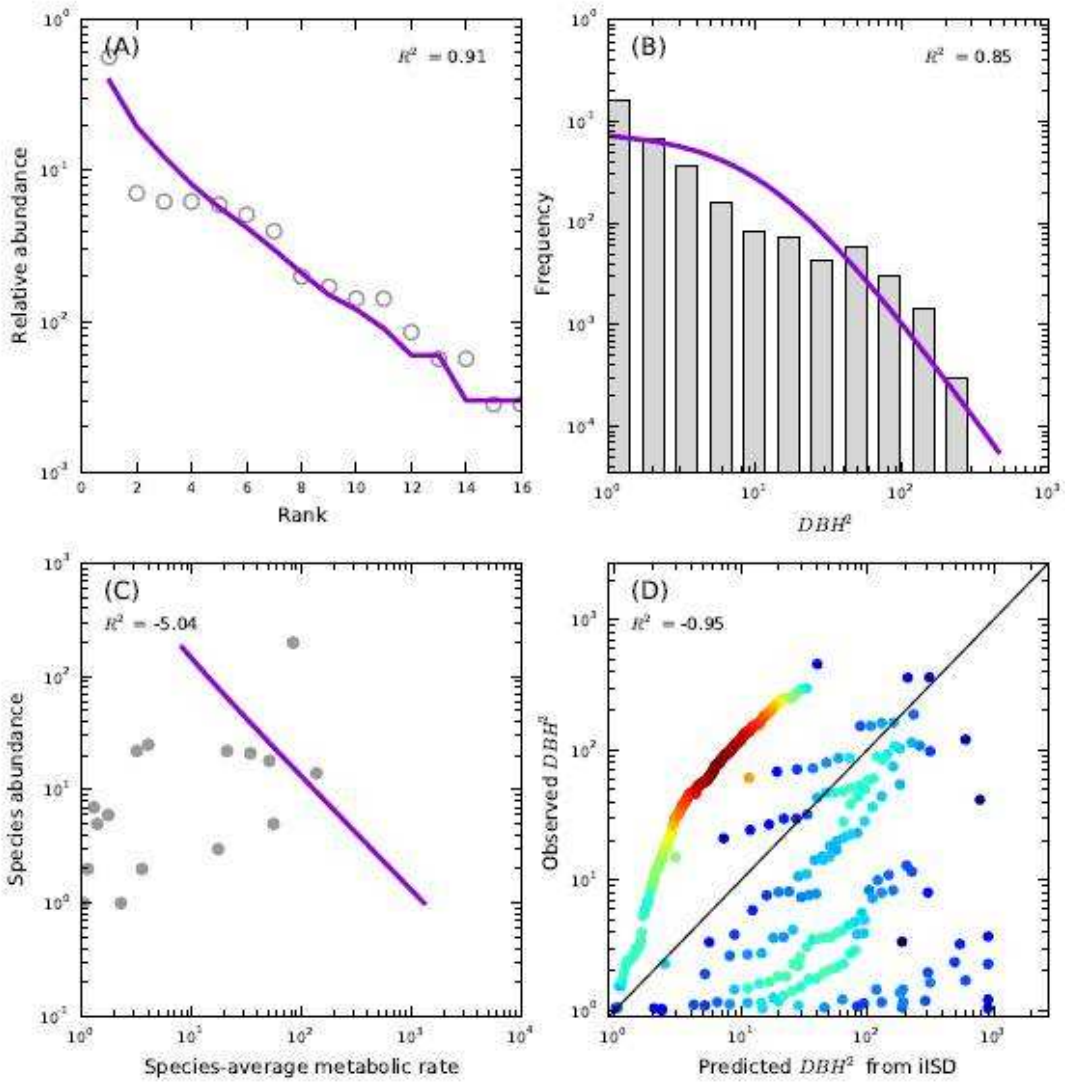


Shirakami, Akaishizawa





Shirakami, Kumagera



# Sherman, sherman

